

MAG/WH 0201
nr 1434

C

membrane - foulant interaction study

Marleen Fontyn



CENTRALE LANDBOUWCATALOGUS



0000 0454 7929

40951

Promotoren: dr.ir. K. van 't Riet
hoogleraar in de Levensmiddelenproceskunde

dr. B.H. Bijsterbosch
hoogleraar in de Fysische en Kolloïdchemie

A MEMBRANE - FOULANT INTERACTION STUDY

Marleen Fontyn

Proefschrift

ter verkrijging van de graad van
doctor in de landbouw- en milieuwetenschappen
op gezag van de rector magnificus
dr. H.C. van der Plas
in het openbaar te verdedigen
op donderdag 27 juni 1991
des namiddags te vier uur in de aula
van de Landbouwniversiteit te Wageningen

idn = 540145

BIBLIOTHEEK
LANDBOUWUNIVERSITEIT
WAGENINGEN

STELLINGEN

1 Na passieve adsorptie (membraan ondergedompeld in een polymeeroplossing) meten Kim *et al.* een hogere relatieve waterflux dan na convectieve behandeling van het membraan (ultrafiltratie van de polymeeroplossing). Door concentratie (polarisatie) van het geultrafiltreerde polymeer aan het membraanoppervlak als enige verklaring hiervoor naar voren te schuiven gaan de auteurs onterecht voorbij aan de verandering van de polymeerconformatie bij druk.

K.J. Kim, A.G. Fane and C.J.D. Fell. The performance of ultrafiltration membranes pretreated by polymers. *Desalination*, 1988, 70, 229-249.

2 De methode van Cabral *et al.* om de performance van een holle vezel membraan-unit uit te drukken door een gemiddelde flux berekend via integratie, zonder de eindfiltratietijd en de vorm van de flux-versus-tijd-curve weer te geven, houdt geen rekening met het feit dat membranen altijd een poriegrootteverdeling hebben.

J.M.S. Cabral, B. Casale and C. L. Cooney. Effect of antifoam agents and efficiency of cleaning procedures on the cross-flow filtration of microbial suspensions. *Biotechnology Letters*, 1985, 7, 749-752.

3 De suggestie om het fractale concept toe te passen op de poriegrootteverdelingen van ultrafiltratiemembranen is weinig realistisch aangezien het concept alleen geldig is indien het aantal poriën $N(r)$ met een bepaalde diameter r evenredig is met r^{-x} (met x een reëel getal) over enkele decades in r .

F. Petrus Cuperus. Characterization of ultrafiltration membranes. Pore structure and top layer thickness. Proefschrift Universiteit Twente, 1990.

4 Met behulp van kleine hoek Röntgenverstrooiing moet het in principe mogelijk zijn de poriegrootteverdeling van ultrafiltratiemembranen te bepalen.

5 Vervanging van de huidige tempereermethode in het chocolade-kristallisatieproces door een eenvoudige koeltechniek gebruik makende van vetkristalkiemen zou het proces aanzienlijk economischer kunnen maken.

T. Koyano, I. Hachiya and K. Sato. Fat polymorphism and crystal seeding effects on fat bloom stability of dark chocolate. *Food Structure*, 1990, 9, 231-240.

6 Bij de bepaling van poriegrootteverdelingen in ultrafiltratiemembranen kunnen de nadelen van transmissie-elektronenmicroscopie (grote risico's om artefacten te krijgen bij het snijden) en deze van scanning-elektronenmicroscopie (te lage resolutie) overkomen worden door gebruik te maken van veld-emissie scanning-elektronenmicroscopie.

K.J. Kim, A.G. Fane, C.J.D. Fell, T. Suzuki and M.R. Dickson. Quantitative microscopic study of surface characteristics of ultrafiltration membranes. *J. Membrane Sci.*, 1990, 54, 89-102.

7 Alhoewel de Lorentz-verdeling nagenoeg onbekend blijkt te zijn bij fysisch-chemici, biedt ze ook daar tal van mogelijkheden, getuige haar veelvuldige toepassing in de analytische chemie bij profiel-fitting.

8 Een gemeenschappelijk beleid (en dus samengevoegde budgetten) in Frans-Vlaanderen, Vlaanderen en Nederland op het gebied van cultuur, wetenschap, politiek, onderwijs en sociale zaken, zou gunstig zijn voor het gehele maatschappelijke leven in de genoemde gebieden.

9 Een fundamentele en pretentieuze-wetenschappelijke opstelling door commerciële onderzoeksinstituten heeft een negatief effect op de toekenning van onderzoekopdrachten door kleine en middelgrote ondernemingen.

10 Het zou getuigen van een juiste ethiek als bij de te fotograferen berghelling, met of zonder beklimmers, een schietlood werd gehangen.

M. Fontyn

A membrane - foulant interaction study.

Wageningen, 27 juni 1991.

VOORWOORD

Bij het totstandkomen van een proefschrift zijn altijd veel mensen betrokken. Dit wil zeggen dat ook dit voorliggende onderzoek slechts zover is gekomen door de hulp, daadwerkelijk en mentaal, van heel wat personen. Enkelen wil ik met name noemen.

Het Biotechnion is een goede werkplek. Het lab op de zesde verdieping en later op het tweede bordes kende bijna altijd ruimtegebrek en dat is een stimulerende omgeving gebleken. In kamer 509, eerst nog leeg, maar spoedig vol, vond ik een goed klankbord. Dank jullie wel Nico, Wouter, Matthijs, Marcel, Lou, Henk en Monique. Bij Johan Weldring vond ik steeds een gewillig oor en een behulpzame hand. Tekenkamer, fotolocatie, magazijn, technische dienst, automatiseringsdienst en sekretariaat herbergen bekwame mensen.

Op de vakgroep Fysische en Kolloïdchemie vond ik altijd mensen bereid om over typische moeilijkheden in het onderzoek te discussiëren.

Zonder hulp en welwillendheid van Joop Weseman en dr. W.G. de Ruig (Rikilt) zouden er nooit ATR-IR-metingen uitgevoerd zijn. Met Markus Oldani (ABB, Baden, Zwitserland) heb ik tijdens geapprecieerde discussies van gedachten kunnen wisselen over XPS en ATR-IR aan membranen. De meettechnische en inhoudelijke kennis van Ed Biemond (Akzo Research Laboratoria Arnhem) van XPS en van David Johnson (The Centre for Surface and Materials Analysis, UMIST, Manchester) van FAB MS was van grote waarde voor het onderzoek. Dank jullie.

In de membraan-vervuilings- en karakteriseringsclub hielden we gezellige en stimulerende bijeenkomsten over de voortgang van de onderzoeken. Toen waren dat Jan-Henk, Lowie, Erik, Gert, Petrus, Maarten, Carien en Jos.

Marjo Broertjes, Gerard Bonekamp, Jean-Paul Vincken, Joop Stoots, Ben Deijkers, Cornelis Visser, Ellert Camminga, Mark Verhagen en Marian Geluk hebben als doctoraalstudenten een wezenlijke bijdrage geleverd bij de uitvoering van het onderzoek en het uitkristalliseren van ideeën. Dank jullie ook voor jullie enthousiasme.

Voorwoord

Eerste en laatste voorwaarde voor dit onderzoek waren Klaas van 't Riet en Bert Bijsterbosch. Zij zijn in 1984 gezamenlijk dit onderzoek gestart en bij het afronden ervan hebben zij veel doorzettingsvermogen getoond. Dank jullie, Bert en Klaas. Ik zal niet licht vergeten hoe jullie in jullie eigen vakgroep op jullie eigen manier mensen weten te motiveren.

Het onderzoek beschreven in dit proefschrift werd uitgevoerd met de financiële steun van het IOP-membranen van het Ministerie van Economische Zaken. Als zodanig lag de uitvoering bij de Programma Commissie Membranen en Stichting Technische Wetenschappen. Akzo en Otare's hebben ook financieel bijgedragen.

CONTENTS

Chapter 1	
Introduction	1
Chapter 2	
Characterization of polymers on ultrafiltration membranes by permeation and adsorption	7
Chapter 3	
Pore size distribution measurements of pristine and fouled polysulfone membranes: method development, membrane characterization and adsorption mechanism	29
Chapter 4	
Surface spectroscopic studies of pristine and fouled membranes.	
Part I. Method development and pristine membrane characterization	55
Chapter 5	
Surface spectroscopic studies of pristine and fouled membranes.	
Part II. Method development and adsorption mechanism	77
Chapter 6	
General discussion	93
Summary	97
Samenvatting	101
Curriculum vitae	105

Chapter 3 will be submitted as:

M. Fontyn, J.-P. Vincken, E. Camminga, M.F.J.M. Verhagen, K. van 't Riet and B.H. Bijsterbosch

Chapter 4 has been published as:

M. Fontyn, K. van 't Riet and B.H. Bijsterbosch. *Colloids and Surfaces*, 1991, 54, 331-347.

Chapter 5 has been published as:

M. Fontyn, K. van 't Riet and B.H. Bijsterbosch. *Colloids and Surfaces*, 1991, 54, 349-362.

CHAPTER 1

INTRODUCTION

1.1. GENERAL INTRODUCTION

Membrane filtration has grown from a laboratory-scale technique in the 1960's to an industrial technology nowadays. Water purification, preconcentration of milk before spray drying, concentration of whole egg and egg white, removal of alcohol from wine, clarification of fruit juices, separation of valuable products from waste streams, combined reaction by enzymes and separation of substrates and products, are such diverse examples of process operations where membranes are widely employed.

Gradual flux decline has always been one of the major drawbacks of membrane processes. This problem has been tackled in several ways, of which the change in configuration of membrane and feed from unstirred dead-end to stirred dead-end and cross-flow filtration is a typical example. Optimization of the flow channel, increasing the cross-flow velocity or decreasing the viscosity by increasing the temperature are then obvious measures. Backflushing [1, 2], pulsing the feed solution [3], using small electrical current pulses [4, 5] and rotating [6] and corrugated [7] membranes also enhance the mass transfer coefficient and thus the flux.

Solution-treatment by prefiltration or feed hydrolysis, ion exchange or pH alteration are other ways of fighting the flux decrease.

Most of the mentioned methods deal with the problem in a process-engineering way. The causes of the flux decline still remain present but are manifest to a lesser extent.

As membrane processes are gaining further impetus, the problem of flux decrease requires more extensive investigation. Concentration polarization during separation and concentration on one hand and fouling of the membrane on the other are the two relevant aspects to be studied. Modelling of concentration polarization has traditionally obtained much attention from the engineering (macroscopic) side. However, studying the fouling problem in a physical chemical way was a new approach only introduced in the early 1980's. In this relation it is worth mentioning that chemical and physical treatment of the membrane surface has been shown to lead to flux enhancement [8-13]. The latter investigations have indicated interactions between the membrane and the

solutes in the feed to be the cause of the early stages of the flux decrease. The physical chemical way of investigating has since gained acceleration. This study aims at investigating physical chemical adsorption phenomena on membranes and the importance of the results for e.g. process engineering.

1.2. DEFINING THE PROBLEM

An illustrative example of the fouling problem relates to the foaming phenomena that are often encountered in large scale fermentation processes. Anti-foaming agents (AFAs) are used to reduce these problems. Also in the sugar refining industry can AFAs hardly be missed, like in the process of washing potatoes for starch production an AFA is continuously dosed. In all cases it appears over and over again that the AFA probably influences the performance of a membrane process further downstream [2, 14-16]. The permeability of the membrane is frequently lowered and the retention behaviour altered.

To test the hypothesis that AFAs are responsible for the flux problems, in the early stages of this project some orienting experiments have been performed. Solutions or dispersions of a number of AFAs were ultrafiltered through different kinds of membranes (Figure 1). AFAs like Struktol SB 2087 and Union Carbide SAG 5693 hardly affect the permeability of the hydrophilic polyacrylonitril (PAN) membrane, but others like Struktol J 660 definitively have a fouling effect, under the conditions used in the experiment. On the other hand, Struktol SB 2087 and Union Carbide SAG 5693 used in combination with the hydrophobic polysulfone (PSf) membrane lead to unacceptably high resistances. J 660 has just the opposite effect again. Apparently, the hydrophobic/hydrophilic balance in the AFA, in relation to the same ratio on the membrane surface plays a decisive role.

Figure 2 depicts the ultrafiltration of SAG 5693, siloxane and polypropylene glycol (PPG) 2000 on a PSf membrane. After 15 minutes the membrane is totally useless when using SAG 5693 or PPG 2000, one of its constituents. Siloxane, the other constituent of SAG 5693, however, doesn't show any flux lowering effect.

From these examples it appears that hydrophobicity/hydrophilicity of membranes as well as adsorbing solute very probably are of importance. This research aims at model studies of the physical chemistry of macromolecular adsorption to membrane materials and its importance for process engineering.

The observation that specific interactions between membranes and AFAs apparently control membrane permeability has led us to focussing on membrane fouling as an adsorption phenomenon. Concentration polarization and gel layer phenomena have not been investigated.

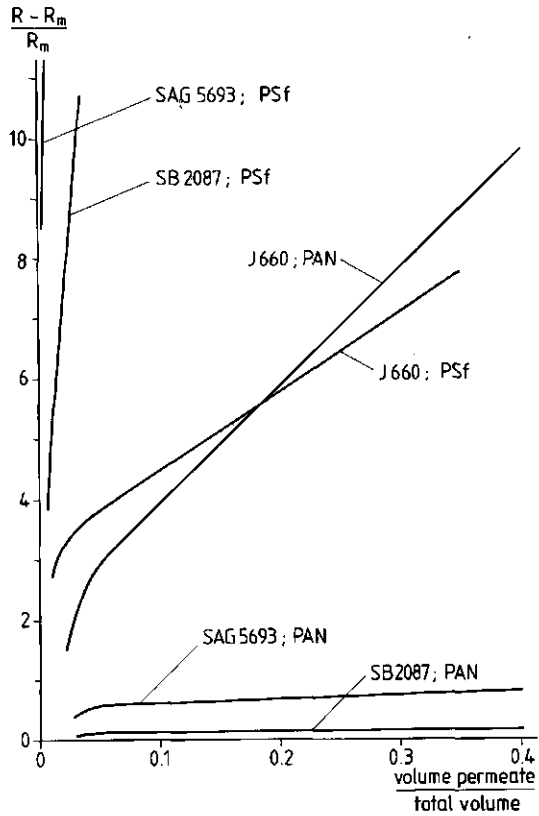


Figure 1. Relative resistance [(observed resistance R - membrane resistance R_m) / R_m] versus relative volume of permeate for some combinations of membranes and anti-foaming agents. $C_{\text{AFA}} = 2000$ ppm.

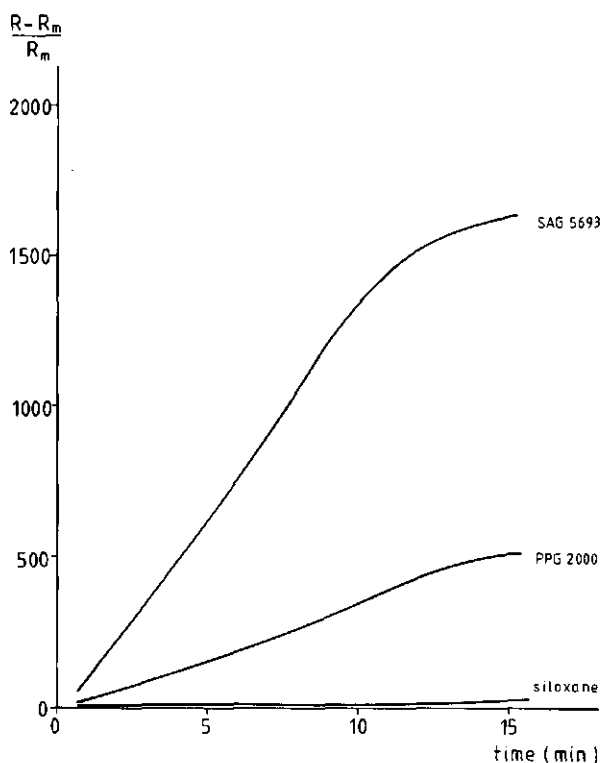


Figure 2. Relative resistance versus time for an Amicon PM 10 PSf membrane in combination with some solutions (2000 ppm) of anti-foaming agents.

1.3. MODEL SYSTEM AND CHARACTERIZATION TECHNIQUES

For the reasons mentioned in relation to Figures 1 and 2 PPG was selected as one of the model compounds in this research project. Other model compounds have been chosen on the basis of their similarity in chemical structure with PPG. Polyethylene glycol (PEG) is the hydrophilic counterpart of PPG and block copolymers of ethylene oxide - propylene oxide (EO-PO-EO) are amphiphilic.

PSf membranes are chemically and microbiologically resistant and in view of these properties widely used in practice. Therefore, the PSf membrane was selected as the model membrane.

The elucidation of interaction phenomena has led to the use of spectroscopic techniques. These had to be techniques enabling the characterization of layers on a polymeric surface of only a few nanometers thickness, which led to the

choice of X-ray photoelectron spectroscopy (XPS), fast atom bombardment mass spectrometry (FAB MS) and attenuated total reflection infrared spectroscopy (ATR IR).

Permeability properties were preferably to be displayed by pore size or pore size distribution (PSD). In particular, a method has been developed for comparing the permeability characteristics of pristine and fouled membranes.

1.4. OUTLINE OF THIS THESIS

This thesis is concerned with the elucidation of the surface structure of some selected membranes and with the interaction mechanisms between foulant and membrane. It has been structured in the following way.

Chapter 2 is dealing semi-quantitatively with the influence of permeation and adsorption of model compounds on flux decrease. It is particularly relating the chemical composition of the foulants with that of the membrane.

In chapter 3 a method for characterization of PSDs has been developed and the characteristics of pristine and fouled membranes are compared. Finally, the physical aspects of adsorption are elaborated on.

Characterization of the pristine and fouled PSf membranes by advanced surface-sensitive spectroscopic techniques is discussed in chapters 4 and 5. Since also the chemical aspects of adsorption are discussed, chapter 5 emphasizes the fouling problem from a molecular point of view.

Finally, a general discussion is given in chapter 6.

REFERENCES

- 1 B.R. Breslau, E.A. Agranat, A.J. Testa, S. Messinger and R.A. Cross. Hollow Fiber Ultrafiltration. *Chem. Eng. Progr.*, 1975, **71**, 74-80.
- 2 K.H. Kroner, H. Schütte, H. Hustedt and M.-R. Kula. Cross-flow Filtration in the Downstream Processing of Enzymes. *Process Biochemistry*, 1984, **19**, 67-74.
- 3 H. Bauser, H. Chmiel, N. Stroh and E. Walitza. Interfacial Effects with Microfiltration Membranes. *J. Membrane Sci.*, 1982, **11**, 321-332.
- 4 W.R. Bowen, R.S. Kingdom and H.A.M. Sabuni. Electrically Enhanced Membrane Separation Processes. Proceedings of the International Congress on Membranes and Membrane Processes (ICOM'87), Japan, Tokyo, June 8-12, 1987.

- 5 R.J. Wakeman and E.S. Tarleton. Membrane Fouling in Crossflow Microfiltration by the Use of Electric Fields. *Chem. Eng. Sci.*, 1987, 42, 829-842.
- 6 M. López-Leiva. Ultrafiltration in Rotary Annular Flow. Ph. D. Thesis, University of Lund, Sweden, 1979.
- 7 I.G. Rácz, J. Groot Wassink and R. Klaassen. Mass Transfer, Fluid Flow and Membrane Properties in Flat and Corrugated Plate Hyperfiltration Modules. *Desalination*, 1986, 60, 213-222.
- 8 A. Noshay and L.M. Robeson. Sulfonated Polysulfone. *J. Applied Polymer Sci.*, 1976, 20, 1885-1903.
- 9 F.-J. Müller, W. Krieger, W. Kissing and R. Reiner. Reduction on Membrane Fouling in Reverse Osmosis by Means of Surface Modifications of the Membranes. In: *Fundamentals and Applications of Surface Phenomena Associated with Fouling and Cleaning in Food Processing*. Eds. B. Hallström, D.B. Lund and Ch. Trägårdh. Tylösand, Sweden, April 6-9, 1981.
- 10 L.M. Speaker and K.R. Bynum. Oriented Monolayer Assemblies to Modify Fouling Properties of Membranes. In: *Physicochemical Aspects of Polymer Surfaces*. Volume 2. Ed. K.L. Mittal. Plenum Press, New York and London, 1983.
- 11 A.G. Fane, C.J.D. Fell and K.J. Kim. The Effect of Surfactant Pretreatment on the Ultrafiltration of Proteins. *Desalination*, 1985, 53, 37-55.
- 12 K.E. Kinzer, D.R. Lloyd, M.S. Gay, J.P. Wightman, B.C. Johnson and J.E. McGrath. Phase Inversion Sulfonated Polysulphone Membranes. *J. Membrane Sci.*, 1985, 22, 1-29.
- 13 T.W. Beihoffer and J.E. Glass. Hydrophilic Modification of Engineering Polymers. *Polymer*, 1986, 27, 1626-1632.
- 14 J.M.S. Cabral, B. Casale and C.L. Cooney. Effect of Antifoam Agents and Efficiency of Cleaning Procedures on the Cross-Flow Filtration of Microbial Suspensions. *Biotechnology Letters*, 1985, 7, 749-752.
- 15 T.R. Hanssens. Personal Communication.
- 16 B.R. Slomp. Personal Communication.

CHAPTER 2

CHARACTERIZATION OF POLYMERS ON ULTRAFILTRATION MEMBRANES BY PERMEATION AND ADSORPTION

ABSTRACT

Membrane fouling is a negative quality aspect of ultrafiltration that is often taken for granted. However, interpreting fouling phenomena in terms of the characteristics of membranes and solutes might quite well contribute to overcoming this problem. This study aims at investigating the effects of polymer adsorption on permeation through membranes and at quantitatively characterizing the interactions. Different types of membranes and solutes have been investigated.

The molecular mass of the solutes appears to affect the adsorption resistance (R_a) as do the chemical natures of solute and membrane. Experiments with ethylene oxide / propylene oxide block copolymers indicate hydrophobicity to be of major importance. Expressing this characteristic in terms of the hydrophilic - lipophilic balance (HLB) does not provide a very useful parameter, although it illustrates the qualitative tendency of R_a to decrease with decreasing hydrophobicity of the polymer.

Adsorption of methylene blue on an intact DDS GR61 membrane and on its polysulfone (PSf) active layer without support layer, demonstrates that adsorption in the pores must be accounted for. The adsorbed amount of polypropylene glycol (PPG) 1200 per geometric surface area (Γ_a') on the intact GR61 and on the PSf layer without support layer can be fitted by a Langmuir-type isotherm. Subtraction of both reveals the Γ_a' on the sublayer. The corresponding maxima in Γ_a' are $21 \text{ g.m}^{-2}\text{geo}$ for the entire membrane and $10 \text{ g.m}^{-2}\text{geo}$ for the PSf layer.

R_a of the complete GR61 membrane does not show a linear relationship with the adsorbed amount. For the present case the Γ_a' in the very porous sublayer is slightly higher than in the less porous PSf layer, but the more effective narrowing of the smaller pores in the PSf as compared to those in the porous sublayer causes the flux to be controlled by the PSf layer.

2.1. INTRODUCTION

Membrane fouling is a phenomenon causing the pure water flux to hardly ever regain its original value. This aspect contributes negatively to the costs of ultrafiltration processes, which are high anyway. These costs are often taken for granted if the ultrafiltration unit meets the primary goals but, preferably, the costs should be reduced.

Studies on laboratory scale have indicated that adsorption of the solutes that have to be filtered might be responsible for this fouling phenomenon and thus for the decreased permeate flux [1-7]. Hydrophobic forces are held responsible, but are not easy to assess quantitatively.

The interaction between membrane and solute can be altered by changing the membrane surface composition. Presorption of polymers, surfactants and other compounds [4, 6, 8-12], chemical modification of the composing polymer [13] and plasma treatment [14] have been shown to be feasible in enhancing the membrane flux. However, their effect can only be predicted qualitatively.

Characterization of membranes and fouling solutes is an important step in understanding the fundamental backgrounds [e.g. 15]. Quantitative measures for chemical interactions in practical systems have been developed in the field of bacterial adhesion [16-21]. The importance of bacterial adhesion in membrane fouling has also been displayed [22].

Interactions of polymers with surfaces can be quantified by such theoretical or empirical parameters as the ζ -potential, the hydrodynamic layer thickness δ_h , the interfacial tension γ , the heat of mixing of several compounds, the thermodynamic interaction parameter χ , the contact angle and the wettability [23-27]. These parameters can be measured or calculated for well-characterized adsorbants and for clean and homogeneous surfaces. Derived measures as the hydrophobic fragmental constant, the HLB (number or temperature) and the phase inversion temperature (PIT) [28-30] are applicable in more practical cases. However, they describe the complex membrane-solute interaction rather incompletely, if not poorly.

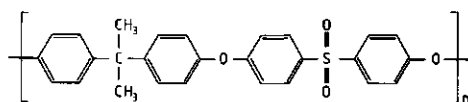
The aim of this study is to investigate the effects of adsorption of different polymers on different types of membranes and the possibility of quantitatively characterizing the interactions in the selected model systems. Emphasis will be on effects that are additional to the sieving effect of ultrafiltration membranes. Permeation measurements and adsorption isotherms have been used as tools. These investigations should initiate more fundamental research with regard to the consequences of polymer adsorption on membranes.

2.2. MATERIALS AND METHODS

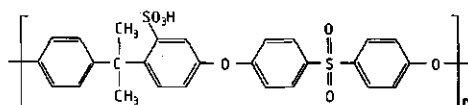
2.2.1. Membranes

Four types of membranes with molecular mass cut off values (MMCO) of 20000 g.mol^{-1} have been used. Table 1 and Figure 1 comprise some of their features. The differences in the types of polymers are the basis for their selection.

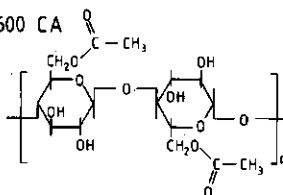
GR 61 PSf



GS 61 SPSf



CA 600 CA



IRIS 3038 PAN

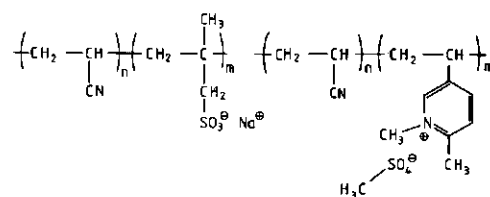


Figure 1. Chemical structure of the polymers used in casting the membranes.

Table 1. Some data on the membranes.

	GR61 PP	GS61 PP	CA600	IRIS3038
Manufacturer	DDS Nakskov, DK	DDS Nakskov, DK	DDS Nakskov, DK	Rhône-Poulenc Paris, F
Polymer type	PSf (Udel)	SPSf (Udel)	CA	PAN copolymer [31]
MMCO	20000	20000	20000	20000
Sublayer type	filter paper (non-woven)	filter paper (non-woven)		nylon
Batch	400-013	104-02	219-005	
R_m (Nsm ⁻³)	1 *10 ¹⁰	6 *10 ⁹	2 *10 ¹⁰	3 *10 ⁹

2.2.2. Compounds

Polypropylene glycol

Polypropylene glycols (PPG) with four different molecular masses (MM) have been employed: 400, 1200 and 2000 (Fluka AG, Buchs, CH, 81350, 81370 and 81380) and 4000 (Serva Feinbiochimica, Heidelberg, D, 46241, analytical grade for GC). PPG is uncharged.

Polyethylene glycol

Selected MMs of polyethylene glycol (PEG) were: 300, 1000, 1500, 3000 and 20000 (Merck, Darmstadt, Schuchardt, D, Art. 807484, 807488, 807489, 819015 and 9732).

Block copolymers of ethylene oxide / propylene oxide

Block copolymers of ethylene oxide (EO) and propylene oxide (PO) were obtained from ICI France S.A. (Clamart, F, Synperonic PE). They are also uncharged. Table 2 summarizes the MMs and the statistically most likely compositions of the EO/PO blocks and the PPGs and PEGs.

Polyvinyl pyrrolidone

Linear polyvinyl pyrrolidone (PVP) from BASF (Ludwigshafen, D, Kollidon K12, K17 and K25) with MMs of ca. 3200, 8000 and 17400 [32] was used. At pH = 7 it is uncharged.

Table 2. Molecular mass of the EO (M_{EO}) and PO (M_{PO}) parts of the PEGs, PPGs and Synperonic PE block copolymers and their statistically most probable configuration.

Compound	M_{PO}	M_{EO}	Configuration
PEG 300	-	300	EO ₇
1000	-	1000	EO ₂₃
1500	-	1500	EO ₃₄
3000	-	3000	EO ₆₈
20000	-	20000	EO ₄₅₅
PPG 400	400	-	PO ₇
1200	1200	-	PO ₂₁
2000	2000	-	PO ₃₄
4000	4000	-	PO ₆₉
L42	1200	300	EO ₃ -PO ₂₁ -EO ₃
L43	1200	500	EO ₆ -PO ₂₁ -EO ₆
L44	1200	800	EO ₉ -PO ₂₁ -EO ₉
L72	2050	500	EO ₆ -PO ₃₅ -EO ₆
P75	2050	2050	EO ₂₃ -PO ₃₅ -EO ₂₃
F77	2050	4800	EO ₅₄ -PO ₃₅ -EO ₅₄
P84	2250	1500	EO ₁₇ -PO ₃₉ -EO ₁₇
L92	2750	700	EO ₈ -PO ₄₇ -EO ₈

Polyvinyl alcohol

Poval 105 polyvinyl alcohol (PVA) (Konam NV., Amsterdam, NL) is uncharged and shows little or no branching. MM (weight averaged) is 46500, as measured by gel permeation chromatography. The acetate content is yet 1.9 mol%, number averaged [33, 34].

Carboxymethyl cellulose

AKU CMC LZ-853 (Akzo Zout Chemie, Industrial Colloids, Arnhem, NL) is a 99.5% pure, anionic carboxymethyl cellulose (CMC) with a DP of 1000 (MM of 220000) and a degree of substitution (DS) with the carboxymethyl groups of 0.95. It is applied in the chemical and food industry as binder and stabilizer and for its rheological properties.

Figure 2 shows the monomeric chemical structure of the compounds used.

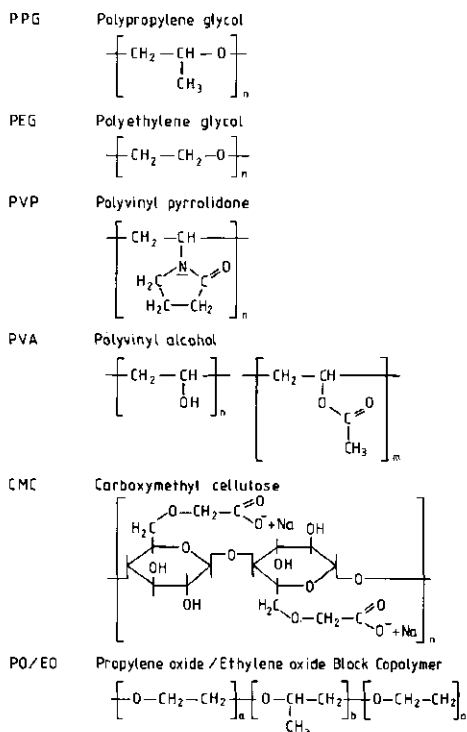


Figure 2. Chemical structure of the monomers of PPG, PEG, PVP, PVA, CMC and EO/PO.

2.2.3. Resistance determination

Resistances have been measured in a dead-end cell (Amicon, Grace & Co, Danvers, MA, type 8400) at 25°C and with constant stirrer speed. The effective membrane area was $4.18 \times 10^{-3} \text{ m}^2$ and the trans-membrane pressure $4 \times 10^5 \text{ Pa}$. Resistance (Nsm^{-3}) is defined as the ratio of the trans-membrane pressure (Pa) to the flow through the membrane (m.s^{-1}). Membrane and adsorption resistances (R_m and R_a) were determined using distilled water. R_m is the resistance of the pristine membrane and R_a that of the membrane with an adsorption layer. The ultrafiltration resistances (R_{uf}) were measured using a 1 g.kg^{-1} solution of the compound under consideration and a membrane with an adsorption layer.

2.2.4. Adsorption procedure

The pristine membranes were tightened in a cell with the same configuration as the dead-end cell and were contacted with a 1 g.kg^{-1} solution of the compound during 24 hours, at 25°C , which leads to adsorption saturation.

2.2.5. Specific surface area determination

Small pieces of GR61 (with and without support layer) with known geometric (geo) surface area were shaken in a solution of methylene blue (MB) (J.T. Baker, Deventer, NL, laboratory grade, 2273) of a given concentration for 24 hours. Depletion measurements (accomplished by measuring the extinction at $\lambda = 664 \text{ nm}$) with a range of increasing MB concentrations provide the maximum adsorbed amount $\Gamma_{a,\text{max}}$ (g.m^{-2}). The specific surface area can then be calculated assuming an MB molecular area of 10^{-18} m^2 , which is an average of vertical and flat oriented molecules [35].

2.2.6. Determination of PPG 1200 concentration

Pieces of GR61 (without support layer) with known total surface area were shaken in a PPG solution for 24 hours, at 25°C . Depletion measurements were executed by a iodometric method [36]. A solution containing 2% (m:v) KI and 0.05% (m:v) I_2 (Merck, Darmstadt, D, p.a., Art 5043 and 4761) was mixed with the PPG (in a volume ratio 1:6). The resulting extinction at $\lambda = 500 \text{ nm}$ was measured after 4 minutes.

2.3. RESULTS AND DISCUSSION

2.3.1. Adsorption as assessed by permeation measurements

The block diagrams in Figure 3 give R_m (lower bar), R_a (middle bar) and R_{uf} (higher bar) for four different membranes and five different compounds. By comparing the pure water fluxes (R_m) of the different membranes, according to their manufacturers each having an MMCO of 20000, it is obvious that the MMCO offers little mainstay for characterizing the pure water flux through a

membrane. The observed differences are due to different manufacturers using different definitions, determination methods, membrane preparation techniques, materials, etc.

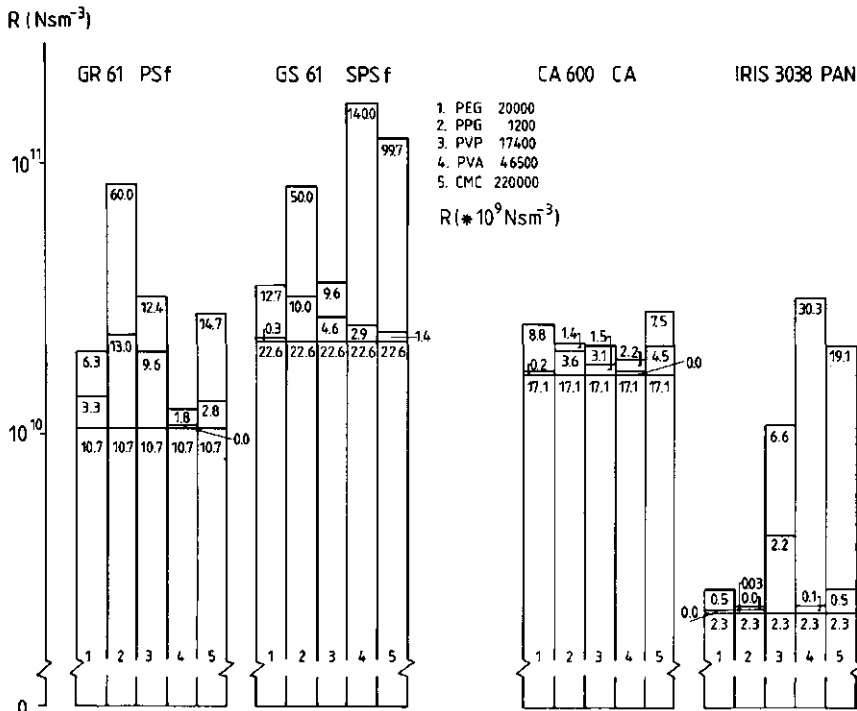


Figure 3. R_m (lower bar), R_a (middle bar) and R_{uf} (upper bar) for different compounds on different types of membrane. Values are given in $\ast 10^9 \text{Nsm}^{-3}$.

By comparing the various compounds it is also clear that MM alone can not explain the effects on adsorption and ultrafiltration (R_a and R_{uf}). The whole spectrum of interactions between polymer molecules themselves, polymer and membrane, polymer and solvent, and solvent and membrane is responsible for the effects observed during adsorption and ultrafiltration. Consequently, the solubility of the compound, its affinity for the membrane material and its ability to form aggregates, as well as the membrane material, its wettability by the solvent and the pore size distribution (PSD) are factors affecting R_a and R_{uf} .

Despite their tendency to get easily fouled, as shown in Figure 3, PSf membranes are widely used in industry because of their chemical and microbiological stability and temperature resistance. Therefore, the commercial GR61 PSf membrane was chosen as a model for further study.

Figure 4 shows the adsorption resistance (R_a) of GR61 for different MMs of PEG, PPG and PVP. As expected, an increase in MM of PPG causes R_a to increase. For PVP this increase in R_a is also manifest, but to a lesser extent than for PPG. Any influence of MM on R_a for PEG is absent though. An increase in MM can obviously result in an increase of R_a to an extent that is different for each of the adsorbing compounds.

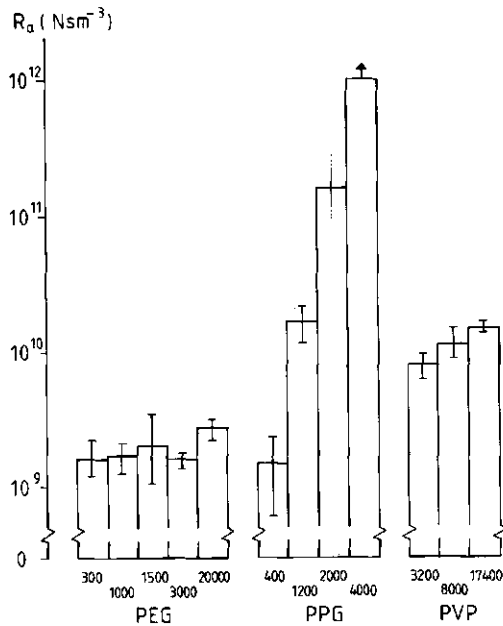


Figure 4. R_a on GR61 for different MMs of PEG, PPG and PVP.

Hydrophobic forces are frequently mentioned as being the main cause of interaction of dissolved compounds with a membrane. The results of Figure 4 agree with this conception, as PPG is strongly hydrophobic, while PVP and PEG are more hydrophilic. To elaborate this hypothesis, block copolymers of EO and PO with a gradient in hydrophobicity have been studied.

In Table 3 the EO and/or PO compounds are arranged according to total MM and expressing the corresponding R_a values. Oligomers of PO or EO with ca. 7 units (PEG 300 and PPG 400) exhibit the same, low, R_a , which seems thus to be independent of the nature of the compound. In contrast, PPG 1200 (21 monomers) shows a tenfold higher R_a than PEG 1000 or PEG 1500 (23 and 34

monomers respectively) despite their nearly similar chemical structure (only one additional CH_3 group in the PO monomer). If 13 PO monomers of PPG 2000 are replaced by 9 EO units on each side of the PO block ($\text{EO}_9\text{-PO}_{21}\text{-EO}_9$ or L44), thus retaining the same MM, the R_a drops with a factor 10. A smaller number of EO units on each side of PPG 2000 ($\text{EO}_6\text{-PO}_{35}\text{-EO}_6$ or L72) already lowers the R_a on PSf with a factor 5. Even doubling the amount of EO units as compared to the amount of PO units (EO_{68} or PEG 3000 versus PO_{34} or PPG 2000) does not cause R_a to rise above the value of PEG 300 and PPG 400. On the contrary, R_a for PEG 3000 is 100 times lower than for PPG 2000.

Table 3. R_a , including its range, for compounds that have been arranged in terms of increasing MM. The last column expresses the corresponding HLB values.

Compound	MM ($\text{g}\cdot\text{mol}^{-1}$)	R_a (* 10^{10} Nsm $^{-3}$)	R_a range (* 10^{10} Nsm $^{-3}$)	HLB (-)
PEG 300	300	0.16	0.05	11.81
PPG 400	400	0.15	0.08	8.45
PEG 1000	1000	0.17	0.04	17.09
PPG 1200	1200	1.67	0.48	6.35
PEG 1500	1500	0.20	0.12	20.75
PPG 2000	2000	15.85		4.40
L44	2000	1.68	0.38	12.29
L72	2550	3.36	0.82	8.21
PEG 3000	3000	0.16	0.02	31.94
L92	3450	9.65	0.77	7.73
P84	3750	2.52	0.13	14.87
P75	4100	2.76	0.19	19.43

From Table 3 it can be concluded that a small change in PO number in the block copolymers (L44, L72, L92) can exhibit large effects on the R_a , and only a small amount of EO is necessary to alter drastically the adsorption tendency of PPG (PPG 1200, L44 and PPG 2000, L72, P75). This conclusion agrees with the hypothesis that hydrophobicity is an important aspect in polymer fouling of membranes.

For block copolymers with a constant number of EO monomers but increasing PO content, a drastic increase in R_a is observed (Figure 5). The strongly decreased solubility in water and the affinity for PSf (thus the hydrophobicity) can be considered responsible for this increase. This is also demonstrated in

Figure 6, where an increase in the number of EO monomers at constant PO content causes a reduction in R_a of GR61.

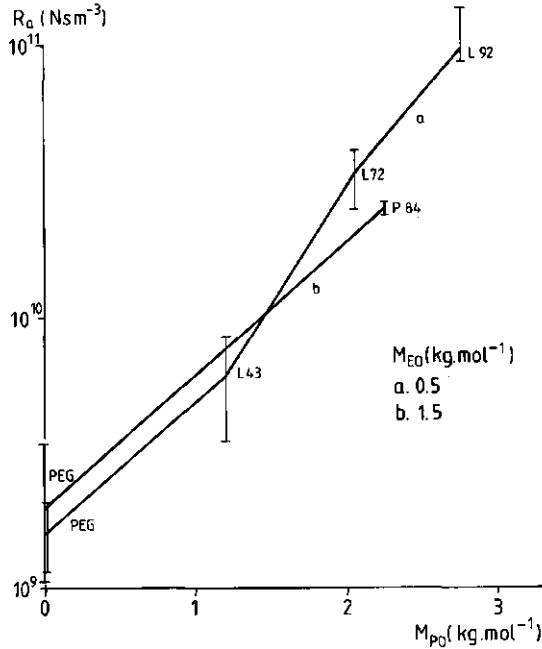


Figure 5. R_a as a function of the MM of the PO part (M_{PO}) in the EO/PO compound. The constant MM of the EO part (M_{EO}) is 0.5 and 1.5 kg mol^{-1} , respectively.

With regard to the interpretation of polymer adsorption on membranes it can be remarked that descriptions for clean and well-characterized surfaces and polymers are available or these data can be determined reliably. Nevertheless, the inferred parameters can not be applied to membranes, since the surface chemistry of membranes is usually not known, surfaces are rough and porous and the characterization in terms of pore sizes is still a controversial subject. Consequently, data for membranes are either not existing or, at least, not very reliable.

Because the parameters required for describing polymer adsorption are rather inaccessible in the case of membranes, it is worthwhile investigating more phenomenologically-oriented characterizations. Among these, the hydrophilic-lipophilic balance (HLB) based on the employment of group contributions [30], is most widely used.

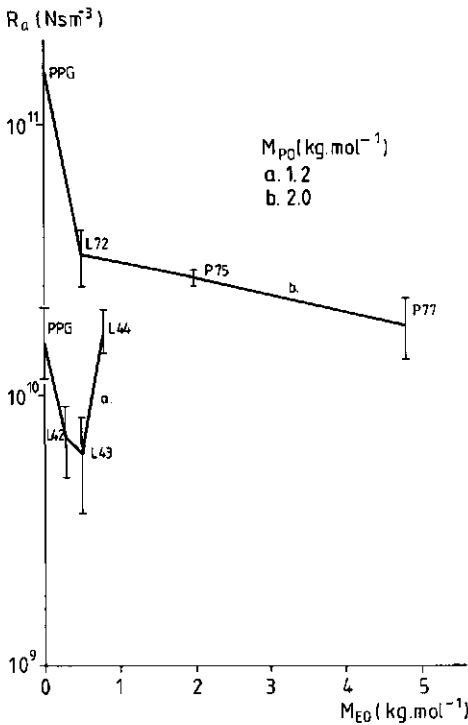


Figure 6. R_a as a function of the MM of the EO part (M_{EO}) in the EO/PO compound. The constant MM of the PO part (M_{PO}) is 1.2 and 2.0 kg.mol^{-1} , respectively.

In this study the HLB of the adsorbing EO end PO polymers is calculated as $7 + \Sigma(\text{hydrophilic group number}) - \Sigma(\text{hydrophobic group number})$, according to the most general formula (summation of group contributions [24]). Group numbers of 0.33 and -0.15 have been calculated for the EO and PO monomers, respectively.

Figure 7 gives the relation between R_a and HLB for the different compounds. For polymers with a comparable MM the R_a tends to decrease with increasing HLB, meaning with increasing hydrophilicity. No straightforward relation between HLB and R_a exists, however, as illustrated e.g. by the EO/PO block copolymers L92, L72 and PPG 400. Although they are characterized by almost the same HLB, their R_a on PSf is quite different. Apparently, the MM of the compounds is not sufficiently accounted for in the HLB to completely interpret the adsorption resistance on PSf. HLB does not give any information on the conformation of the EO/PO block copolymer in the solution nor at an interface like a polymeric membrane.

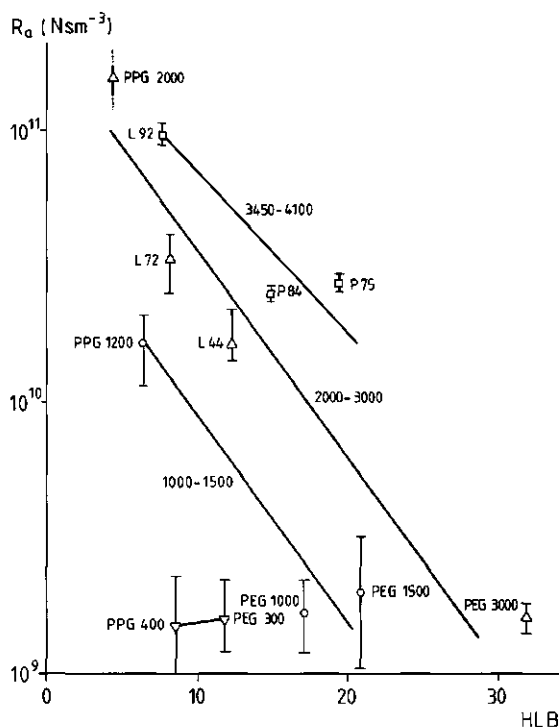


Figure 7. R_a as a function of HLB. Different lines refer to compounds of similar MM.

Nevertheless, the inference that at almost constant MM R_a tends to decrease with decreasing hydrophobicity and that increasing MM at constant HLB leads to an increase in R_a is useful. The degree of adsorption is determined by the hydrophobicity; the MM is determining the blocking of the membrane pores. Both aspects together determine the R_a .

It has to be concluded that the effect of the chemical nature of compounds and membranes is not yet well quantifiable. HLB is not the only intrinsic quantity to characterize the adsorption effect of EO and/or PO polymers on the GR61 PSf membrane. In view of the fouling problem it is thus important to develop other methods for elucidating the geometrical and chemical characteristics of the membrane surface. A first attempt, in which several surface-selective spectroscopical techniques are combined, has already been published [37].

2.3.2. Adsorption isotherms

The MB method assesses the external surface area of the membrane together with that in the pores that are accessible for MB molecules. Monolayer adsorption and the absence of dimerisation of MB molecules are assumed. Van den Boomgaard *et al.* [38] have shown that this technique is useful for membranes.

Two different experiments have been performed, one with the intact membrane (PSf and support layer) and one with the PSf layer only (the support layer can easily be removed). The intact GR61 membrane reveals a specific surface area of $2350 \pm 200 \text{ m}^2 \cdot \text{m}^{-2} \text{geo}$, the PSf layer alone of $1800 \pm 200 \text{ m}^2 \cdot \text{m}^{-2} \text{geo}$, indicating that MB adsorbs also on the support layer of GR61.

These results emphasize that the total surface area of membranes by far exceeds their geometrical value. The major part of the surface area is located in the porous structure (of the PSf layer and the support layer).

The adsorption isotherm of PPG 1200 on the PSf layer of the GR61 without support layer is shown in Figure 8, curve a. The adsorbed amount (Γ_a) increases gradually with the equilibrium PPG concentration ($[\text{PPG}]_{\text{eq}}$), but seems to level off. The adsorption isotherm for the complete GR61 membrane (Figure 8, curve b) is much steeper.

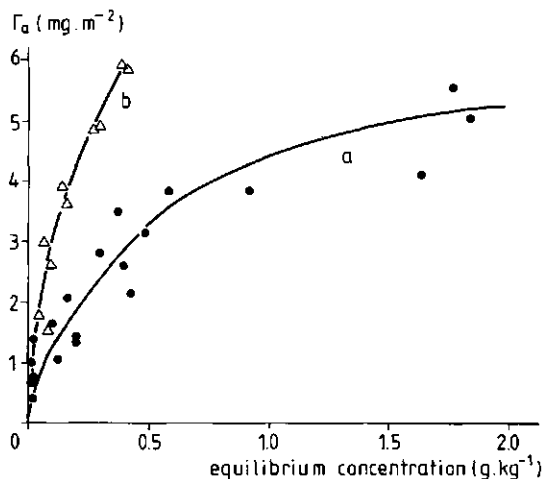


Figure 8. Adsorption isotherm for PPG 1200 a. PSf layer ($1800 \text{ m}^2 \cdot \text{m}^{-2} \text{geo}$), b. GR61 ($2350 \text{ m}^2 \cdot \text{m}^{-2} \text{geo}$).

In order to enable comparison with literature data both adsorption isotherms have been converted to isotherms of Γ_a' (the adsorbed amount per m^2 geometric surface area) as a function of $[PPG]_{eq}$. Although, strictly taken, Langmuir adsorption isotherms only apply for simple systems (no polymers) with homogeneous surfaces, for monolayer adsorption and for saturation at high concentration both data sets have been linearized according to the Langmuir isotherm $\Gamma_a' = (k_1' * [PPG]_{eq}) / (1 + k_2' * [PPG]_{eq})$ (Figure 9, curves GR61 and PSf). If it is assumed that Γ_a' for GR61 equals the sum of Γ_a' of the PSf layer and that of the substructure, the Langmuir isotherm for the PPG adsorption on the support layer can be calculated (Figure 9, curve sub). Table 4 summarizes the Langmuir characteristics for each layer.

By way of comparison, protein adsorption on membranes as measured by e.g. van den Boomgaard *et al.* [38], Matthiasson *et al.* [1, 3], Hanemaaijer *et al.* [39] and Brink and Romijn [6] can be considered. For the intact GR61 membrane for α -lactalbumin (α -la) Γ_a' max values of 1740 and 1100 $mg \cdot m^{-2} \cdot geo$ have been observed [39 and 6, respectively]. For β -lactoglobulin (β -lg) the reported values are in agreement, ca. 760 $mg \cdot m^{-2} \cdot geo$. The Γ_a' max values from literature [6, 39] are about 10 to 20 times lower than the maximum adsorbed amount of PPG 1200. PSf globules prepared by the phase inversion technique exhibited maximum protein adsorption densities of 3.2 and 2.9 $mg \cdot m^{-2}$ respectively (at a pH of ca. 5 (i.e. the IEP)) [39]. If it is assumed that the surface of the PSf globules is non-porous and exhibits the same adsorption

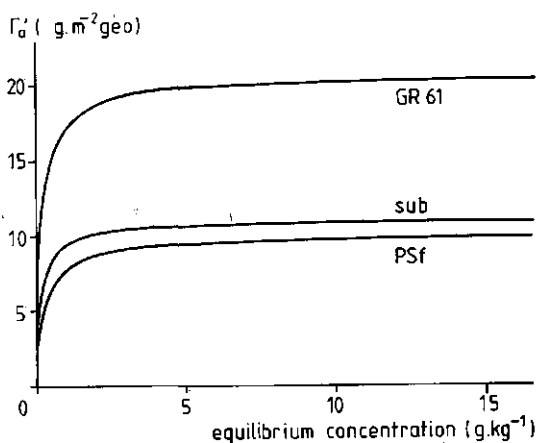


Figure 9. Constructed Langmuir adsorption isotherms for PPG on the intact GR61, the PSf layer and the sublayer.

Table 4. Langmuir characteristics for the complete GR61 membrane, the PSf layer alone and the substructure.

	GR61	PSf	sublayer
k_1' (kg.m ⁻² geo)	95.33	34.02	62.63
k_2 (kg.g ⁻¹)	4.6	3.4	5.7
Γ_a' max (g.m ⁻² geo)	21	10	11

characteristics as the flat sheet (membrane), the specific surface area of the GR61 membrane (PSf) can be calculated and compared to that obtained with MB in this study. Values of ca. 340 [6] and 550 [39] and of ca. 260 m².m⁻²geo are found for α -la and β -lg, respectively. These have to be compared with the ca. 2000 m².m⁻²geo obtained by the MB method. Apparently, the effective thicknesses of the adsorbed layer, a consequence of the MM of the adsorbants in combination with the solvent conditions, are such that the pores in GR61 are less accessible for β -lg than for MB and even more so for α -la. Also different pieces of GR61 can have different specific surface area.

Matthiasson *et al.* [3] measured a Γ_a' max of 30 mg.m⁻²geo for BSA on GR61 at pH 7, which is not the IEP. Even if it is taken into account that more BSA will adsorb at the IEP, that value is remarkably lower than usually observed for proteins. This may be due to BSA being a much larger molecule than α -la and β -lg, so that adsorption of BSA can not take place in the smaller pores of the GR61 membrane.

If the protein radius is approaching the pore radius, the largest part of the adsorption will be on the membrane surface, only a minor part taking place in the pores.

All specific surface area determination methods reveal values that are much higher than corresponding with the external surface only. Obviously PPG adsorption takes place on top of the membrane surface as well as in the pores of the PSf and of the support layer.

2.3.3. Adsorption resistance versus adsorbed amount

Figure 10 represents R_a of the complete GR61 membrane versus the adsorbed amount per geometrical surface area.

During the adsorption process the PPG 1200 has to diffuse through the PSf

layer before it reaches the support layer. However, the more effective narrowing of the smaller pores in the PSf layer than of those in the porous sublayer causes the flux to be controlled by the first. So adsorption in the pores of the support layer is not the determining factor of the R_a .

To further assess the importance of PPG adsorption with regard to flux decrease and membrane fouling, a better characterization of the (distribution of the) pores is desirable. This can be accomplished by selecting appropriate calibration compounds and permeation conditions [40]. If the membrane and its pores are characterized in this way, fluxes after adsorption and fouling can probably be predicted.

At all events, these permeation and adsorption experiments demonstrate that the performance of a membrane is dependent of the chemical and physical interactions occurring between the membrane itself and the solute.

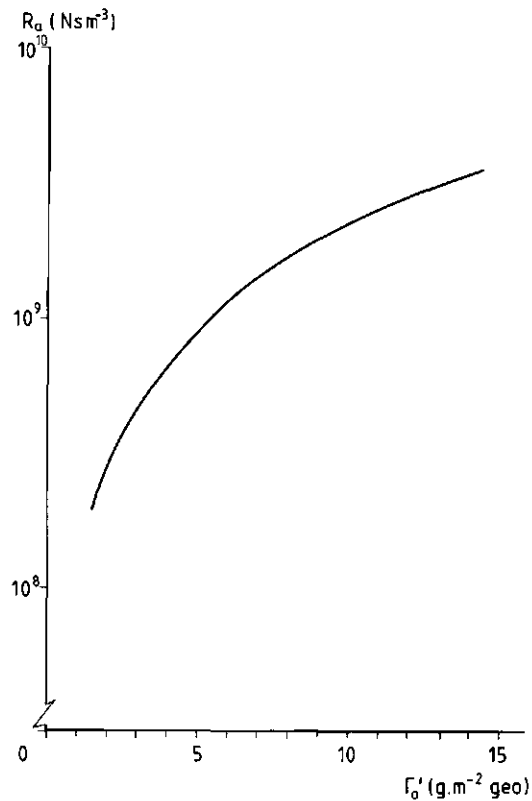


Figure 10. R_a as a function of the adsorbed amount of PPG 1200 for GR61.

2.4. CONCLUSIONS

From ultrafiltration experiments with several high-molecular compounds on various types of membranes it is obvious that sieving is only one aspect of the process. Probably even more important, adsorption phenomena as governed by the chemical nature of the membrane and the adsorbing compound determine the resistance to flow. This second aspect is not easily comprised in a characteristic parameter, however. Nevertheless, at constant MM, R_a tends to decrease with increasing HLB, illustrating that it can be most useful to have detailed knowledge on the physical chemical properties of the membrane surface and the compounds to be filtered.

The specific surface area, as determined by adsorption of MB reveals values of 2350 and 1800 $m^2 \cdot m^{-2} \text{geo}$ for the complete GR61 membrane and the PSf layer, respectively. These values are characteristic for highly porous materials. Adsorption of PPG 1200 on the PSf layer thus occurs to a lesser extent than on the intact GR61. Linearization of the experimental adsorption data according to a Langmuir-type isotherm reveals saturation at 10 and 21 $g \cdot m^{-2} \text{geo}$ respectively. The very porous support layer adsorbs to a greater extent than the skin and the more porous part under the skin of the PSf layer. PPG adsorption takes place on top of the membrane surface as well as in the pores of the membrane.

In the present case, the relation between R_a and Γ_a' is not linear, in contrast to what has been reported for other systems. Although the amount adsorbed in the support layer may be higher than in the PSf layer, the effect on the flux of the latter is dominant due to the smaller pores. Consequently, for a better understanding of fouling of ultrafiltration membranes, also knowledge of their porosity or PS(D) is of utmost importance.

ACKNOWLEDGEMENTS

The author would like to thank J.A.M. Stoots, M.F.J.M. Verhagen and M.A. Geluk for their contributions to this research.

REFERENCES

- 1 E. Matthiasson. The Role of Macromolecular Adsorption in Fouling of Ultrafiltration Membranes. *J. Membrane Sci.*, 1983, **16**, 23-36.
- 2 L.J. Zeman. Adsorption effects in Rejection of Macromolecules by Ultrafiltration Membranes. *J. Membrane Sci.*, 1983, **15**, 213-230.
- 3 E. Matthiasson, B. Hallström and B. Sivik. Adsorption Phenomena in Fouling of Ultrafiltration Membranes. In: *Engineering and Food. Volume 1.* Ed. B.M. McKenna. Elsevier, Amsterdam, 1984, 139-149. Proceedings from the Third International Congress on Engineering and Food, Dublin, Ireland, September, 1983.
- 4 A.S. Michaels, C.R. Robertson and H. Reihanian. Mitigation of Protein Fouling of Lipophilic Membranes by Presorption of Hydrophilic Polymers. The 1987 International Congress on Membranes and Membrane Processes, Tokyo, Japan, June 8-12, 1987.
- 5 P. Heinemann, J.A. Howell and R.A. Bryan. Microfiltration of Protein Solutions: Effect of Fouling on Rejection. *Desalination*, 1988, **68**, 243-250.
- 6 L.E.S. Brink and D.J. Romijn. Reducing the Protein Fouling of Polysulfone Surfaces and Polysulfone Ultrafiltration Membranes. Optimization of the Type of Presorbed Layer. *Desalination*, 1990, **78**, 209-233.
- 7 J.H. Hanemaaijer, T. Robbertsen, Th. van den Boomgaard and J.W. Gunnink. Fouling on Ultrafiltration Membranes. The Role of Protein Adsorption and Salt Precipitation. *J. Membrane Sci.*, 1989, **40**, 199-218.
- 8 P.M. van der Velden and C.A. Smolders. Solute/Membrane Interactions of Sodium Dodecyl Sulfate with Uncharged and Cation Exchange Membranes. *J. Colloid Interface Sci.*, 1977, **61**, 446-454.
- 9 L.M. Speaker and K.R. Bynum. Oriented Monolayer Assemblies to Modify Fouling Propensities of Membranes. In: *Physicochemical Aspects of Polymer Surfaces. Volume 2.* Ed. K.L. Mittal. Plenum Press, New York and London, 1983.
- 10 A.G. Fane, C.J.D. Fell and K.J. Kim. The Effect of Surfactant Pretreatment on the Ultrafiltration of Proteins. *Desalination*, 1985, **53**, 37-55.
- 11 L.M. Speaker. AFT (Anti Fouling Technology) for Membranes and Nonpermeable Surfaces. Proceedings of the Second International Conference on Fouling and Cleaning in the Food Processing, Madison, Wisconsin, July, 1985.
- 12 K.J. Kim, A.G. Fane and C.J.D. Fell. The Performance of Ultrafiltration Membranes Pretreated by Polymers. *Desalination*, 1988, **70**, 229-249.
- 13 F.-J. Müller, W. Krieger, W. Kissing and R. Reiner. Reduction on Membrane Fouling in Reverse Osmosis by Means of Surface Modifications of the Membranes. In: *Fundamentals and Applications of Surface Phenomena Associated with Fouling and Cleaning in Food Processing.* Eds. B. Hallström, D.B. Lund, Ch. Trägårdh. Työlösand, Sweden, April 6-9, 1981.

- 14 J. Wolff, H. Steinhauser and G. Ellinghorst. Tailoring of Ultrafiltration Membranes by Plasma Treatment and Their Application for the Desalination and Concentration of Water-Soluble Organic Substances. *J. Membrane Sci.*, 1988, **36**, 207-214.
- 15 J.-L. Nilsson. A Study of Ultrafiltration Membrane Fouling. PhD Thesis, Lund University, Lund, Sweden, 1989.
- 16 D.F. Gerson. Cell Surface Energy, Contact Angle and Phase Partition. I. Lymphocytic Cell Lines in Biphasic Aqueous Mixtures. *Biochimica et Biophysica Acta*, 1980, **602**, 269-280.
- 17 D.F. Gerson and J. Akit. Cell Surface Energy, Contact Angle and Phase Partition. II. Bacterial Cells in Biphasic Aqueous Mixtures. *Biochimica et Biophysica Acta*, 1980, **602**, 281-284.
- 18 W. Norde. Forces and Energies Involved in Adhesion and Adsorption. Adsorption of Biopolymers and Its relevance for Particle Adhesion: a Physico-Chemical Approach. In: *Bacterial Adhesion and Preventive Dentistry*. Eds. J.M. ten Cate, S.A. Leach and J. Arends. IRL Press Ltd., Oxford, England, 1984, 1-17.
- 19 M. Rosenberg. Bacterial Adherence to Hydrocarbons: a Useful Technique for Studying Cell Surface Hydrophobicity. *FEMS Microbiology Letters*, 1984, **22**, 289-295.
- 20 M.C.M. van Loosdrecht, J. Lyklema, W. Norde, G. Schraa and A.J.B. Zehnder. The Role of Bacterial Cell Wall Hydrophobicity in Adhesion. *Applied and Environmental Microbiology*, 1987, **53**, 1893-1897.
- 21 M.C.M. van Loosdrecht, J. Lyklema, W. Norde, G. Schraa and A.J.B. Zehnder. Electrophoretic Mobility and Hydrophobicity as a Measure to Predict the Initial Steps of Bacterial Adhesion. *Applied and Environmental Microbiology*, 1987, **53**, 1898-1901.
- 22 H.-C. Flemming and G. Schaule. Biofouling on Membranes - A Microbiological Approach. *Desalination*, 1988, **70**, 95-119.
- 23 A.W. Adamson. *Physical Chemistry of Surfaces*. Interscience Publishers, 1967, 2nd Ed.
- 24 D.W. van Krevelen and P.J. Hoftyzer. *Properties of Polymers. Their Estimation and Correlation with Chemical Structure*. Elsevier Scientific Publishing Company, Amsterdam, Oxford, New York, 1976.
- 25 M.A. Cohen Stuart, Th. van den Boomgaard, S.M. Zourab and J. Lyklema. The Layer Thickness of Adsorbed Nonionic Surfactants: Comparison between electrokinetic and Film Thickness Methods. *Colloids and Surfaces*, 1984, **9**, 163-172.
- 26 M.A. Cohen Stuart, F.H.W.H. Waajen T. Cosgrove, B. Vincent and T.L. Crowley. The Hydrodynamic Thickness of Adsorbed Polymeric Layers. *Macromolecules*, 1984, **17**, 1825-1830.
- 27 M.A. Cohen Stuart and J.W. Mulder. Adsorbed Polymers in Aqueous Media. The Relation between Zeta Potential, Layer Thickness and Ionic Strength. *Colloids and Surfaces*, 1985, **15**, 49-55.

- 28 R.F. Rekker and H.M. de Kort. The Hydrophobic Fragmental Constant; an Extension to a 1000 Data Point Set. *Eur. J. Med. Chem. - Chimica Therapeutica*, 1979, 14, 479-488.
- 29 K. Shinoda and H. Kunieda. Phase Properties of Emulsions: PIT and HLB. In: *Encyclopedia of Emulsion Technology*. Volume 1. Basic Theory. Ed. P. Becher. M. Dekker, Inc., New York and Basel, 1983, 337-367.
- 30 P. Becher. HLB - A Survey. In: *Surfactants in Solution*. Volume 3. Eds. K.L. Mittal and B. Lindman. Plenum Press, New York and London, 1984, 1925-1946.
- 31 Q.T. Nguyen, Ph. Aptel and J. Néel. Characterization of Ultrafiltration Membranes. Part I. - Water and Organic Solvent Permeabilities. *J. Membrane Sci.*, 1979, 5, 235-251.
- 32 M.A. Cohen Stuart. Flexible Polymers at a Solid-Liquid Interface. The Adsorption of Polyvinyl Pyrrolidone onto Silica. PhD Thesis. Agricultural University Wageningen, Wageningen, The Netherlands, 1980.
- 33 B.J.R. Scholtens. Copolymers at a Liquid-Liquid Interface and Their Retarding Effect on Mass Transfer between Both Phases. PhD Thesis. Agricultural University Wageningen, Wageningen, The Netherlands, 1977.
- 34 L.K. Koopal. Inference of Polymer Adsorption from Electrical Double Layer Measurements. The Silver Iodide - Polyvinyl Alcohol System. PhD Thesis. Agricultural University Wageningen, Wageningen, The Netherlands, 1978.
- 35 H.J. van den Hul. The Specific Surface Area of a Silveriodide Suspension. PhD Thesis, Rijksuniversiteit Utrecht, The Netherlands, 1966.
- 36 A. van den Boomgaard. The Effect of Electrolytes on Emulsions Stabilized by Nonionic Surfactants. PhD Thesis. Agricultural University Wageningen, Wageningen, The Netherlands, 1985.
- 37 M. Fontyn, B.H. Bijsterbosch and K. van 't Riet. Chemical Characterization of Ultrafiltration Membranes by Spectroscopic Techniques. *J. Membrane Sci.*, 1988, 36, 141-145.
- 38 Th. van den Boomgaard, T. Robbertsen, W. Versluis and J.H. Hanemaaijer. Membrane Fouling in Ultrafiltration of Dairy Liquids. *Membraantechnologie in Nederland*, 1986, 1, 42.
- 39 J.H. Hanemaaijer, T. Robbertsen, D.J. Romijn, Th. van den Boomgaard and L.E.S. Brink. Fouling of Ultrafiltration Membranes: Pore Narrowing Caused by Protein Adsorption. *Membraantechnologie in Nederland*, 1987, 2, 49.
- 40 M. Fontyn, J.-P. Vincken, K. van 't Riet and B.H. Bijsterbosch. Pore Size Distribution Measurements of Pristine and Fouled Membranes: Method Development, Membrane Characterization and Adsorption Mechanism. Chapter 3 of this thesis, to be published.

CHAPTER 3

PORE SIZE DISTRIBUTION MEASUREMENTS OF PRISTINE AND FOULED POLYSULFONE MEMBRANES: METHOD DEVELOPMENT, MEMBRANE CHARACTERIZATION AND ADSORPTION MECHANISM

ABSTRACT

Dextrans were selected to characterize the pore size distributions of pristine and fouled polysulfone membranes in terms of retention curves. The measurements were standardized such that adsorption, configuration and concentration polarization effects were minimized.

To convert retention curves into pore size distributions (PSDs) a simple model is employed. It assumes that the Hagen-Poiseuille relation holds, that pore blocking by dextran is excluded, that a homogeneous solution is present above the membrane and that the PSDs show a long tail Lorentz distribution.

The reproducibility of the PSD for any particular piece of DDS GR61 PP membrane is very good, whereas large variations are observed among different pieces of membrane. The implication is that data on fouled membranes always have to be related to those of the same sample in the pristine state.

Adsorption of polypropylene glycol (PPG) results in an alteration of the PSD: the centre shifts towards larger pores, the distribution becomes wider and the total number of pores decreases. Small pores are supposedly blocked by PPG and become excluded from permeation, whereas pores of intermediate size do not seem to be affected. PPG adsorption inside the large pores causes pore narrowing and flux reduction. It can be concluded that PPG adsorbs on top of the polysulfone membrane as well as on the walls inside the larger pores.

3.1. INTRODUCTION

The literature on fouling of ultrafiltration membranes strongly emphasizes the engineering aspects of the phenomenon. Observed flux declines are usually described in terms of such models as only comprising empirical parameters. Attempts to understand the molecular background and to relate aspects of physical and polymer chemistry with the process descriptions, however, gradually emerged during the last few years [1-4]. Better characterization of

the membranes has become an important issue in this approach. Especially physical and chemical characterizations of pristine and fouled membranes are very useful in this respect.

Physical characterization in terms of molecular mass cut-off (MMCO) determination and pore size (PS) or pore size distribution (PSD) measurements, has received detailed attention in literature [5-9]. However, MMCO data, usually provided by the manufacturers, appear to be less useful in this respect. A membrane can be characterized by its PS(D), e.g. by using N₂ adsorption-desorption pore volume determination, thermoporometry, Hg porosimetry and permeation of macrosolutes. Many factors, such as drying of the membrane and the process conditions during the permeation, can affect the results and should be taken into account. Therefore, the experimental method, the calibration compounds and the process conditions must be reported together with the results. This problem has already duly been elaborated in literature [10-17].

In this paper the physical characterization of pristine DDS GR61 PP polysulfone (PSf) ultrafiltration membranes as well as of these membranes being fouled by adsorption of polypropylene glycol (PPG) is reported. This characterization was accomplished by permeation of macrosolutes (dextrans). The chemical characterization of these fouled and pristine membranes has been accomplished by surface spectroscopy [18, 19]. The first objective of this study is to select a proper macrosolute and to standardize the process conditions for the PSD measurements. The macrosolute has to be usable for the pristine as well as for the PPG fouled membranes. The second objective is to get a better understanding of the physical mechanism of fouling by adsorption on the membrane by modelling the PSD change.

3.2. SELECTION OF THE CALIBRATION COMPOUND

It is obvious that the calibration compounds have to meet strict requirements. Preferably the compound is monodisperse or has at least a well known molecular mass distribution (MMD) (a). It must be applicable as received from the manufacturer, rather than having to spend time in purifying and characterizing the compound. It must be readily available in a wide range of molecular mass (MM) and at acceptable prices (b). Furthermore, it should not form aggregates (c), has to be of a rigid spherical form (d) and should not show affinity for the membrane (e). These last three requirements can be largely met by choosing the appropriate solvent and proper process conditions.

If membranes fouled with an adsorption layer have to be characterized, an additional requirement is that the calibration compound should not show any affinity for the foulant on the membrane (f). Several possible calibration compounds have been considered, such as proteins, dextrans, polyethylene oxide (PEO), polyvinyl pyrrolidone (PVP), polyvinyl alcohol (PVA) and polyvinyl acetate (PVAc).

(a) (b) Molecular Mass Distribution, Availability

Only proteins are monodisperse, the other compounds showing various degrees of polydispersity (as expressed in M_w/M_n , mass averaged MM/number averaged MM). PEO standards for HPLC, e.g., show an M_w/M_n of ca. 1.1. These standards are very pure, but costly. Other, more bulky, PEOs have broad MMDs (M_w/M_n in the order of 10-100) and contain impurities. Dextrans are available in different MMDs, with polydispersities ranging from 1.5 to 20 and at acceptable prices. Due to these reasons PEO has not been selected.

(c) Association

Globular proteins sometimes show association behaviour, as has also been observed for PEO and PVP. Polyethylene glycol 20000, e.g., associates to clusters of 100 molecules or more if the temperature is raised [20]. On the other hand, at low concentration polarization levels and under favourable conditions for fractionation no significant physical interactions are observed between dextrans of similar size [21, 22]. Association and dissociation phenomena of dextrans can also be prevented by employing dilute salt solutions [23, 24]. For dextrans with MM larger than 2000, the χ interaction parameter of the polymers with water is strongly dependent on concentration, but almost independent of the MM of dextran [24]. For these reasons PVP and PEO have not been used as the calibration compound.

(d) Rigid Spheres

If proteins were to serve as calibration compounds, they must be globular in order to behave as rigid spherical molecules in the filtration. For each protein with a specific MM, the appropriate solvent quality conditions would have to be established separately, as well as several experiments would have to be performed to obtain the whole retention curve.

Literature about solvent quality [25, 26] and molecule structure [24, 27] does indicate that dextran molecules (5% branched via α -(1 \rightarrow 3)-linkages) can be regarded as spheres. Dextran conformation in solution is essentially unaffected by addition of electrolytes, at least at 25°C [28]. Solutions of hydrolyzed dextrans are Newtonian and do not show flow birefringence. Dextran T70 and T40 (Pharmacia Fine Chemicals) do not exhibit any orientation under flow conditions at 0.5% (m/m) in water [29]. Although at high pressures deformation can possibly occur [16], at pressures below $0.1 \cdot 10^5$ Pa no deformation is observed [30]. For the present purpose dextrans can be considered to behave as hard spheres.

(e) Adsorption

Because we aim at pore size determination of PSf membranes, the calibration compounds should not adsorb onto this material under ultrafiltration conditions. It is well-known that proteins do exhibit high adsorption resistances on PSf, due to their amphiphilic character [2, 31, 32]. Dextrans do not reveal any adsorption on a hydrophobic material such as polycarbonate Nuclepore membranes [30]. It is therefore expected that dextran will not adsorb on PSf.

(f) Affinity for Foulant

The calibration compound selected for PSD determination must not interact with the adsorbed PPG layer either. The most appropriate calibration compound will thus have to be essentially hydrophilic, because PPG is hydrophobic. In this respect dextran is a better compound than proteins.

In view of the considerations presented in this section, dextran was selected as the most suitable calibration compound.

3.3. MATERIALS AND METHODS

3.3.1. Ultrafiltration

Membrane

De Danske Sukkerfabrikker (DDS) GR61 PP membranes, made up of Udel PSf (polyethersulfone + bisphenol A) [33], were investigated. The support layer of these membranes consists of cellulose. The MMCO value as quoted by the manufacturer is 20000 g.mol^{-1} . The experimentally measured pure water membrane resistance R_m can range from 0.4 to $1.3 \cdot 10^{10} \text{ Nsm}^{-3}$. Further information on the chemical structure can be found in Fontyn *et al.* [18].

Calibration Compound

Dextran is a biopolysaccharide produced by *Leuconostoc mesenteroides* strain B512 [34, 35]. The MMDs for the different T fractions as provided by the manufacturer (Pharmacia Fine Chemicals, Uppsala, S) were used (Table 1).

Table 1. Properties of dextran fractions. Mass averaged MM (M_m) and number averaged MM (M_n) in $\cdot 10^3 \text{ g.mol}^{-1}$, intrinsic viscosity $[\eta]$ (20°C) in ml.g^{-1} .

Dextran	M_m	M_n	$[\eta]$	M_m/M_n
T10	9.9	5.7	9.0	1.74
T20	22.3	15.0	14.8	1.49
T40	35.6	19.8	19	1.80
T70	73.4	42.4	26	1.73
T110	101.0	62.0	31	1.63
T2000	1751.0	305.8	70	5.73

Foulant

Polypropylene glycol (PPG) (Fluka AG, Buchs, CH, 81370) with an average MM of 1200 was used. PPG can be considered a model compound for an anti-foaming agent, having hydrophobic properties but being soluble in water.

Adsorption Procedure

A pristine GR61 PSf membrane was tightened in a cell and exposed to a 1 g.kg^{-1} aqueous solution of the compound at 25°C . After 24 hours the solution was replaced by pure water, allowing the measurement of the overall resistance, which equals the sum of R_m and the adsorption resistance R_a .

Permeation Procedure

A GR61 PSf membrane, either or not fouled, was installed in an Amicon (Grace, Danvers, MA) stirred cell type M8400, with an effective membrane area of $4.18 \times 10^{-3} \text{ m}^2$. Total volume amounted to 350 ml and the stirrer speed was kept constant. Pressure was controlled by a manometer. Flow was continuously measured.

3.3.2. Gel Permeation Chromatography

Columns

The MMDs of the ultrafiltered dextran fractions were assessed by employing Bio-Gel® TSK 40-XL and TSK 30-XL gel filtration HPLC columns in series (7.8 × 300 mm) (Bio-Rad, Richmond, CA) [36]. As a guard column, Bio-Gel® TSK Guard was installed between injection and columns. The volume of the total system is 22.1 ml, the void volume is 11.7 ml.

Elution Procedure

Samples of 20 μl were injected (Knauer, Berlin, D, injection valve) and transported to the columns at $1.0 \text{ ml}\cdot\text{min}^{-1}$ (Knauer HPLC pump type 64.00). Detection of the signal after separation (30°C) was established by a refractive index detector at 40°C (Erma Optical Works Ltd, Tokyo, Japan, type ERC 7510). The elution liquid was a 0.05 M potassium acetate (KAc) (Merck, Darmstadt, D, Art 4820) / acetic acid (HAc) (id., Art 58) buffer with a pH of 5.0.

Data were processed, via an integrator (SP 4290, Spectra Physics, San Jose, CA), in a PC.

3.4. SELECTION OF PROCESS CONDITIONS

The conditions for dextran permeation must be such that no adsorption on the PSf membrane (membrane resistance unaltered by adsorption) and no deformation of dextrans take place and that concentration polarization levels are kept at a minimum. The selection was performed on the basis of experimental measurements of the different parameters, as given below.

3.4.1. Adsorption

Molecular Mass (Distribution)

The adsorption and ultrafiltration resistances R_a and R_{uf} of Dextran T fractions of various MM are compared in Figure 1. R_a (insert) is almost equal for the different fractions. The average R_a of $2.8 \cdot 10^9 \text{ Nsm}^{-3}$ ($\pm 1.0 \cdot 10^9$) is only a small addition to the pure water membrane resistance R_m of $10.3 \cdot 10^9 \text{ Nsm}^{-3}$. The flow through the GR61 membranes is thus hardly affected by the adsorption of any Dextran T. However, this increase in resistance will change the pore size distribution (PSD) to a small extent. The ultrafiltration on the other hand is obviously influenced by the size of the dextrans. To prevent the influence of adsorption during retention measurement only the first few ml of permeate, thus only two or three minutes permeation, were used. Adsorption can be ignored during this short period of time.

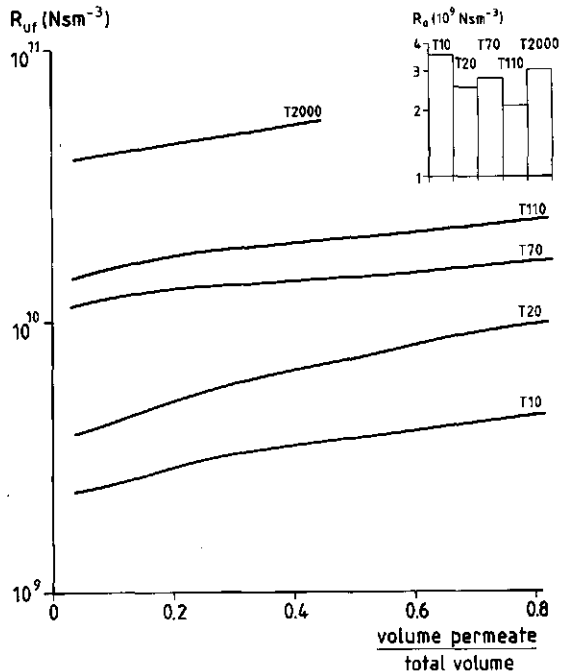


Figure 1. R_a and R_{uf} as a function of relative permeate volume for different Dextran T fractions.

Because the manufacturer estimates the MMCO value of the GR61 at 20000 g.mol^{-1} , for the PSD measurement a mixture of dextrans with MMDs ranging around this value must be selected. To cover the whole pore size range a

mixture of Dextrans T10:T40 in a ratio of 2:3 (mm) was chosen. The MM ranges between 5000 and 100000 g.mol⁻¹, covering dextran Stokes radii between ca. 1.8 and ca. 8.4 nm [21, 22, 24].

pH and Ionic Strength

Gel permeation chromatography (GPC) or size exclusion chromatography (SEC) of dextrans require ionic strengths (I) lower than 0.1 M and a pH of ca. 5 [37, 38]. In this way adsorption of dextrans on the column matrix is avoided and any acidic fractions of the dextrans are eluted at the same elution volume or MM as the neutral fractions. In view of the GPC analysis a KAc / HAc buffer of I = 0.05 M at pH = 5 is selected as the solvent in the PSD measurement [38]. These solvent conditions do not affect R_a and R_{uf} and therewith the result of the PSD measurement.

Temperature

All experiments were performed at 25°C.

Concentration

Although ultrafiltration resistances increase immediately even at low concentration values, the adsorption resistance is only affected at concentrations higher than 2 g.kg⁻¹. An optimal concentration of the dextran solution would be one that is lower than 2 g.kg⁻¹.

3.4.2. Concentration Polarization and Deformation

Concentration and Pressure

Table 2 illustrates that the ultrafiltration resistance increases at increasing pressures which might be due to concentration polarization and dextran deformation. However, the pressure used during adsorption measurement does not significantly affect the adsorption capacity of T70 on PSf.

At constant concentration and fixed MM, lowering the pressure difference reveals an increased retention and a steeper retention curve (Figure 2). At a constant pressure of 0.1 *10⁵ Pa, decreasing the concentration from 5 to 1 g.kg⁻¹ also causes a steeper retention curve and a shift towards higher retentions. At a pressure of 0.5 *10⁵ Pa, however, alterations in the retention curve are not significant (Figure 2). The corresponding ultrafiltration resistances increase with increasing concentration and pressure.

Table 2. R_a and R_{uf} (at volume permeate/total volume = 0.3) of GR61 at different transmembrane pressures ΔP . Dextran T70; $c = 1 \text{ g.kg}^{-1}$; $\text{pH} = 7$; $I = 0$; $R_m = 5.04 \cdot 10^9 \text{ Nsm}^{-3}$.

	$\Delta P (\cdot 10^5 \text{ Pa})$					
	0.1	0.5	1.0	1.5	2.0	4.0
R_a ($\cdot 10^9 \text{ Nsm}^{-3}$)	0.54	0.01	1.40	0.98	0.66	1.52
R_{uf} at $V_p/V_t=0.3$ ($\cdot 10^9 \text{ Nsm}^{-3}$)	1.44	1.53	3.06	4.92	7.35	20.50

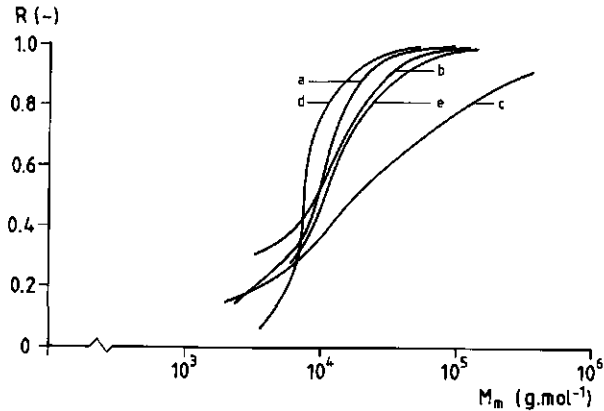


Figure 2. Retention (R) curve of GR61 for the dextran mixture under different conditions of concentration and pressure (g.kg^{-1} and $\cdot 10^5 \text{ Pa}$ respectively) a. $C=5 / \Delta P=0.1$, b. $C=5 / \Delta P=0.5$, c. $C=5 / \Delta P=1.0$, d. $C=1 / \Delta P=0.1$ and e. $C=1 / \Delta P=0.5$.

From these results it ensues that pressure and concentration must be as low as possible. Considering detection limits and the accuracy in pressure control, a pressure of $0.5 \cdot 10^5 \text{ Pa}$, and due to accuracy in GPHPC a dextran concentration of 5 g.kg^{-1} were finally selected.

3.4.3. Selection of conditions

Table 3 summarizes the conditions selected in retention measurements.

Table 3. Standardized process conditions for retention measurement.

Calibration compound	mixture of Dextran T10 and T40 in a ratio of 2:3 (m:m)
Concentration	5 g.kg ⁻¹
Temperature	25°C
Solvent	KAc / HAc
pH	5.0
I	0.05 M
ΔP	0.5 *10 ⁵ Pa

The first 3 ml of the dextran permeate through the GR61 was always discarded. A subsequent sample of 5 ml was collected and analysed by HPGPC to determine the MMD of the permeated dextrans.

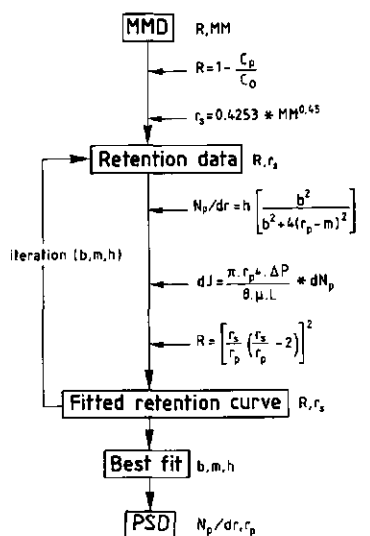
3.5. MODELLING OF PORE SIZE DISTRIBUTION

In studying membrane fouling it is of utmost importance to trace the narrowing or blocking of pores, the corresponding shift in pore sizes and the alteration of the membrane surface. This can be accomplished by the conversion of observed retention curves into PSDs, a process that requires models for the flux decrease and for the physical structure of the membrane. The choice of these models is not really critical, since we are dealing only with the relative differences between pristine and fouled membranes.

Therefore, the following simple assumptions have been made. The flow through a pore is proceeding according to Hagen-Poiseuille [39], corresponding with cylindrical pores of a length equal to the thickness of the active membrane layer. Hydrodynamic lag (steric hindrance) is accounted for according to Ferry [40], excluding the effects of adsorption and of pore blocking by the calibration compound and assuming a homogeneous solution above the membrane. The overall retention of dextran molecules of a given size through pores of different sizes is the weighted sum of the retention coefficients through all pore sizes separately. The pore sizes are supposed to be long tail Lorentz distributed [41].

For the conversion of the MM of dextrans into effective hydrodynamic radii r_s (effective radii for pore penetration) several equations exist. Kassotis *et al.* [42], using the results of Granath [21], formulated r_s (Å) = 0.4253 * MM^{0.45}. This equation is valid for dextrans in water at 20°C. Basedow *et al.* [23] established that the effective hydrodynamic radius (radius for pore penetration) complies with the equation r_s (Å) = 0.115 * MM^{0.581} (water and dilute salt concentrations, 25°C). Significant differences between both equations only show up for MMs exceeding 10⁵, values that were not involved in this study. For convenience reasons the equation of Kassotis *et al.* has been used.

Figure 3 schematizes the consecutive steps in the calculation of the PSD from the MMDs generated from GPC and the retention data.



C_p concentration permeate	C_0 concentration mixture
b width at half height	m centre
h height	μ viscosity
L pore length	J flow

Figure 3. Scheme of the elaboration from MMDs to PSD.

3.6. RESULTS

3.6.1. Pristine membranes

Typical retention data from repeated measurements of a GR61 PSf membrane have been fitted according to the scheme given in Figure 3. The best fit (Figure 4) reveals a Stokes radius at $R = 0.5$, $r_{s,0.5}$, of 2.65 nm. The shape of the curve can be characterized by σ , the mathematical mean of the Stokes radii at retentions 0.25 and 0.75. It gives an impression of the steepness of the retention curve. For the typical curve in Figure 4, σ is 2.93 nm.

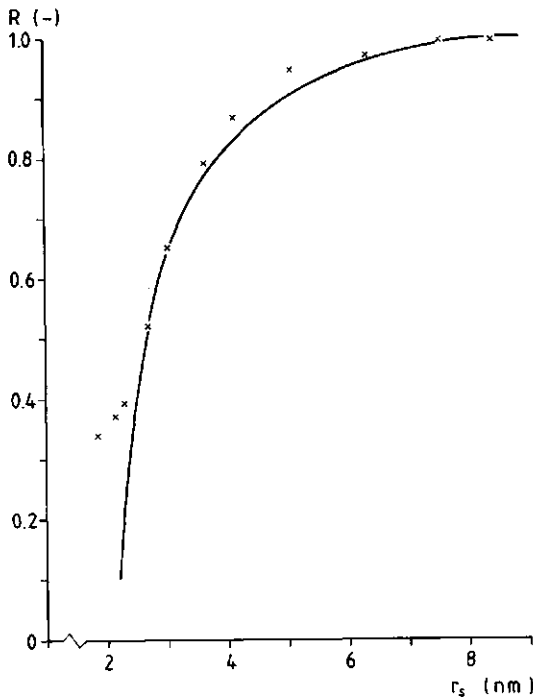


Figure 4. Experimental and fitted retention curve for a pristine GR61. $J_m = 3.49 \cdot 10^{-6} \text{ m.s}^{-1}$.

Conversion of the best fit into a PSD (Figure 5) shows a distribution around 3 nm and a width at half height, b , of 0.5 nm. The maximum frequency of the number of pores $N_p(\text{max})/dr$ in this particular membrane at $3 (\pm 0.05) \text{ nm}$ is $1.2 \cdot 10^{12} \text{ nm}^{-1}$. The total number of pores $N_p(\text{total})$ is calculated by integrating the PSD from 0 to 10 nm and appears to be $9.1 \cdot 10^{12}$, corresponding to $2.2 \cdot 10^{15} \text{ pores.m}^{-2}$.

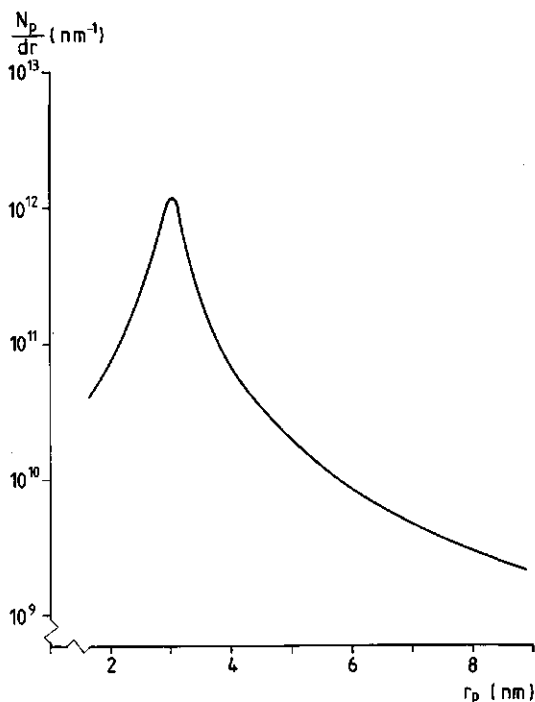


Figure 5. PSD for a pristine GR61.

Comparison of the obtained PSD with literature data for the same type of membrane is hardly possible. Only Hanemaaijer *et al.* [32] obtained a "characteristic" pore size (r_p^* , their own definition) of ca. 9 nm, which is of the same order of magnitude. However, using the overall flux and the mentioned r_p^* , this corresponds with a N_p^* (total) of $2.7 \cdot 10^{18}$ pores.m⁻², which is a factor 1000 higher than calculated according to our model. In their analysis, another piece of membrane and other calibration compounds and process conditions were used. Moreover, other assumptions were made in calculating the PS(D). These results for the pristine membrane illustrate that they should only be interpreted relatively, in combination with those for the fouled membrane.

The inaccuracy in the measurement of the retention coefficient of a given membrane (same type, same batch, same cut) is ± 0.08 , meaning that no significant differences in the best fit for the retention curve are obtained. Consequently, the PSD of one piece of membrane appeared to be reproducible.

In contrast, different pieces of membrane of the same type and batch can

exhibit large flux differences. Also large variations in the retention coefficients are observed, in the range of ± 0.23 , resulting in other best retention fits and thus other PSDs. Regarding the search for differences in PSD between pristine and fouled membranes, these results emphasize that for each fouled membrane, the pristine situation has to be examined first.

3.6.2. Fouled Membranes

A pristine GR61 membrane after having been contacted with a PPG solution exhibits an additional adsorption resistance R_a of $1.20 \cdot 10^9 \text{ Nsm}^{-3}$ on top of the pure water membrane resistance of $5.05 \cdot 10^9 \text{ Nsm}^{-3}$ (Table 4).

Table 4. Flux, retention and PSD characteristics for the pristine as compared to the PPG-adsorbed GR61.

	Pristine	Adsorbed
Flux (m.s^{-1})	$9.9 \cdot 10^{-6}$	$8.0 \cdot 10^{-6}$
Retention (fit)		
$r_{s,0.5}$ (nm)	3.26	2.97
σ (nm)	3.45	3.15
Pore size distribution		
centre, m (nm)	2	4
width at 1/2 height, b (nm)	1.0	1.5
$N_p(\text{max})/dr$ (nm^{-1})	$2.7 \cdot 10^{12}$	$2.6 \cdot 10^{11}$
$N_p(\text{total})$ (pores.m^{-2})	$9.2 \cdot 10^{15}$	$1.3 \cdot 10^{15}$

The adsorption of PPG causes a shift in retention as shown in Figure 6. Some characteristics of the best fit to this typical data, taken from repeated measurements, are given in Table 4. The dextran size at half retention, $r_{s,0.5}$, shifts from 3.26 nm for the pristine to 2.97 nm for the fouled membrane. The retention curve becomes slightly steeper than that of the pristine membrane (σ changes from 3.45 to 3.15 nm).

Typical PSD characteristics for both membranes are given in Figure 7 and summarized in Table 4. The centre of the distribution, m, changes from 2 to 4 nm and the width at half height, b, from 1.0 to 1.5 nm. Due to PPG adsorption the smaller pores in the pristine membrane are largely excluded from permeation, whereas access to the larger pores becomes restricted. The total number of accessible pores drops from $9.2 \cdot 10^{15} \text{ pores.m}^{-2}$ in the pristine

membrane to $1.3 \cdot 10^{15}$ pores. m^{-2} in the coated membrane.

A GR61 PSf membrane fouled by β -lactoglobulin at its IEP (pH = 4) has been characterized [32] by a "characteristic" pore size r_p^* of 2.5 nm. This means that also in this case a strong pore narrowing as compared to the pristine membrane has occurred. Calculating (with the overall flux of that membrane and the mentioned pore size) the total number of pores of that size amounts to $N_p^*(total) = 5.2 \cdot 10^{19}$ pores. m^{-2} , showing it to be higher than the N_p^* of the pristine membrane at the r_p^* of 9 nm.

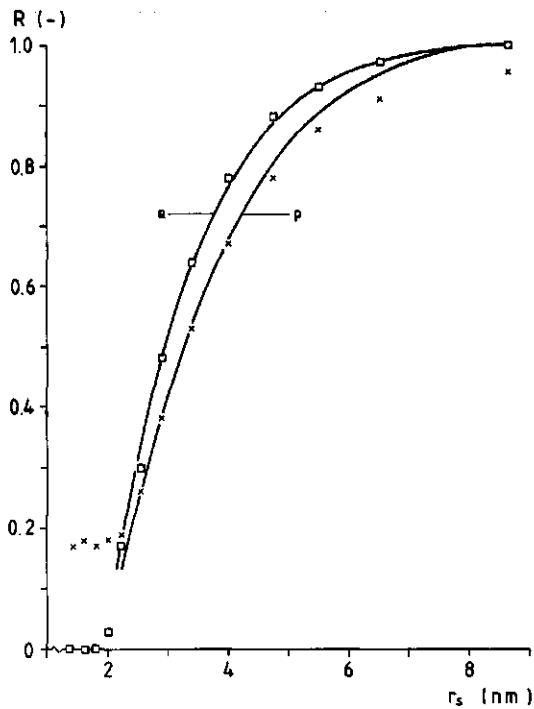


Figure 6. Experimental and fitted retention curve for the pristine (p) and PPG-adsorbed (a) GR61. $J_m = 9.9 \cdot 10^{-6}$ $m.s^{-1}$; $J_{m+a} = 8.0 \cdot 10^{-6}$ $m.s^{-1}$.

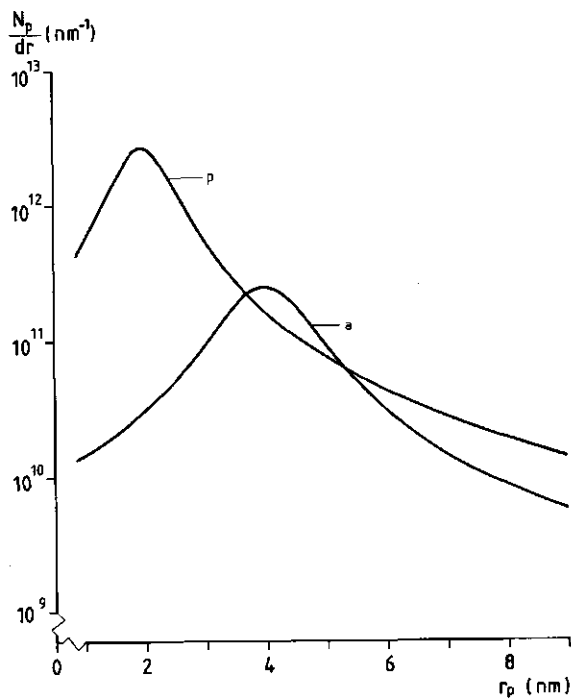


Figure 7. PSD for the pristine (p) and PPG-adsorbed (a) GR61.

3.7. DISCUSSION - MECHANISM OF ADSORPTION

An explanation for the effect of adsorption on PSD is schematized in Figure 8. The PSD is roughly divided in small (category I), intermediate (category II) and large pores (category III). PPG starts to be adsorbed on the membrane surface. Pores of category I are too small for PPG to penetrate and thus to permeate or to get adsorbed onto the pore wall. The PPG molecules are adsorbed around and entrapped in the pore opening, but are probably not swept away by water (and dextran) molecules during the flux (and retention) measurement. The PPG molecules thus definitely block these pores and exclude them from contributing to the flux. These pores give maximum retention.

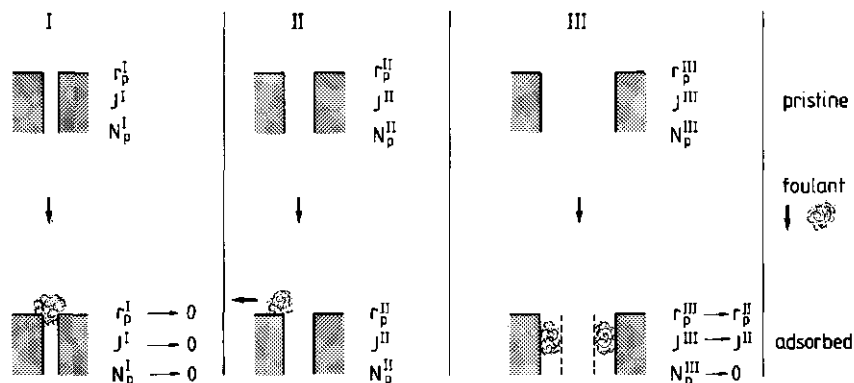


Figure 8. Schematic representation of the processes proceeding in the different pore size ranges in a pristine and a fouled membrane.

Adsorption around the pore opening leads to a pore entrance narrowing that prevents PPG molecules from permeating into the pores of category II during the adsorption experiment. Therefore no adsorption takes place onto the pore wall. However, during flux and retention measurement the water and dextran molecules can sweep away those molecules that are only partially adsorbed around the pore opening at just a few sites. During measurement water and dextran molecules permeate undisturbed through these pores. Flux and retention exhibited by these intermediate pores is thus equal in the pristine and the fouled membrane.

The large pores of category III are completely penetrable for PPG molecules, which can adsorb onto the pore wall. During flux and retention measurement these molecules are not swept away by the water and dextran molecules. Due to the adsorption the pore size shifts to smaller values, so that pores of category III in the pristine membrane are reduced to a lower category in the fouled membrane. The number of pores of category III and thus their contribution to the flux in the fouled membrane diminishes.

Figure 7 can be interpreted in terms of this adsorption model. On the basis of (extrapolated) intrinsic viscosity data and the disc-coil model configuration the PPG molecule can be characterized by an overall size of 2 to 3 nm radius (r_{PPG}) [43]. No unfolding upon adsorption is assumed.

On the basis of an adsorption model that only comprises pores of category I and III, Figure 9a is generated, based on curve p in Figure 7. It results in a continuously decreasing PSD with increasing pore radius. This model can not explain the observed maximum and the partially higher N_p/dr than in the pristine membrane.

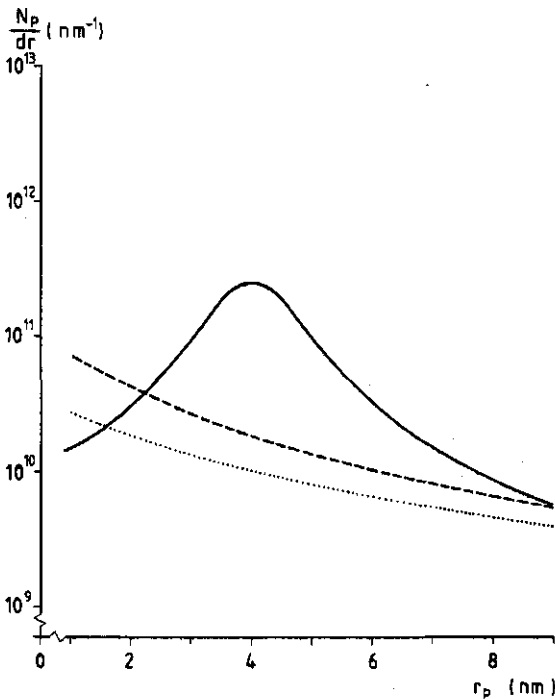


Figure 9a. Experimental (full line) and modelled PSD without category II pores (dashed line $r_{ppG} = 2$ nm, dotted line $r_{ppG} = 3$ nm) for GR61 with adsorbed PPG.

In Figure 9b the existence of category II pores is incorporated, with $r_p < r_{ppG}$ for category I, $r_{ppG} < r_p < 2r_{ppG}$ for category II and $r_p > 2r_{ppG}$ for category III pores with a pore narrowing of $2r_{ppG}$. The generated PSD better reflects the experimental data: a maximum, a wider PSD and a higher number of pores per dr than in the pristine membrane PSD may be obtained. This adsorption model gives a much better approximation of the experimental PSD than the simplified one given in Figure 9a.

More accurate knowledge on the size of the PPG would be necessary to refine the model. Possibly, the incorporation of the different ranges of the repulsive forces between PPG and PSf and between dispersed and adsorbed PPG will improve the estimation of the observed PSD. Multilayer PPG adsorption on a PSf pore wall that is already covered by a monolayer could be another refinement.

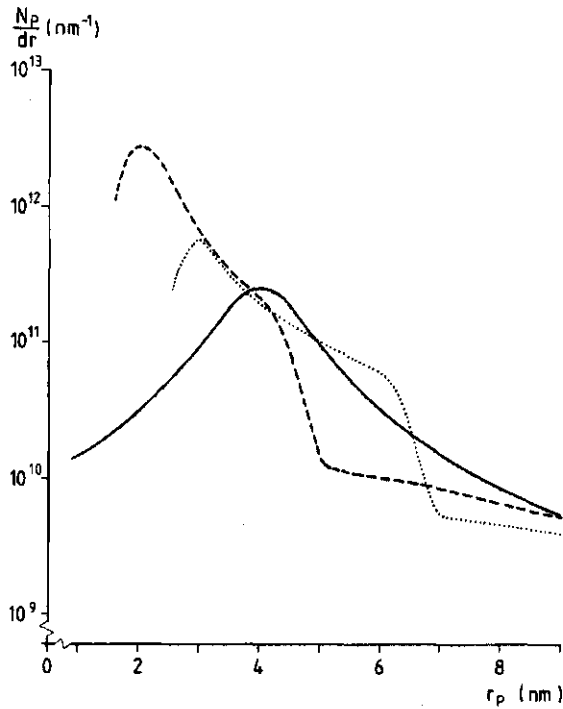


Figure 9b. Experimental (full line) and modelled PSD with category II pores (dashed line $r_{ppG} = 2$ nm, dotted line $r_{ppG} = 3$ nm) for GR61 with adsorbed PPG.

If a difference in pore narrowing for category III pores is assumed for $2r_{ppG} < r_p < 3r_{ppG}$ and $r_p > 3r_{ppG}$ ($r_p - r_{ppG}$ and $r_p - 2r_{ppG}$, respectively), the resultant PSD (Figure 9c) even better estimates the higher N_p/dr . The assumption originates from the fact that only one PPG molecule can enter the smallest pores of the category III, resulting in unsaturated adsorption (not fully packed adsorption layer).

For the experimental data in Figure 7 the following conclusions can be drawn.

In the range of about 5.5 nm and up, in the fouled membrane N_p^{III} has decreased. The corresponding curve lies below the curve for the pristine membrane in this pore radius range. Below about 5.5 nm the sum of the narrowed pores of category III and the unaltered pores of category II causes the occurrence of a higher number of pores in the fouled membrane PSD as compared to the pristine form. Unsaturated adsorption in pores of radii smaller than circa 5.5 nm, present in the pristine membrane, together with pores of

category II causes the fouled membrane PSD to show a maximum that can be higher than that of the pristine membrane. Together with the blocked pores of category I a declining region at smaller pore radii occurs. Here curve a lies considerably below curve p.

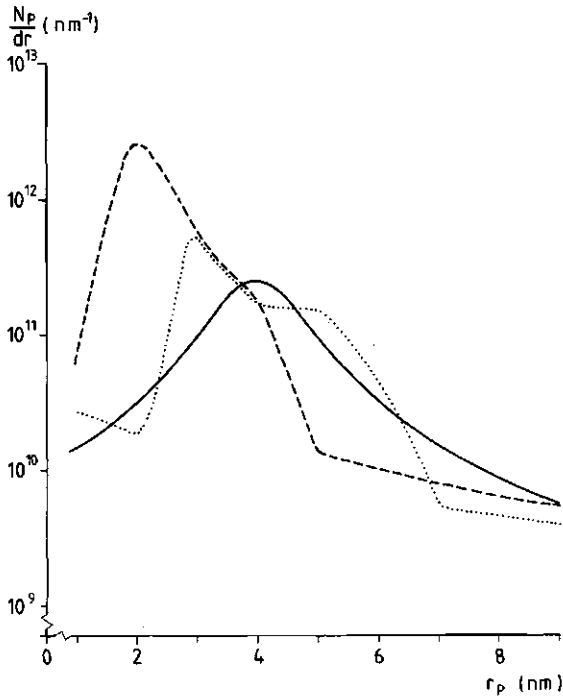


Figure 9c. Experimental (full line) and modelled PSD with category II pores and partial filling of category III pores (dashed line $r_{ppG} = 2$ nm, dotted line $r_{ppG} = 3$ nm) for GR61 with adsorbed PPG.

A quantitative interpretation of the adsorption mechanism not relating the PSD of the fouled membrane to that of the pristine membrane, would depend on the validity of the models for the transport of solvent and solutes through pores of different sizes and the physical models concerning the adsorption of macrosolutes on polymer surfaces. In this case, where it always concerns a comparison of pristine and fouled membrane PSDs, it is not all that important whether the PSDs are constructed with sophisticated or simple models.

The qualitative interpretation is valid for the specified conditions of PPG adsorption: aqueous solution, pressureless, etc. The disc-coil configuration of PPG in solution is well-established. It is known that macromolecules adsorbed on a surface may exhibit another configurational and migrational behaviour.

Nevertheless, the qualitative interpretation of differences in PSD data remains valid for the same reason as cited above.

The given interpretation is to some extent an idealized one, since the relevant processes do not change abruptly but go through a transition at the beginning and at the end of each pore size range. However, from the observed results the conclusion can be drawn that PPG adsorption is not only occurring at the geometric (external) surface of the membrane, but also takes place inside the pores.

3.8. CONCLUSIONS

Dextrans are found to be appropriate compounds for measuring the retention curve of pristine GR61 PSf membranes and the same membranes fouled by adsorption of PPG. Standardized process conditions, enacted to minimize dextran adsorption onto and into the membrane, dextran deformation and concentration polarization and to maximize the accuracy of the measurement (Table 3), result in reproducible data for each individual membrane.

Due to large differences in properties between separate membranes of the same type and batch, any PSD measurement of a fouled membrane must be preceded by the physical characterization of the same membrane in the pristine state, in order to enable any interpretation of the adsorption mechanism.

The procedure for obtaining the PSDs enables to compare the pristine and adsorbed membranes. The postulated model for adsorption of PPG (Figure 8) satisfactorily explains the alteration in the PSD of a pristine membrane due to fouling. The smaller pores become completely blocked and do not contribute to the flux anymore, whereas the largest pores become more narrow. This process causes a decreased contribution to the flux of this category of pores. Pores intermediate in size can be conceived as unaltered by adsorption.

ACKNOWLEDGEMENTS

The author would like to thank J.-P. Vincken, E. Camminga and M.F.J.M. Verhagen for their contributions to this research.

LIST OF SYMBOLS

b	width at half height of the PSD	[m]
C	concentration	[kg.kg ⁻¹]
C ₀	concentration in the feed	[kg.kg ⁻¹]
C _p	concentration in the permeate	[kg.kg ⁻¹]
h	height of the PSD	[m ⁻¹]
I	ionic strength	[kg.kg ⁻¹]
J	flow	[m.s ⁻¹]
J _m	membrane flux	[m.s ⁻¹]
L	pore length	[m]
m	centre of the PSD	[m]
M _m	mass averaged MM	[kg.mol ⁻¹]
M _n	number averaged MM	[kg.mol ⁻¹]
M _m /M _n	polydispersity	[-]
N _p	number of pores	[m ⁻²]
N _p (total)	total number of pores	[m ⁻²]
N _p /dr	frequency of the number of pores	[m ⁻¹]
N _p (max)/dr	maximum frequency of the number of pores	[m ⁻¹]
ΔP	transmembrane pressure	[Pa]
r _p	pore radius	[m]
r _s	effective hydrodynamic pore radius	[m]
r _{s,0.5}	Stokes radius at half retention	[m]
r _{PPG}	overall radius of the PPG molecule	[m]
R	retention, 1 - C _p /C ₀	[-]
R _a	adsorption resistance	[Nsm ⁻³]
R _m	membrane resistance	[Nsm ⁻³]
R _{uf}	ultrafiltration resistance	[Nsm ⁻³]
V _p	permeate volume	[m ³]
V _t	total volume	[m ³]
[η]	intrinsic viscosity	[m ³ .kg ⁻¹]
μ	viscosity	[m ² .s ⁻¹]
σ	slope of the retention curve	[m]
x	interaction parameter	[-]

REFERENCES

- 1 J.-Y. Chen and W. Pusch. Solute - Membrane Interactions in Hyperfiltration. *J. Applied Polymer Sci.*, 1987, 33, 1809-1822.
- 2 A.S. Michaels, C.R. Robertson and H. Reihanian. Mitigation of Protein Fouling of Lipophilic Ultrafiltration Membranes by Presorption of Hydrophilic Polymers. The 1987 International Congress on Membranes and Membrane Processes, Tokyo, Japan, June 8-12, 1987.
- 3 K.J. Kim, A.G. Fane and C.J.D. Fell. The Performance of Ultrafiltration Membranes Pretreated by Polymers. *Desalination*, 1988, 70, 229-249.
- 4 J. Wolff, H. Steinhäuser and G. Ellinghorst. Tailoring of Ultrafiltration Membranes by Plasma Treatment and their Application for the Desalination and the Concentration of Water-Soluble Organic Substances. *J. Membrane Sci.*, 1988, 36, 207-214.
- 5 W. Pusch and A. Walch. Membrane Structure and Its Correlation with

- Membrane Permeability. *J. Membrane Sci.*, 1982, 10, 325-360.
- 6 I. Jitsuhara and S. Kimura. Structures and Properties of Charged Ultrafiltration Membranes Made of Sulfonated Polysulfone. *J. Chem. Eng. Japan*, 1983, 16(5), 389-393.
 - 7 C.A. Smolders and E. Vugteveen. New Characterization Methods for Anisotropic Ultrafiltration Membranes. *Polym. Mater. Sci. Eng.*, 1984, 50, 177-181.
 - 8 L. Zeman and G. Tkáčik. Pore Volume Distribution in Ultrafiltration Membranes. *Polym. Mater. Sci. Eng.*, 1984, 50, 169-176.
 - 9 P.I. Dalven, J.R. Hildebrandt, A. Shamir, A.J. Lacetti, L.T. Hodgins and H.P. Gregor. Acrylonitrile-Based Copolymers: Synthesis, Characterization, and Formation of Ultrafiltration Membranes Utilized for the Immobilization of Proteins. *J. Applied Polymer Sci.*, 1985, 30, 1113-1132.
 - 10 J. Desbrières, M. Rinaudo, M. Brun and J.F. Quinson. Relation entre le taux de rétention et la distribution des pores dans une membrane d'ultrafiltration. *Journal de chimie physique*, 1981, 78(2), 187-191.
 - 11 L. Zeman and M. Wales. Steric Rejection of Polymeric Solutes by Membranes with Uniform Pore Size Distribution. *Sep. Sci. Technol.*, 1981, 16, 275-290.
 - 12 G. Capannelli, F. Vigo and S. Munari. Ultrafiltration Membranes - Characterization Methods. *J. Membrane Sci.*, 1983, 15, 289-313.
 - 13 Q.T. Nguyen and J. Néel. Characterization of Ultrafiltration Membranes. Part III. Role of Solvent Media and Conformational Changes in Ultrafiltration of Synthetic Polymers. *J. Membrane Sci.*, 1983, 14, 97-109.
 - 14 Q.T. Nguyen and J. Néel. Characterization of Ultrafiltration Membranes. Part IV. Influence of the Deformation of Macromolecular Solutes on the Transport through Ultrafiltration Membranes. *J. Membrane Sci.*, 1983, 14, 111-128.
 - 15 L.J. Zeman. Adsorption Effects in Rejection of Macromolecules by Ultrafiltration Membranes. *J. Membrane Sci.*, 1983, 15, 213-230.
 - 16 A.N. Cherkasov, A.E. Polotskii, V.S. Galenko, V.P. Zhemkov and L.Yu. Gorelova. Peculiarities of the Ultrafiltration of Linear Flexible-Chain Polymers. *Kolloidnyi Zhurnal*, 1984, 46(1), 185-186.
 - 17 B.D. Mitchell and W.M. Deen. Theoretical Effects of Macromolecule Concentration and Charge on Membrane Rejection Coefficient. *J. Membrane Sci.*, 1984, 19, 75-100.
 - 18 M. Fontyn, K. van 't Riet and B.H. Bijsterbosch. Surface Spectroscopic Studies of Pristine and Fouled Membranes. Part I. Method Development and Pristine Membrane Characterization. *Colloids and Surfaces*, 1991, 54, 331-347. Chapter 4 of this thesis.
 - 19 M. Fontyn, K. van 't Riet and B.H. Bijsterbosch. Surface Spectroscopic Studies of Pristine and Fouled Membranes. Part II. Method Development and Fouled Membrane Characterization. *Colloids and Surfaces*, 1991, 54, 349-362. Chapter 5 of this thesis.

- 20 W. Burchard. Solution Thermodynamics of Non-Ionic Water-Soluble Polymers. In: Chemistry and Technology of Water-Soluble Polymers. C.A. Finch Ed., Plenum Press, New York and London, 1983, p125.
- 21 K.A. Granath. Solution Properties of Branched Dextran. *J. Colloid Sci.*, 1958, 13, 308-328.
- 22 E.A. Lange. Molecular and Macromolecular Sieving by Asymmetric Ultrafiltration Membranes. University Microfilms International, MI, USA, 1984, Stanford University.
- 23 A.M. Basedow, K.H. Ebert. Production, Characterization and Solution Properties of Dextran Fractions of Narrow Molecular Weight Distributions. *J. Polym. Sci., Polym. Symp.*, 1979, 66, 101-115.
- 24 A.M. Basedow, K.H. Ebert and W. Feigenbutz. Polymer-Solvent Interactions: Dextran in Water and DMSO. *Makromol. Chem.*, 1980, 181, 1071-1080.
- 25 C. Tanford. Physical Chemistry of Macromolecules. John Wiley and Sons, New York, 1961.
- 26 H. Yamakawa. Modern Theory of Polymer Solutions. Harper and Row, New York, 1971.
- 27 K. Gekko. Solution Properties of Dextran and Its Ionic Derivatives. ACS Symp. Series, 1981, 150, American Chemical Society, Washington, D.C.
- 28 C.A. Finch Ed. Chemistry and Technology of Water-Soluble Polymers. Plenum Press, New York and London, 1983.
- 29 D.B. Sellen. Light Scattering Rayleigh Linewidth Measurements on Some Dextran Solutions. *Polymer*, 1975, 16, 561-564.
- 30 T.D. Long, D.L. Jacobs and J.L. Anderson. Configurational Effects on Membrane Rejection. *J. Membrane Sci.*, 1981, 9, 13-27.
- 31 E. Matthiasson. The Role of Macromolecular Adsorption in Fouling of Ultrafiltration Membranes. *J. Membrane Sci.*, 1983, 16, 23-36.
- 32 J.H. Hanemaaijer, T.W. Robbertsen, T.H. van den Boomgaard and J.W. Gunnink. Fouling of Ultrafiltration Membranes. The Role of Protein Adsorption and Salt Precipitation. *J. Membrane Sci.*, 1989, 40, 199-218.
- 33 M. Fontyn, B.H. Bijsterbosch and K. van 't Riet. Chemical Characterization of Ultrafiltration Membranes by Spectroscopic Techniques. *J. Membrane Sci.*, 1988, 36, 141-145.
- 34 Dextran Fractions, Dextran Sulphate, DEAE-Dextran, Defined Polymers for Biological Research, Pharmacia Fine Chemicals, Uppsala, Sweden, DX April 1980-7.
- 35 V. Hlady, J Lyklema and G.F. Fler. Effect of Polydispersity on the Adsorption of Dextran on Silver Iodide. *J. Colloid Interface Sci.*, 1982, 87, 395-406.
- 36 H. Sasaki, T. Matsuda, O. Ishikawa, T. Takamatsu, K. Tanaka, Y. Kato and T. Hashimoto. New Series of TSK-Gel PW Type for High Performance Gel

- Filtration Chromatography. Sci. Report of Toyo Soda, Mfg. Co., Ltd., 1985, 29, 37-54.
- 37 B.G. Belenkii and L.Z. Vilenchik. Modern Liquid Chromatography of Macromolecules. J. Chromatography Library - Volume 25, Elsevier, Amsterdam, 1983.
 - 38 H.A. Deckers, C. Olieman, F.M. Rombouts and W. Pilnik. Calibration and Application of High - Performance Size Exclusion Columns for Molecular Weight Distribution of Pectins. Carbohydrate Polymers, 1986, 6, 361-378.
 - 39 J. Grimson. Mechanics and Thermodynamics of Fluids. McGraw Hill, London, 1970.
 - 40 J.D. Ferry. Ultrafilter Membranes and Ultrafiltration. Chemical Reviews, 1936, 18, 373-455.
 - 41 S. Gasiorowicz. Quantum Physics. Chapter 23. Selected Topics in Radiative Transitions. J. Wiley and Sons, Inc., New York, 1974.
 - 42 J. Kassotis, J. Shmidt, L.T. Hodgins and H.P. Gregor. Modelling of the Pore Size Distribution of Ultrafiltration Membranes. J. Membrane Sci., 1985, 22, 61-76.
 - 43 L.S. Sandell and D.A.I. Goring. A Comparison of the Intrinsic Viscosities of Oligomeric Propylene Glycols with the Behavior Predicted for Models in Aqueous Solution at 25°. Macromolecules, 1970, 3, 50-54.

CHAPTER 4**SURFACE SPECTROSCOPIC STUDIES OF PRISTINE AND FOULED MEMBRANES. PART I. METHOD DEVELOPMENT AND PRISTINE MEMBRANE CHARACTERIZATION**

ABSTRACT

Studying the adsorption mechanism of foulants on polysulfone (PSf) membrane surfaces requires chemically and physically well characterized membranes. This report deals with the chemical characterization of DDS GR61 PP and Dorr-Oliver S10 membranes by surface sensitive spectroscopy, to subsequently investigate the interactions with solutes during fouling (Part II).

Attenuated total reflection Fourier transform infrared spectroscopy (ATR FTIR) reveals the type of PSf used, Udel (polyethersulfone (PESf) + bisphenol A) and Victrex (PESf), respectively. Fast atom bombardment mass spectrometry (FAB MS), however, indicates also the presence of minor amounts of bisphenol A in the S10 surface. This might be caused by admixing of bisphenol A or block-copolymerization of Victrex with Udel. Deviations from the calculated bulk composition in both membrane surfaces (as detected by X-ray photoelectron spectroscopy (XPS)) are due to the preferential location of SO₂ functional groups in the bulk and aryl-O-aryl and aryl-C-aryl groups at the surface. This conclusion is supported by angular dependent XPS. In contrast to the presumed chemical structure the element N is detected. Combination of all spectroscopic data illustrates this to be due to the presence of dimethylformamide (DMF) in the surfaces, DMF being the solvent employed during manufacturing of the PSf membranes.

The GR61 and S10 could be characterized to such an extent that better insight in the surface structure and chemistry is obtained. Part II will show that these results as well as the method can be used to analyse fouled membranes.

4.1. INTRODUCTION

Characterization of pristine and fouled membranes is receiving considerable attention nowadays in view of such aspects as novel membrane processes, modelling of separation and transport mechanisms and the severe problems resulting from fouling. Many macro- as well as microscopical phenomena are being dealt with, such as process engineering aspects, thermo- and permporometry, pore size and pore volume (distribution) measurements, determination of the skin thickness, electron microscopy, etc. [1 - 7]. In describing fouling, the balance of molecular and atomic forces, as expressed by the hydrophobicity of all materials contributing in the membrane process (membrane, solutes, solvents), plays a dominant role. Solute-membrane interactions will take place on the outer surface as well as in the membrane pores. The effect of changing a hydrophobic into a hydrophilic surface on the performance of the membrane process is revealed by experiments with coatings, adsorption layers, polymer and surfactant pretreatment and plasma treatment [8 - 14]. A good measure for hydrophobicity is actually still lacking. Contact angle measurements are widely used in this connection although its data are known to be dependent on the pore size. Probably, the elaboration of the sticking bubble technique [15] can be useful in quantifying the hydrophobicity.

A fundamental study of membrane fouling faces the problem of insufficient knowledge of the chemistry of the surfaces. The review by Larrabee and Shaffner [16] (601 references in 1981) accentuates the potentialities of spectroscopic techniques for surface characterization of various types of materials. Nevertheless, only during the past decade have they thoroughly been employed to investigate polymer materials, as recently reviewed [17, 18]. Some studies of synthetic membrane surfaces are reported [15, 19-21]. However, a comprehensive investigation of the surfaces, atomic composition and molecular configuration are not dealt with. Advanced surface spectroscopy is a powerful tool to achieve this.

Using these techniques on membranes may involve some disadvantages; e.g. their application on non-smooth, non-conducting surfaces, the possible dependence of the results on pore size, the effect of drying the membrane, may create some uncertainties. Nevertheless, this paper demonstrates that additional membrane knowledge can be gained by employing these non-standard techniques on membranes.

In this paper a combination of different spectroscopic techniques is applied to polysulfone (PSf) membranes. The aim is to reveal the chemical composition of

and the molecular configuration in the surfaces in order to better understand the membrane fouling properties. It has to be stipulated that these techniques only provide information on the outer surface. It is assumed that the results are equally applicable to the inner surface of the pores.

4.2. MATERIALS AND METHODS

4.2.1. Membranes

Table 1 resumes the characteristics of the commercial polysulfone (PSf) membranes investigated. Prior to use the membranes were rinsed with microfiltered distilled water for at least 36 hours. Small pieces of membrane were then dried for one hour in an oven at 100°C. All beakers were covered by aluminum foil and not by Parafilm, since the latter contains fouling silicone oil, as experimentally inferred from X-ray photoelectron spectroscopy (XPS) and fast atom bombardment mass spectrometry (FAB MS) in this study.

Table 1. Data on GR61 and S10 membranes.

	GR61	S10
Manufacturer	De Danske Sukkerfabrikker (Naskov, DK)	Dorr-Oliver (Stamford, Connecticut, USA)
Batch	400-013	(purchased in 1985)
Polysulfone type	Udel [19, 21]	Victrex [19]
Support layer	filter paper	nonwoven polyethylene (Paifec, DuPont)
Conservation	water, 50% glycerol, 3.6% propanoic acid, 0.8% caustic soda	water, glycerol, SDSS
γ_d (mNm ⁻¹) [15]	65.8 > 72.0 (batch 158-010)	(66.8 for S30)
Pure water membrane resistance R_m (*10 ¹⁰ Nsm ⁻³)	0.5 - 1.1	0.2 - 0.5

A number of membranes were prepared by TNO (Netherlands Organization for Applied Scientific Research, Zeist, NL) on the laboratory scale by casting a polymer / dimethylformamide (DMF) solution on a nonwoven polyester support (type Villedon FO 2406, Freudenberg, D), directly followed by coagulation in water at 20°C. Two types of PSf (Udel and Victrex) were used, differing in chemical structure by the presence or absence of a bisphenol A part in the monomer [19]. After coagulation the membranes were rinsed several times in demineralised water and stored in the wet state at 0°C. Prior to use they were subjected to the same treatment as described for the commercial membranes. Some properties of these membranes are shown in Table 2.

Table 2. Data on TNO PSf membranes.

	Udel TNO 18	Victrex TNO 18	Victrex TNO 20	Victrex TNO 22
PSf type	Udel P3500	Victrex 200P	Victrex 200P	Victrex 200P
Concentration casting solution (% mass)	18	18	20	22
Casting thickness (μm)	250	200	250	250
R_m ($\cdot 10^{10} \text{ Nsm}^{-3}$)	1.4-2.0	1.2-2.4	5.1-7.2	18-36

4.2.2. Surface-Sensitive Spectroscopy

Attenuated Total Reflection Fourier Transform Infrared Spectroscopy (ATR FTIR)

Comprehensive treatises of the ATR technique can be found in [22 - 24]. The differences and advantages of FT in comparison with a grating instrument are summarized in [18, 25]. The application of (ATR) (FT) IR to polymers is assessed by the vast amount of literature [18, 20, 23, 24, 26, 27].

Although the ATR IR technique does not need ultra high vacuum (UHV), the exposed surfaces are usually dry. For the investigation of polymeric films, where the process application is always under wet conditions, the analysis of the dried membranes requires the results about the configuration of the surface molecules to be interpreted with due care since they may have been

reoriented in the drying process. Despite this drawback, until now no other characterization method of the membrane surface has provided so much information.

For all ATR IR measurements an IFS 85 (Bruker Analytische Messtechnik GmbH, Karlsruhe, D), equipped with a DTGS detector and a Harrick ATR unit (Harrick, Ossining, USA) was used. The dry membrane samples were cut to the size of the KRS5^{45°} parallelepiped-shaped ATR crystal (10x5x1 mm) and single-sided tightened. Typically, 1000 scans of sample and background reference (aluminum) were recorded (resolution 1 cm⁻¹) to improve the signal-to-noise ratio. No depth-profiling analysis was done (only one angle of incidence). The absorption spectra were linearly water vapour and baseline corrected. The wavenumber scale has been calibrated with a cellulose triacetate (CTA) film.

The penetration depth d_p of the IR radiation depends on its wavelength, on the refractive index of the internal reflection element (IRE) and on the angle of incidence with the normal to the sample surface. It is typically in the μm order. The physical basis for depth analysis justifies to consider $1/2 d_p$ as a measure for the thickness of the analysed surface [28]. In our specific case the angle of incidence was 45° implying penetration depths ($1/2 d_p$) between 2.5 and 0.25 μm . By choosing the appropriate IRE crystal and ATR equipment and by employing an FT instrument, the range of information about the surface is enhanced.

X-Ray Photoelectron Spectroscopy (XPS)

Details about principles and instrumentation of XPS are given in e.g. [18, 29 - 32]. Many applications to polymers as well as other materials are reviewed in [16, 17, 32]. Until now membrane surfaces have rarely been analysed by XPS [15, 19-21].

XPS data give information about the atomic composition and chemical structure of the surface. Typical electron escaping depths are in the nm order. By changing the angle between the normal to the surface and the axis to the analyser differences between bulk and surface composition of the polymer sample can be visualized. Detection of surface enrichments with some chemical groups and the unravelling of the surface configuration of different block-copolymers are possible accomplishments of XPS analysis [17, 19, 33]. The integration of XPS results with data obtained from other techniques gives a better insight in the overall topography of surfaces, which is important with respect to different applications of the materials [33].

Since XPS uses UHV (10^{-7} - 10^{-8} Pa), and thus dry samples are studied, interpretation of the data is subject to the same restrictions as in the ATR IR technique.

XPS spectra were recorded using an ESCALAB MKII (VG Scientific, East Grinstead, Sussex, GB) which employs non-monochromatized $MgK\alpha$ X-rays and a hemispherical mirror analyser. Typically, 20 scans per region were recorded with a constant analyser energy of 50 eV. Binding energy scales were charge-corrected by setting the C-C peak of the C1s to 284.5 eV. The sensitivity factors were taken from Wagner *et al.* [34].

The dry membranes (ca. 1 cm^2) were mounted on the sample holder by double sided tape. Electrons escaping perpendicularly to and under an angle of 40° with the surface were analysed. The depths analysed in these cases were ca. 5 and ca. 1 nm, respectively. These depths are apparent, based on the statistical concept of mean free-path length in a homogeneous solid. The C1s peak was decomposed assuming that the shape of the lower binding energy side of the first peak is the same for the following peaks (equal Gauss-Lorentz ratio) and that peak width at half height is equal.

Fast Atom Bombardment Mass Spectrometry (FAB MS)

To minimize the need for neutralization of the insulating sample, an alternative for the primary ion beam in secondary-ion mass spectrometry (SIMS) is the use of fast atoms. This technique is known as FAB MS. The spectra produced by FAB MS are essentially the same as those obtained by SIMS [17, 35, 36]. The mass spectra of the negatively charged fragments can also be a powerful probe in detecting groups with electronegative elements such as oxygen and halides [17].

In FAB MS and static SIMS the first few atomic layers are analysed [17, 37]. SIMS is more surface sensitive and has a higher molecular specificity than XPS.

FAB MS analyses were carried out on a VG SIMSLAB (VG Ionex, Sussex, GB). Square sections of the dried membranes were mounted on titanium sample stubs. The samples were bombarded with a 2 keV beam of argon atoms, producing a target current of 1.0 nA in an analysis area of approximately 15 mm^2 . During spectral acquisition, secondary ions were energy filtered and then separated according to mass by a VG MM12-1200 quadrupole spectrometer. Positive and negative spectra were acquired by scanning through the mass range 0 - 300 amu. At large secondary ion response the primary-beam current was reduced to 0.1 nA to prevent detector saturation. Similarly, if the signal

was sufficient at 1.0 nA, the spectra were recorded in the range 100 - 400 amu. Where necessary, charge neutralization was carried out using a 500 eV beam of electrons.

To allow comparison of different spectra relative intensities were taken to compensate for different experimental conditions. The positive FAB mass spectra were normalized with respect to mass-to-charge fragments $m/z=15^+$ (CH_3^+) and the negative spectra to $m/z=13^-$ (CH^-).

4.3. RESULTS AND DISCUSSION

4.3.1. XPS

Table 3 gives the atomic composition of all PSf membranes for two different depths, as averaged over several measurements. Relative differences exceeding 5% (90% confidence) between the averages are significant.

Table 3. Atomic composition (XPS) of GR61, S10, Udel TNO 18, Victrex TNO 18, 20 and 22 and calculated values assuming that N is from DMF.

Membrane	Atom%						
	C	C ^a	S	S ^a	O	O ^a	N
GR61 90°	77.5	80.4	2.7	3.2	17.0	16.5	2.9
GR61 40°	77.6	81.4	2.3	2.8	16.6	15.7	3.8
S10 90°	72.2	73.3	5.5	6.0	20.7	20.7	1.7
S10 40°	73.9	75.0	5.0	5.4	19.6	19.6	1.5
Udel TNO 18 90°	75.8	78.8	3.4	4.0	17.6	17.1	3.2
Udel TNO 18 40°	76.6	80.7	2.8	3.5	16.6	15.8	3.9
Victrex TNO 18 90°	66.0	67.7	1.9	2.5	27.6	29.8	4.6
Victrex TNO 20 90°	66.7	68.7	3.4	4.4	25.4	27.0	4.4
Victrex TNO 22 90°	67.1	68.4	4.0	4.7	25.9	26.9	2.9
Victrex TNO 18 40°	70.6	73.4	1.7	2.2	23.5	24.4	4.2
Victrex TNO 20 40°	74.2	78.2	2.5	3.2	18.9	18.6	4.4
Victrex TNO 22 40°	71.3	73.6	2.7	3.2	22.6	23.1	3.3
Udel calculated	84.4		3.1		12.5		-
Victrex calculated	75.0		6.3		18.8		-

^a After deduction of DMF contribution.

GR61 (Udel) and S10 (Vicat) membranes exhibit less C and S and more O in the surfaces analysed perpendicularly and at 40° (furtheron to be called 90° and 40° surface) compared to the calculated composition. Nitrogen is unexpectedly present in the surface of both membranes. FAB MS analysis (see section FAB MS) illustrates that this nitrogen probably originates from the solvent DMF used during preparation of the membranes.

Although no additives were employed in their preparation, the reference Udel and Vicat PSf membranes (all marked with TNO in Table 3) also show nitrogen to be present. Obviously, this nitrogen can only originate from the solvent. For the GR61 and S10 membranes this means that in principle the solvent alone can account for the deviating surface composition and admixture molecules have not necessarily to be invoked.

Increasing the Vicat polyethersulfone (PESf) concentration in the casting solution from 18 to 22% (mass%) causes more S (typical for PSfs) and less N (typical for DMF) to be determined, as expected.

The atomic concentrations for both commercial membranes have been corrected for the presence of DMF, assuming homogeneous distribution (columns 3, 5 and 7 in Table 3). The ensuing data appears to better fit the composition calculated on the basis of Udel PSf and Vicat PESf. So, the change in surface composition is partly due to the presence of retained solvent molecules.

Table 3 also shows that corrected and non-corrected 90° surface values for the TNO membranes exhibit the same features as for the commercial membranes: less C and S, as opposed to more O, than in the calculated composition, whereas the DMF-corrected compositions better match than the non-corrected ones.

The 40° surface contains less S and O than the more bulk-like 90° surface in GR61 and S10 as well as in the TNO membranes (Table 3). It seems that the SO₂ functional groups are preferentially located in the bulk of the membranes. This will probably be due to the phase inversion preparation technique. If, before applying the coagulation step, enough solvent evaporates, the solution polymer-solvent becomes gradually more viscous. The casting solution-air interface becomes rigid and any reorientation is prevented. Consequently, the membrane surface will have a chemical composition similar to the overall composition. On the other hand, if time between casting and coagulation is relatively short, in the ternary system the solvent is displaced by the non-solvent until a thermodynamically unstable situation is reached. The solution polymer-solvent becomes more concentrated in polymer. The process of outflow

of solvent and inflow of non-solvent in the polymeric film is slow so that in the early stages of the process the polymer has the possibility to reorient to the thermodynamically most favourable situation and the chemical composition of the surface will differ from the expected overall composition. This has been demonstrated experimentally in reference [15], where also further supporting evidence is cited. In the case of PSf this means that more hydrophilic groups orient to the non-solvent water. More SO₂ groups in the membrane bulk is the consequence.

Data in Table 3 point out that both commercial PSf membrane 40° surfaces are more hydrophobic than the 90° surface (bulk).

The surface of a membrane revealing another than overall composition may especially be important in fouling studies, since the fouling capacity is only related to the ultimate surface structure of the membrane. So many variables during the membrane preparation process affect the surface composition (and the membrane resistance (R_m) for that matter), that it is virtually impossible to predict the actual membrane characteristics. Nevertheless, systematic study of the overall membrane characteristics could give insight into their effect on the surface characteristics.

For the PSf membranes the C1s atomic peak is decomposed into 4 components to obtain further structural information (Table 4). Peaks at binding energies 284.5, 286.1 and 290.5 eV correspond to the C-C and C-S, the C-O and the $\pi \rightarrow \pi^*$ shake up, respectively [32, 38]. The peak at 288.0 eV represents further oxidized carbon (C=O) [32].

The C=O bond appears both in GR61 and S10, although this is not to be expected from the net compositions. If it would be indicative of an oxidized PSf surface, the C amount at 288.0 eV should be higher in the 40° surface than in the 90° surface. The analysis of the TNO 40° surfaces (Table 4) as compared to the 90°, however, does not support the hypothesis of an oxidized surface. Probably, the appearance of the C=O structure has to be attributed to the presence of DMF in the membrane surfaces. The two types of C in DMF correspond to 288.0 and to 286.1 eV [32].

Table 4. Relative importance of the various components of the C1s XPS peak of GR61, S10, Udel TNO 18, Victrex TNO 18, 20 and 22.

Membrane	C%		
	284.5 ^a	286.1 ^a	288.0 ^a
GR61 90°	75.2	21.8	3.1
S10 90°	68.6	25.6	5.8
Udel TNO 18 90°	81.5	16.8	1.7
Udel TNO 18 40°	84.6	14.0	1.4
Victrex TNO 18 90°	69.2	27.3	3.5
Victrex TNO 20 90°	67.6	24.8	7.6
Victrex TNO 22 90°	70.9	26.3	2.8
Victrex TNO 18 40°	75.6	21.6	2.8
Victrex TNO 20 40°	81.1	13.7	5.1
Victrex TNO 22 40°	79.0	17.6	3.4
Udel calculated	85.2	14.8	-
Victrex calculated	83.3	16.7	-

^a Binding energy (eV)

The $\pi \rightarrow \pi^*$ shake up indicates the presence of unsaturated bonds. All samples show this unsaturation (aromaticity in view of the proposed structure). The three lower binding energy peaks have a quantitative meaning. The sum of their peak areas is 100%. The intensity of the shake-up component has been added to the intensity of the main peak at 284.5 eV. The 286.1 eV peak should be due to nearly half the O in PSf; the other half is not bound to C but to S. The C in a C-S bond is the most hydrophobic: it is located between two aromatic phenyl structures Ar-SO₂-Ar which behave as a rather rigid structure.

The results for the C1s peak decomposition for the GR61 and S10 90° surface (Table 4) are in agreement with the observed trend in atomic composition (Table 3). Ar-SO₂-Ar groups are oriented towards the bulk and the Ar-O-Ar groups are more located at the surface.

These surface - bulk differences and differences with the overall calculated composition are also observed for the TNO membranes (Table 4). For Udel TNO 18 the C1s values for the 40° surface almost match the calculated values for the different types of C.

From Table 3 the atom% of O bound to S could be calculated as twice the atom% of S. The difference between the actual atom% of O and that of O bound to S should be the amount of O bound to C, which could be compared

to half the atom% of C bound to O obtained from C1s peak decomposition in Table 4. Fitting this calculation with the observation will be subject to the mentioned alteration in atomic composition from surface to bulk which is not accounted for in the data of the 90° and 40° surface. This is a composition averaged over the respective depths. Matching calculation with observation is also hampered by the inaccuracy introduced when decomposing the C1s peak. One could also think of an enhanced concentration of the chain ends on the surface (R-OH rather than R-O-R) but O1s peak decomposition only reveals O bound to C and to S. Another difficulty is that also the C-N contribution from the DMF partially contributes to the peak at 286.1 eV. Therefore more detailed interpretation would be doubtful.

Increasing the concentration of the casting solution should provide some information about the effect of concentration on the ultimate surface structure and on the porosity of the membrane. Unfortunately, the XPS C1s analysis revealed a hydrocarbonaceous fouling on the surface of the Victrex TNO 20 (very high area% at C-C (and C-S) 284.5 eV for the 40° surface as compared to the 90° surface). The data at 286.1 and 288.0 eV are also subject to this fouling and are thus equally unreliable.

Since the polymer in the most concentrated solution (22%) experiences the highest hindrance against reorientation, the membrane prepared from this solution will exhibit the highest S% in the surface.

However, this possible difference in reorientation for the different Victrex TNO membranes is not the only phenomenon contributing to the observed differences in water flux given in Table 2. Changing the polymer concentration will also affect the porous structure of the membrane, so that these differences in R_m are inconclusive.

Nevertheless, some conclusions can be drawn. The higher the PSf concentration, i.e. the lower the DMF content, the lower the N atom% and the lower the amount of C=O at 288.0 eV, as expected. If no reorientation of SO₂ towards the bulk takes place, the S% should be 6.3% (Victrex). Reorientation is more pronounced at a lower polymer concentration due to less hindrance. This results in a lower S% at a lower polymer concentration.

For the other Victrex TNO samples the peak area% do not differ sufficiently to associate it with differences in chemical composition in the surfaces.

Despite the differences in the chemical configuration of the surfaces and the bulk, it remains clear that GR61 represents more the Udel type of PSf and S10 the Victrex type.

In summary, the observed nitrogen in GR61 and S10 originates from DMF and reorientation of the chemical groups at the membrane surface has taken place. There is less S at the surface rendering it more hydrophobic. This fact is caused by the manufacturing process.

4.3.2. FAB MS

If the FAB MS analysis of GR61 and S10 can be accomplished at low energy, fragments of relatively high mass to charge ratios m/z can be obtained without sample charging, resulting in more information about the chemical structure of the sample surface than if analysed at high energy. Especially for negative FAB MS charging is the major problem.

The positive m/z values 444^+ , 426^+ , 397^+ , 380^+ and 368^+ in the GR61 spectrum originate from the Udel PSf monomer (Figure 1). They are not found in S10, giving strong evidence that in S10 the major monomer is not of the Udel type. The Victrex PESf monomeric ion 232^+ was never determined in any of the membrane samples. Nevertheless, the 249^+ and 184^+ fragments are seen in some GR61 spectra (Figure 1). The bisphenol A part in the Udel monomeric unit with a m/z 210^+ could not be detected, but the bisphenol A ($m/z = 228^+$) (Figure 1) was clearly observed in the spectra of both GR61 and S10. It suggests that Victrex PESf is not the only ingredient used in manufacturing S10. Probably, some Udel PSf or bisphenol A is also incorporated in the S10 surface.

Because of their difficult determination and the huge number of combinations leading to certain mass values, assigning all higher m/z ions is not feasible.

High-intensity m/z fragments from the usual CHO fragmentation are found at 29^+ , 43^+ , 57^+ and 71^+ for both GR61 and S10 (Table 5). S10 seems to have another CHO fragmentation pathway than GR61, as inferred from the higher intensity of the 43^+ , 57^+ and 71^+ fragments relative to the $m/z-2$ fragment. Typically, the ratio $(m/z)/(m/z-2)$ for 43^+ , 57^+ and 71^+ in S10 reaches ca. 1.0 as compared to 0.4 in GR61. This ratio can be used as a criterion to distinguish S10 (Victrex) from GR61 (Udel).

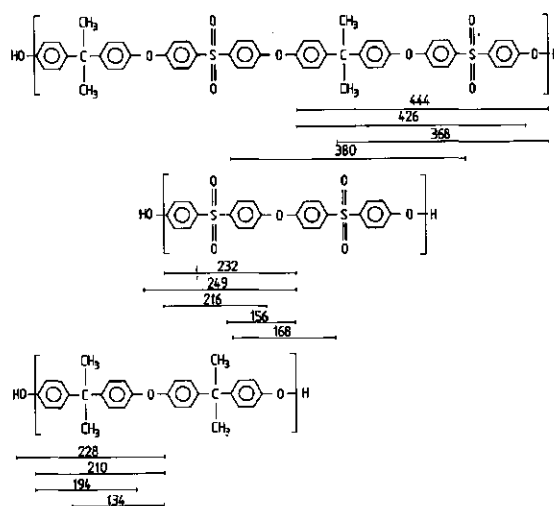


Figure 1. Possible fragmentation pattern of GR61 and S10 membranes in positive FAB MS.

Table 5. Relative intensities of the CHO, aromatic and N fragments (positive FAB MS) in GR61 and S10, and their possible assignment.

m/z	GR61	S10	possible assignment
29	5.04	8.00	$C_2H_5^+$; CHO^+
43	5.15	7.50	$C_3H_7^+$; $C_2H_3O^+$
57	0.96	5.31	$C_4H_9^+$; $C_3H_5O^+$
71	0.21	2.54	$C_5H_{11}^+$; $C_4H_7O^+$
77	0.54	1.27	$C_6H_5^+$
91	0.50	0.62	$C_7H_7^+$
115	0.19	0.32	$C_9H_6^+$
165	0.12	0.08	
28	3.25	8.62	N_2^+ ; CH_3NH^+
42	1.89	2.12	NCO^+

One of the aromatic ions, 115^+ , likely originates from the bisphenol A structure. During fragmentation, the three aliphatic C atoms bound to the phenyl structure presumably form an aromatic ring with two C atoms of that phenyl ring. The intensity ratio of m/z 77^+ , also an aromatic fragment, to 115^+ is a possible criterion to distinguish between Victrex and Udel. If the S10 surface consists mainly of Victrex, with Udel or bisphenol A as a minor

component, this ratio must be higher than for GR61, which is indeed observed (4.0 and 2.8 respectively).

The even-numbered positive fragments 28^+ and 42^+ in Table 5 are almost undoubtedly due to a C-N fragment. Further evidence for this nitrogen compound is constituted by the negative fragments 14^- , 26^- and 42^- , although 14^- and 26^- can also be attributed to the usual CHO fragmentation in negative FAB MS (Table 6). The ratio $24^-:25^-:26^-$ for S10, on the other hand, does not support the presence of N in the S10 surface. But considering the assignments of 28^+ , 42^+ and 42^- , a C-N compound is obviously also present in the S10 surface, as it is in the GR61. The XPS analysis has already shown that it possibly stems from the solvent used during preparation of the membrane. Most common solvents for PSf are dimethylformamide (DMF), N-methylpyrrolidone (NMP) and dimethylsulphoxide (DMSO). DMSO, not being a C-N compound, can obviously be excluded. In none of the spectra fragments possibly referring to NMP are observed. Although present in very low intensity (0.09 in GR61 and 0.05 in S10), $M^+=73^+$ can be assigned to DMF [39]. Other fragments are e.g. 29^+ and 15^+ ; these can also originate from the PSf although the positive even numbered 58^+ and 44^+ strongly suggest to be derived from a nitrogen compound.

Table 6. Relative intensities of typical fragments (negative FAB MS) in GR61 and S10, and their possible assignment.

m/z	GR61	S10	possible assignment
14	0.15	0.14	CH_2^- ; N^-
24	2.63	1.53	C_2^-
25	4.06	3.30	C_2H^-
26	3.51	0.68	C_2H_2^- ; CN^-
42	0.23	0.06	CNO^-
12	0.50	0.30	C^-
24	2.63	1.53	C_2^-
36	0.42	0.11	C_3^-
48	0.34	0.28	C_4^-
60	0.07	0.04	C_5^-
72	0.06	0.04	C_6^-
16	0.69	2.68	O^-
17	0.45	1.69	OH^-

The CHO degradation pattern C_n^- and the O^- and OH^- (Table 6) are also high-intensity fragments in both spectra. The higher O^-/C^- ratio expected in S10 as compared to GR61 is actually observed (9.00 and 1.43, respectively). Very conspicuous in the negative spectra are the sulphur fragments $S^- 32^-$, $SO^- 48^-$, $SO_2^- 64^-$, $SO_3^- 80^-$ and $HSO_4^- 97^-$. The ratio of the relative intensities (I) of SO_2^- to C^- ($64^-/12^-$) is higher in S10 than in GR61 (0.65 and 0.08 respectively), as is expected.

The two criteria, $I(SO_2^-)/I(C^-)[Udel] \ll I(SO_2^-)/I(C^-)[Vitrex]$ and $I(O^-)/I(C^-)[Udel] \ll I(O^-)/I(C^-)[Vitrex]$, can be used to distinguish between a Udel and a Vitrex membrane.

4.3.3. ATR FTIR

Several differences, in terms of extra bands as well as shifts in bands, between GR61 and S10 are clearly observed in the ATR IR spectra (Figure 2 and Table 7). The roughly symmetrical doublet at 1387 and 1365 cm^{-1} , attributed to the symmetrical C-H deformation of $C-(CH_3)_2$, and the band at 1170 cm^{-1} (probably also associated with this structure via skeletal vibration C-C) [40] are only found for GR61, but not for S10. Another striking feature is the absence of the C=C stretch vibration band at 1503 cm^{-1} in S10, probably due to the aromatic rings being located near the aliphatic C-C structure in Udel (Ar-C-Ar). The highest frequency of the C-H stretch of CH_3 at 2968 cm^{-1} is clearly observed in GR61 and rather weakly in S10.

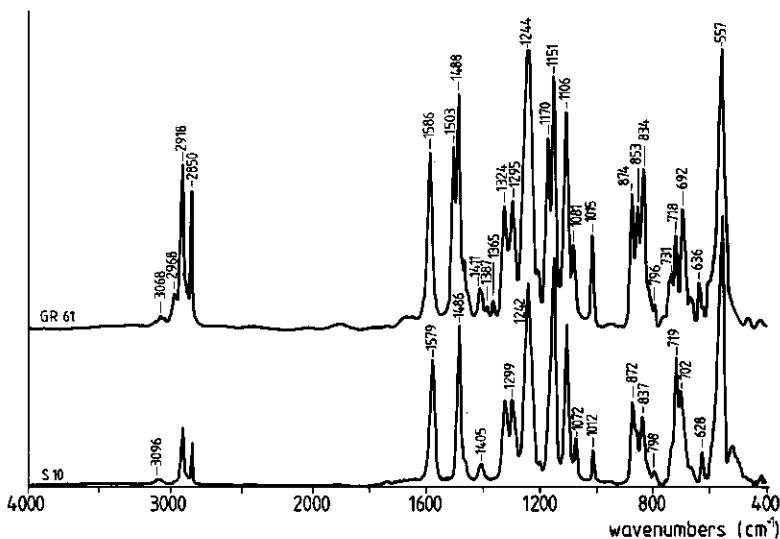


Figure 2. ATR IR spectra of pristine GR61 and S10.

The most conspicuous shifts of band maxima are the C=C stretch band at 1586 for GR61 as compared to 1579 cm^{-1} for S10, the bands probably associated with the phenolic structure (C-O stretch and O-H deformation) at 1411 and 1295 (GR61), 1405 and 1299 cm^{-1} (S10), respectively, and the unassigned band at 1081 (GR61) and 1072 cm^{-1} (S10), respectively. Also the fingerprint region below 1000 cm^{-1} shows a different pattern in vibration bands for GR61 and S10.

The ratio of relative intensities I (band at 558 cm^{-1} as a base) of the aryl ether at 1244 (or 1242) and S=O stretch bands at 1151 cm^{-1} can be taken as a measure for the difference between Udel and Victrex. It is expected to be higher in GR61 than in S10, which is observed indeed (1.25 and 0.88 respectively).

Table 7. ATR IR bands and their possible assignment for GR61 and S10.

Possible assignment	GR61 (cm^{-1})	S10 (cm^{-1})
C-H stretch aromatic aliphatic	3096, 3068, 3037 2968, 2918, 2850	3096, 3068, - -, 2918, 2850
C=C stretch	1586, 1503, 1488 1411	1579, -, 1486 1405
C-H C-(CH ₃) ₂ symm. deform.	1387, 1365	-
S=O stretch -SO ₂ -	1324, 1151 1295	1323, 1151 1299
C-O stretch aryl ether	1244	1242
C-C C-(CH ₃) ₂ skeletal vibr.	1170 1106 1081 1015 874, 835, 834 731, 718, 692 636	- 1106 1072 1012 872, -, 837 -, 719, 702 628

Minor constituents can not be traced in IR. In the case of S10, where FAB mass spectra indicate the presence of bisphenol A, this feature is not observed in the "bulk" ATR IR technique, nor is the presence of small amounts of a nitrogen-containing solvent in both GR61 and S10.

4.4. CONCLUSIONS

The combination of three different surface sensitive spectroscopic techniques, XPS, FAB MS and ATR IR, illustrates the similarities and differences between GR61 and S10 PSf membranes. The first consists of Udel PSf, the second has Victrex PESf as the major compound. A characteristic feature in FAB MS is the higher ratio of intensity of the aromatic m/z fragments 77^+ and 115^+ in S10 than in GR61, correlated with the amount of bisphenol A present in the surfaces. Comparison of GR61 and S10 in XPS shows a higher content of S and O in S10 than in GR61, as is also inferred from FAB MS data. Most conspicuous in ATR IR is the presence or absence of the vibration bands at 1170 and 1503 and the doublet at $1387 - 1365 \text{ cm}^{-1}$ in GR61 and S10, respectively, confirming the major components to be Udel and Victrex. An ultimate criterion to distinguish between S10 and GR61 is the ratio of intensities of m/z fragments (FAB MS) $43^+/41^+$, $57^+/55^+$ and $71^+/69^+$ which is 1.0 for S10 and 0.4 for GR61.

S10 also shows a minor amount of Udel as a constituent which is preferentially located in the uppermost layers, as determined by FAB MS and XPS. For both membranes a gradient in hydrophobicity towards the surface is also inferred from XPS and FAB MS. SO_2 structural groups are more oriented towards the bulk and CH_3 and aryl-C-aryl functions towards the surface.

The unexpected presence of nitrogen originates from the remaining solvent DMF and not necessarily from an additive, as is inferred from reference PSf membranes cast with known components.

ACKNOWLEDGEMENTS

The author wishes to thank mr. M.E.F. Biemond (Akzo Corporate Research, Arnhem, NL) for collecting and elaborating the XPS data. Dr. D. Johnson (Surface Analysis Service, UMIST, Manchester, GB) determined the FAB mass spectra and mr. J.M. Weseman (RIKILT, Wageningen, NL) provided useful tips during acquisition of the ATR IR spectra.

Dr. H.C.W.M. Buys (TNO, MT, Zeist, NL) had the idea about the retained solvent molecules and provided the reference TNO membranes. Fruitful discussions with dr. M. Oldani (ABB, Corporate Research, Baden, CH) are gratefully acknowledged.

This investigation was supported by the Programme Committee on Membrane Technology (PCM) of the Dutch Ministry of Economic Affairs.

REFERENCES

- 1 H.J. Preusser. Die Ultrastruktur einiger feinporiger Membranfiltertypen. I. Elektronenmikroskopische Untersuchungen der Oberflächen. *Kolloid-Z. u. Z. Polymere*, 1972, **250**, 133-141.
- 2 J. Kassotis, J. Schmidt, L.T. Hodgins and H.P. Gregor. Modelling of the Pore Size Distribution of Ultrafiltration Membranes. *J. Membrane Sci.*, 1985, **22**, 61-76.
- 3 F.P. Cuperus, D. Bargeman and C.A. Smolders. Thermoporometry and Permporometry Applied to UF-Membrane Characterization. Workshop on Characterization of Ultrafiltration Membranes, G. Trägård Ed., Lund University, Sweden, September 9-11, 1987, p121.
- 4 G. Schock, A. Miquel and R. Birkenberger. Characterization of Ultrafiltration Membranes: Cutoff Determination by Gelpermeation Chromatography. The 1987 International Congress on Membranes and Membrane Processes, Tokyo, Japan, June 8-12, 1987, p383-384.
- 5 L. Zeman, G. Tkacik and P. Le Parlouer. Characterization of Porous Sublayers in Ultrafiltration Membranes by Thermoporometry. *J. Membrane Sci.*, 1987, **32**, 329-337.
- 6 F.P. Cuperus, D. Bargeman and C.A. Smolders. Characterization of UF Membranes with Monodisperse Gold Sols. *Membraantechnologie in Nederland*, 1988, **3**, 11.
- 7 G.B. van den Berg and C.A. Smolders. The Boundary Layer Resistance Model for Unstirred Ultrafiltration. A New Approach. *J. Membrane Sci.*, 1989, **40**, 149-172.
- 8 F.-J. Müller, W. Krieger, W. Kissing and R. Reiner. Reduction on Membrane Fouling in Reverse Osmosis by Means of Surface Modifications of Membra-

- nes. In: *Fundamentals and Applications of Surface Phenomena Associated with Fouling and Cleaning in Food Processing*. B. Hallström, D.B. Lund, Ch. Trägård. Työlösand, Sweden, April 6-9, 1981, p343-347.
- 9 L.M. Speaker and K.R. Bynum. Oriented Monolayer Assemblies to Modify Fouling Propensities of Membranes. In: *Physicochemical Aspects of Polymer Surfaces*. Vol. 2. Ed. K.L. Mittal, Plenum Press, New York and London, 1983, p817-841.
 - 10 A.G. Fane, C.J.D. Fell and K.J. Kim. The Effect of Surfactant Pretreatment on the Ultrafiltration of Proteins. *Desalination*, 1985, 53, 37-55.
 - 11 A.S. Michaels, C.R. Robertson and H. Reihanian. Mitigation of Protein Fouling of Lipophilic Ultrafiltration Membranes by Presorption of Hydrophilic Polymers. The 1987 International Congress on Membranes and Membrane Processes, Tokyo, Japan, June 8-12, 1987, p17-19.
 - 12 J. Wolff, H. Steinhauer and G. Ellinghorst. Tailoring of Ultrafiltration Membranes by Plasma Treatment and their Application for the Desalination and Concentration of Water-Soluble Organic Substances. *J. Membrane Sci.*, 1988, 36, 207-214.
 - 13 K.J. Kim, A.G. Fane and C.J.D. Fell. The Performance of Ultrafiltration Membranes Pretreated by Polymers. *Desalination*, 1988, 70, 229-249.
 - 14 L.E.S. Brink and D.J. Romijn. Reducing the Protein Fouling of Polysulfone Surfaces and Ultrafiltration Membranes. Optimization of the Type of Coating. *Desalination*, 1990, 78, 209-233.
 - 15 J.T.F. Keurentjes, J.G. Harbrecht, D. Brinkman, J.H. Hanemaaijer, M.A. Cohen Stuart and K. van 't Riet. Hydrophobicity Measurements of Microfiltration and Ultrafiltration Membranes. *J. Membrane Sci.*, 1989, 47, 333-344.
 - 16 G.B. Larrabee and T.J. Shaffner. Surface Characterization. *Anal. Chem.*, 1981, 53, 163R-174R.
 - 17 F. Garbassi and E. Occhiello. Spectroscopic Techniques for the Analysis of Polymer Surfaces and Interfaces. *Anal. Chim. Acta*, 1987, 197, 1-42.
 - 18 J.A. Gardella Jr.. Review. Recent Advances in Ion and Electron Spectroscopy of Polymer Surfaces. *Applied Surface Sci.*, 1988, 31, 72-102.
 - 19 M. Fontyn, B.H. Bijsterbosch and K. van 't Riet. Chemical Characterization of Ultrafiltration Membranes by Spectroscopic Techniques. *J. Membrane Sci.*, 1988, 36, 141-145.
 - 20 M. Oldani and G. Schock. Characterization of Ultrafiltration Membranes by Infrared Spectroscopy, ESCA and Contact Angle Measurements. *J. Membrane Sci.*, 1989, 43, 243-258.
 - 21 J.H. Hanemaaijer, T. Robbertsen, Th. van den Boomgaard and J.W. Gunnink. Fouling of Ultrafiltration Membranes. The Role of Protein Adsorption and Salt Precipitation. *J. Membrane Sci.*, 1989, 40, 199-218.
 - 22 N.J. Harrick. *Internal Reflection Spectroscopy*. Interscience Publishers, New York, 1967.

- 23 J.L. Koenig. Fourier Transform Infrared Spectroscopy of Polymers. In: *Polymer Spectroscopy*. Ed. M. Gordon. Springer Verlag, 1985, p89-154.
- 24 H.A. Willis and V.J.I. Zichy. The Examination of Polymer Surfaces by Infrared Spectroscopy. In: *Polymer Surfaces*. Ed. D.T. Clark and W.J. Feast, Wiley & Sons, 1978.
- 25 G. Gidály and R. Kellner. Simultaneous Qualitative and Quantitative FT-IR-ATR-Spectroscopic Analysis of Submicrometer Organic Films and of the Surface Layer of Bulk Polymer Samples. *Microchim. Acta*, 1981, I, 131-139.
- 26 R. Kellner, G. Fischböck, G. Götzinger, E. Pungor, K. Toth, L. Polos and E. Lindner. FTIR-ATR Spectroscopic Analysis of Bis-Crown-Ether Based PVC-Membrane Surfaces. *Fresenius Z. Anal. Chem.*, 1985, 322, 151-156.
- 27 R. Kellner, G. Götzinger and F. Kashofer. In situ FTIR-ATR Spectroscopic Study of the Protein Adsorption on Hydrophilic and Hydrophobic Surfaces. *Colloquium Spectroscopicum Internationale*, 24 (CSI 24), Garmisch Partenkirchen, West-Germany, September 15-20, 1985. Volume I, p 172-173.
- 28 H.G. Tompkins. The Physical Basis of the Depth of Absorbing Species Using Internal Reflection Spectroscopy. *Applied Spectroscopy*, 1974, 28, 335-341.
- 29 D.T. Clark. The Application of ESCA to Studies of Structure and Bonding in Polymers. In: *Structural Studies of Macromolecules by Spectroscopic Methods*. Ed. K.J. Ivin, J. Wiley & Sons, 1976.
- 30 P.M.A. Sherwood. Photoelectron Spectroscopy. In: *Spectroscopy, Volume 3*. Eds. B.P. Straughan and S. Walker. Chapman and Hall, London, 1976, p240-296.
- 31 J. Augustynski and L. Balsenc. Application of Auger and Electron Spectroscopy to Electrochemical Problems. In: *Modern Aspects of Electrochemistry*. No 13. Eds. B.E. Conway and J. O'M. Bockris, Plenum Press, New York and London, 1979, p251-360.
- 32 D. Briggs and M.P. Seah, Eds. *Practical Surface Analysis by Auger and X-Ray Photoelectron Spectroscopy*. J. Wiley & Sons, 1983.
- 33 M. Gervais, A. Douy, B. Gallot and R. Erre. Surface Studies of Polypeptidic Block Copolymers by Electron Spectroscopy for Chemical Analysis: Poly (N^ε-trifluoroacetyl-L-lysine)-Polysacrosine Diblock Copolymers. *Polymer*, 1986, 27, 1513-1520.
- 34 C.D. Wagner, L.E. Davis, M.V. Zeller, J.A. Taylor, R.A. Raymond and L.H. Gale. Empirical Atomic Sensitivity Factors for Quantitative Analysis by Electron Spectroscopy for Chemical Analysis. *Surface Interf. Anal.*, 1981, 3, 211-225.
- 35 M.P. Seah and D. Briggs. A Perspective on the Analysis of Surfaces and Interfaces. In: *Practical Surface Analysis by Auger and X-Ray Photoelectron Spectroscopy*. D. Briggs and M.P. Seah, Eds., J. Wiley & Sons, 1983, Ch.1, 1-15.
- 36 D. Briggs. SIMS for the Study of Polymer Surfaces: a Review. *Surface Interf. Anal.*, 1986, 9, 391-404.

- 37 J.A. Gardella Jr. and D.M. Hercules. Mass Spectrometry of Molecular Solids. II. Laser Microprobe Mass Analysis of Selected Polymers. *Fresenius Z. Anal. Chem.*, 1981, **308**, 297-303.
- 38 J. Peeling and D.T. Clark. Photooxidation of the Surfaces of Polyphenylene Oxide and Polysulfone. *J. Appl. Polymer Sci.*, 1981, **26**, 3761-3772.
- 39 S.R. Heller and G.W.A. Milne, Eds. EPA/NIH Mass Spectral Data Base, National Bureau of Standards, Washington D.C., 1980-1983.
- 40 L.J. Bellamy. *The Infra-red Spectra of Complex Molecules*. Methuen & Co Ltd., London. J. Wiley & Sons, Inc., New York. 1958, 2nd Ed.

CHAPTER 5

SURFACE SPECTROSCOPIC STUDIES OF PRISTINE AND FOULED MEMBRANES. PART II. METHOD DEVELOPMENT AND ADSORPTION MECHANISM

ABSTRACT

The complicated problem of membrane fouling has been tackled by applying several surface spectroscopical methods. The results elucidate various chemical aspects of the interaction between polysulfone (PSf) membranes and polypropylene glycol (PPG), which combination was chosen as a model system.

All analyses of the DDS GR61 PP and Dorr-Oliver S10 membranes fouled by adsorption of PPG, show that the latter is present as an additional layer on the surfaces. The atomic composition (as revealed by X-ray photoelectron spectroscopy (XPS)) of the pristine membranes changes towards that of PPG in the fouled surfaces.

In fast atom bombardment mass spectrometry (FAB MS) some m/z fragments occur that are not observed in the spectra of the membranes and of the foulant separately. Unfortunately, assignment of these ions which could contribute in clarifying the chemical mechanism of adsorption, is not possible due to their complexity. On the other hand, attenuated total reflection Fourier transform infrared spectroscopy (ATR FTIR) demonstrates that the major interaction between PSf and PPG proceeds through the aryl- $C(CH_3)_2$ -aryl structure in PSf and the CH_3 groups in PPG. Also in S10, consisting mainly of Victrex polyethersulfone with Udel as a minor surface constituent (Part I), this interaction is clearly observed.

This study shows integrated application of various surface spectroscopic techniques to be a powerful means in unravelling the mechanisms of fouling. It is especially helpful in directing research on membrane materials for special purposes or in designing cleaning agents and procedures for membranes.

5.1. INTRODUCTION

Adsorption phenomena in fouling of membranes have extensively been described, e.g. [1 - 4], although mainly for proteins. Solute - membrane interactions are not only important for the primary adsorption, but are also considered important for the further build-up of fouling in membrane processes [5, 6].

Quite generally, adsorption is a well-documented phenomenon [7]. Only, the appropriate data is usually obtained with surfaces that are smooth, well defined and easy to handle. Fundamental research about adsorption at membrane surfaces, on the other hand, has been very scarce. This is probably due to the absence of those characteristics of a model system. However, to enhance the applicability of membranes the mechanisms governing adsorption, especially those related to fouling, need to be known. On a macroscopical scale the alteration of the pore size (distribution) has been investigated [8 - 10], whereas on a molecular scale the configuration of the foulants near the surface has been studied [11].

This paper is concerned with the (chemical) interactions between well characterized polysulfone (PSf) membranes (Part I, chapter 4) and polypropylene glycol (PPG) as a hydrophobic foulant.

To this purpose surface-sensitive spectroscopic techniques revealing the atomic and structural composition of the fouled membranes are employed. Investigating the differences elucidates the functional groups in membrane and foulant that are responsible for the mutual interactions. In particular, a combination of different techniques can lead to useful conclusions [12, 13].

The techniques used focus on the outer membrane surface although the surface area in the pores will be much larger. This is important because the foulant, with a molecular mass (MM) of 1200, has easy access to the inner surface. However, in the authors' opinion the results about the outer surface of the membrane can be generalized.

5.2. MATERIALS AND METHODS

5.2.1. Membranes

Commercial DDS GR61 PP and Dorr-Oliver S10 polysulfone (PSf) membranes are used in the adsorption study. Their treatment and the characterization of the

pristine surfaces, before adsorption, by surface spectroscopy has been described in Part I (chapter 4).

5.2.2. Foulant

PPG $[-\text{CH}(\text{CH}_3)-\text{CH}_2-\text{O}-]_n$ (Fluka AG, Buchs, CH, 81370) with an average molecular mass of 1200 amu was used as the fouling (adsorbing) agent. PPG acts as a model compound for an anti-foaming agent, combining hydrophobic properties with (limited) solubility in water.

5.2.3. Adsorption Procedure

Pieces of the rinsed PSf membranes were exposed to a 1 kg.m^{-3} aqueous PPG solution during 24 hours at atmospheric pressure and 25°C . After equilibration the membranes were washed with 10 ml microfiltered distilled water to remove non-adsorbed PPG molecules and dried in the same way as the pristine membranes (Part I).

Adsorption from the 1 kg.m^{-3} PPG solution on the PSf is completed within 24 hours [24].

5.2.4. Surface-Sensitive Spectroscopy

The basic interactions underlying membrane fouling are not dealt with in the few spectroscopic studies of synthetic membrane surfaces [4, 13 - 15], and thus are still not unravelled. It is of utmost importance to investigate fouled membranes by advanced spectroscopy.

Part I (chapter 4) comprises a review of the employed surface spectroscopic techniques and the applied conditions.

Spectrum subtraction in attenuated total reflection Fourier transform infrared spectroscopy (ATR FTIR) to detect the differences between or the changes in samples is thoroughly discussed in [12, 16 - 18] (scaling factor, assumptions, dangers and possible artefacts, etc.). (Re-)orientation and (slight) modifications of the surface molecules (by contact with an other compound) have been investigated and models for the analysed sample surface were proposed [12, 18 - 20]. Quantitative information on the sample surface is gained by calculating absorbance ratios in pure and modified surfaces [21]. Good contact of the sample with the internal reflection element (IRE) is essential for quantitative measurements and calculation of spectra differences [21, 22],

resulting also in reproducible data. All these aspects were duly taken care off in the interpretation of our difference spectra, which were obtained by minimizing the observed additional vibration band or shift.

The ATR IR spectrum of the pure PPG (viscous liquid) was recorded by spreading a very small droplet on one side of the IRE crystal. The X-ray photoelectron spectroscopy (XPS) spectrum of the pure PPG was acquired after evaporating a solution in dichloromethane on aluminum foil. In fast atom bombardment mass spectrometry (FAB MS) the PPG was smeared out on the stub and dried under a lamp and further analysed under the same conditions as the membranes.

In order to allow proper conclusions to be drawn, spectra of pristine and fouled membranes were always obtained from the same membrane sheet and in the same experiment.

The necessary drying procedure can influence the results of the measurements of the system membrane and foulant equally well as for the pristine membrane. Therefore, the spectroscopic results should be interpreted with care. Measuring the membrane characteristics after wetting the membrane + foulant again will not give any definite answer because even wetting a pristine membrane to the same extent as before drying is very difficult due to a modified physical structure.

5.3. RESULTS AND DISCUSSION

5.3.1. XPS

The analysis for two electron escaping depths, ca. 5 and ca. 0.5 nm, originating from analysis at a 90° and 10° angle with the sample, respectively, of both fouled PSf membranes (Table 1) clearly illustrates the adsorption of a C-O compound. Comparison of the calculated and experimentally determined composition of PPG illustrates that this additional compound is indeed PPG.

The data for S10, 90° in Table 1 are slightly different from the results obtained in Table 3 of Part I (chapter 4). The latter are an average composition while the former are the results for that particular membrane which has been fouled in this study. It is obvious that it contains more N than the average S10.

Table 1. Atomic composition (XPS) of pristine and PPG fouled GR61 and S10, and PPG.

Material	Atom%			
	C	S	O	N
GR61 90°	78.4	2.5	16.2	2.9
GR61+PPG 90°	77.9	2.0	18.1	2.0
GR61 10°	80.6	1.5	14.2	3.7
GR61+PPG 10°	78.8	1.1	18.3	1.7
S10 90°	69.8	3.5	22.7	4.0
S10+PPG 90°	69.8	4.2	24.4	1.6
S10 10°	70.7	3.3	22.2	3.9
S10+PPG 10°	75.1	2.7	21.1	1.0
PPG	75.0	-	25.0	-
Udel calculated	84.4	3.1	12.5	-
Victrex calculated	75.0	6.3	18.8	-
PPG calculated	75.0	-	25.0	-

The C1s decomposed peak at 290.5 eV ($\pi \rightarrow \pi^*$ shake up satellite) is not used in this analysis (only of qualitative interest) (Table 2). It is absent in the PPG sample.

Table 2. C1s peak decomposition (XPS) of pristine and PPG fouled GR61 and S10, and of PPG.

Material	C %		
	284.5 ^a	286.1 ^a	288.0 ^a
GR61	69.5	24.7	5.8
GR61+PPG	65.6	29.8	4.6
S10	61.2	30.1	8.7
S10+PPG	60.1	34.8	5.1
PPG	29.6	70.3	-
Udel calculated	85.2	14.8	-
Victrex calculated	83.3	16.7	-
PPG calculated	33.3	66.7	-

^a Binding energy (eV)

The adsorption of PPG causes a drop in the C=O signal (288.0 eV) because PPG does not contribute to it and the dimethylformamide (DMF) layer is masked (Table 2). The C-O contribution (286.1 eV) in both fouled membranes is increased since it makes up 2/3 of the C content in PPG (Table 2).

5.3.2. FAB MS

Important smaller mass to charge m/z fragments in the positive spectrum of PPG (Figure 1.a.i) are the non-typical CHO fragmentation products 31^+ ($\text{CH}_2=^+\text{OH}$) and 45^+ ($\text{CH}_3\text{-CH}^+\text{OH}$). Dipropylene glycol fragments are found at 87^+ ($\text{X-C}_2\text{H}_5^+$), 99^+ ($\text{X-C}_3\text{H}_5^+$), 101^+ ($\text{X-C}_3\text{H}_7^+$) and 115^+ ($\text{X-C}_3\text{H}_5\text{O}^+$), with X being the monomeric unit of PPG. Fragments headed under the series $\text{X}_n\text{-H}$ ($58n + 1$), respectively $\text{X}_n\text{-C}_3\text{H}_5$ ($58n + 41$), with 58 being the mass of the monomeric unit of PPG, are comparable to those in the degradation of polyethylene oxide [23]. For a third series (251^+ , 309^+ , 367^+), it is not certain whether it should be assigned to $\text{X}_n + 19$ with $n = 4, 5, 6$ or to $\text{X}_n + 77$ with $n = 3, 4, 5$. (The higher m/z are not shown in the Figure 1.a.i).

Both positive spectra of the fouled GR61 and S10 in Figure 1.a.ii and iii show m/z ions that are equally typical for the PSf fragmentation pattern and the PPG degradation. Other fragments exclusively originate from the combination of PSf and PPG.

Typical PSf fragments (77^+ , 91^+ and 165^+ from aromatic ring degradation, respectively 28^+ and 42^+ from the nitrogen compound) show a diminished intensity. The adsorbed layer apparently causes a less deep monitoring of the PSf surface layer.

Among other fragments those at 59^+ , 117^+ and 175^+ identify the adsorbed compound as PPG ($\text{X}_n\text{-H}$). Comparison of the intensity ratios of the PPG and/or PSf ions $31^+/29^+$, $59^+/57^+$ and $117^+/115^+$ for the pristine PSf membranes and the pure PPG with these ratios for the membranes with an adsorbed PPG layer (membrane + PPG) (Table 3), indicates that the intensities of the concerned mass fragments are constituted partly of PPG and partly of PSf.

Besides various non-typical fragments (C_nH_x^- , $\text{C}_n\text{H}_x\text{O}_y^-$, O^- and OH^-), the smaller mass negative spectrum of PPG (Figure 1.b.i, higher m/z are not shown) shows the typical 75^- through 249^- series $^-\text{O-X}_n\text{-H}$ (consecutive differences of 58 amu) and fragments corresponding with loss of oxygen and/or hydrogen comparable to those observed in the degradation of polyethylene oxide (117^- $^-\text{O-X-C}_3\text{H}_7$, 115^- $^-\text{O-X-C}_3\text{H}_5$, 113^- $^-\text{O-X-C}_3\text{H}_3$) [23].

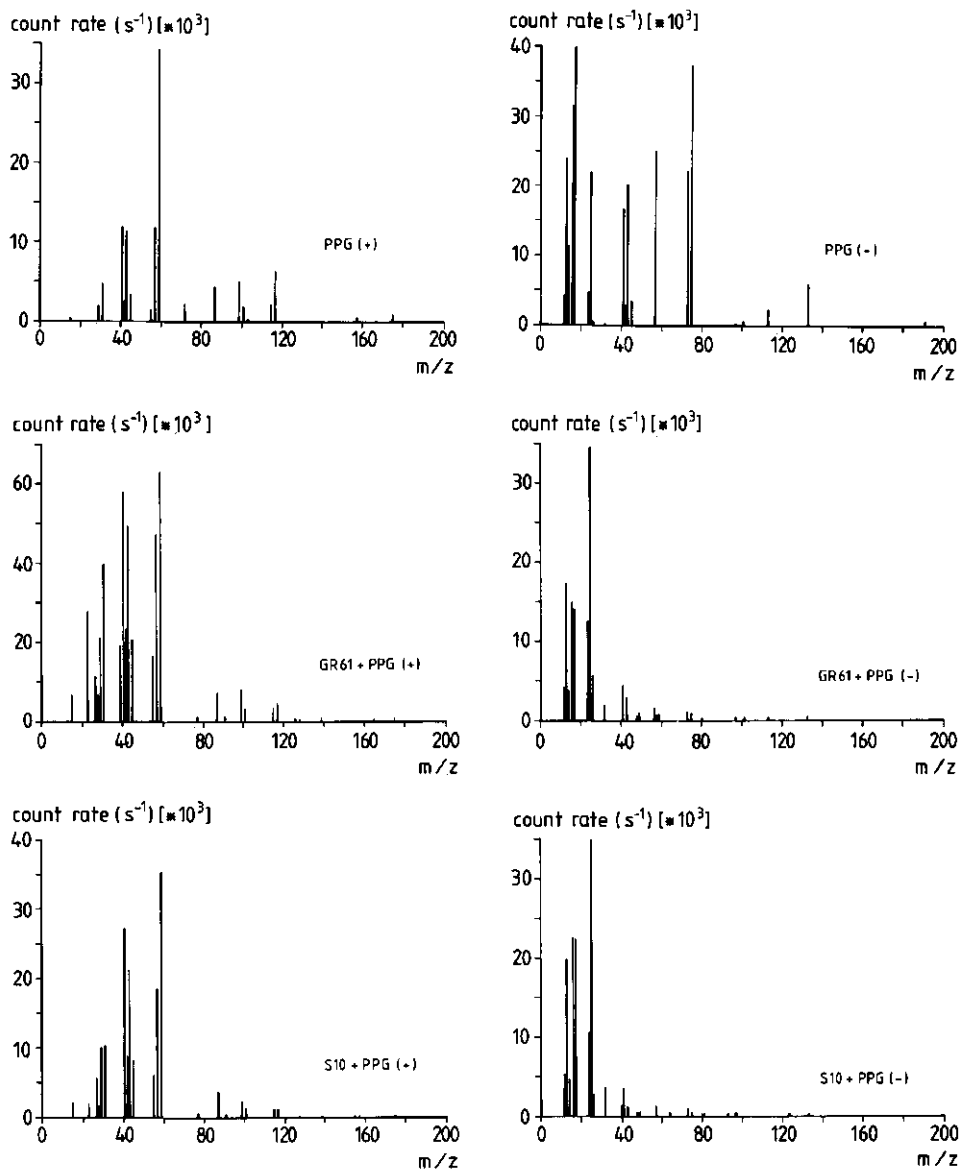


Figure 1. a. Positive and b. negative FAB mass spectra of i. PPG, ii. GR61 + PPG and iii. S10 + PPG.

Table 3. Intensity ratios of m/z fragments (positive FAB MS) typical for PPG or PSf or the combination PSf + PPG in GR61 and S10.

	Intensity Ratio				
	GR61	S10	PPG	GR61+PPG	S10+PPG
31/29	0.11	0.09	2.43	1.88	1.03
59/57	0.20	0.06	2.90	1.34	1.94
117/115	0.40	0.43	2.90	1.27	1.09
155/157			0.12	2.05	0.83
213/215			0.10	3.37	1.27
271/273			0.63	6.80	3.86
329/331			0.45	5.08	2.25
387/389			-	4.23	1.62

The negative spectrum of GR61 + PPG (Figure 1.b.ii) is clearly distinguished from the spectrum of the pristine GR61 by the fingerprint fragments 17^- , 41^- , 57^- , 73^- and 113^- (Table 4). These fragments and the decreased relative intensities of the S fragments (Table 4) easily identify the adsorbed layer as PPG. The diminished ratio of intensities of the oxygen ions $16^-/17^-$ in the two combination spectra (0.96 and 1.01) compared to those for the pristine GR61 and S10 (1.53 and 1.58 respectively) is also caused by the corresponding low ratio in PPG (0.79).

If fragments can be traced that neither correspond to the pristine membrane, nor to the PPG, and if these ions can be assigned as partly comprising PSf and partly PPG, the chemical mechanism of the adsorption between PSf and PPG may be unravelled. The first series to be considered in this connection ranges from 155^+ to 387^+ , the terms mutually differing by 58 amu and having an m/z being 2 amu lower than in a similar series for pure PPG. It is uncertain whether this series of new fragments exclusively originates from PPG, or that it is a combination of PPG and PSf. In the combination spectrum the intensity ratio of these m/z to $m/z+2$ fragments is higher than in the PPG spectrum (Table 3), suggesting that the ion $m/z+2$ is more easily obtained from the pure PPG than from the combination PSf + PPG. Since these combination fragments can also be derived from multimers of propylene glycol (PG) coupled to a fragment with m/z 96, or from the series 251^+ through 367^+ shortened with a 96 fragment, any further conclusions about an interaction and its chemical nature can not be drawn.

Table 4. Relative intensities of typical m/z fragments (negative FAB MS) in the pristine GR61 and S10, in PPG and in the combination PSf + PPG, and their possible assignment.

m/z assignment	Relative Intensities				
	GR61	S10	GR61+PPG	S10+PPG	PPG
32 S ⁻	64.93	40.54	0.11	0.19	
48 SO ⁻	34.17	27.94	0.04	0.03	
64 SO ₂ ⁻	3.80	19.27	0.02	0.02	
80 SO ₃ ⁻	1.76	5.34	0.006	0.012	
97 HSO ₄ ⁻	1.89	1.21	0.004	0.003	
17 OH ⁻	0.45	1.69	1.29	1.12	1.67
41 C ₂ HO ⁻			0.21	0.18	0.70
57 C ₃ H ₅ O ⁻			0.09	0.06	1.05
73 C ₃ H ₅ O ₂ ⁻			0.07	0.04	0.93
75 ⁻ O-X-H			0.06	0.03	1.56
113 ⁻ O-X-C ₃ H ₃			0.009	0.001	0.097
133 ⁻ O-X ₂ -H			0.004	0.002	0.250

The series 255⁺, 313⁺ and 371⁺, another type of combination fragments typical for membranes with a PPG layer, can unfortunately neither be assigned to a certain structure.

The negative spectra of GR61 and S10 covered by PPG do also not give information about the adsorption mechanism.

5.3.3. ATR IR

Characteristic features in the ATR IR spectrum of PPG (Figure 2 and Table 5) as compared to the pristine PSf membranes (Part I) are the C-H stretch region (only the aliphatic one at wavenumbers below 3000 cm⁻¹), the C-O stretch at 1099 cm⁻¹, which is due to the aliphatic ether bond, and the CH₃ symmetrical deformation at 1373 cm⁻¹.

The spectra of the fouled membranes (Figure 3) very much resemble those of the pristine PSfs, due to the depth of analysis of ATR IR as compared to the thickness of the adsorbed PPG layer. However, as compared to the corresponding pristine membrane spectra, they show weaker C-H bands. It is not likely that this is due to an artefact because of the reproducibility for this particular membrane. This phenomenon is not found by XPS and FAB MS.

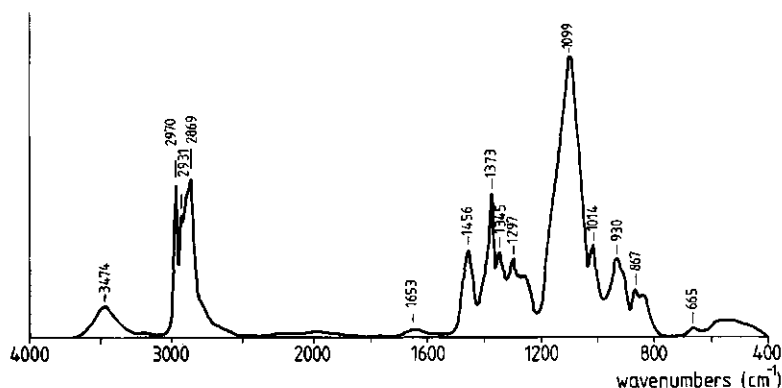


Figure 2. ATR IR spectrum of the pure component PPG.

Table 5. ATR IR bands of PPG and their possible assignment.

Wavenumber (cm^{-1})	Possible assignment
3474	O-H stretch
2970 and 2869	C-H stretch CH_3 asymmetrical and symmetrical
2931	CH_2
2894	CH
1456	CH_2 deformation and CH_3 asymmetrical deformation
1373	CH_3 symmetrical deformation
1345	C-H bending
1297	
1263	
1099	C-O stretch aliphatic ether
930	
668	

In S10 + PPG as well as in GR61 + PPG the CH_3 symmetrical deformation at 1373 cm^{-1} , characteristic for PPG, is observed (Table 6). Also the sharp band of the C-H (CH_3) stretch in PPG at 2970 cm^{-1} is well determined in GR61 + PPG (at 2970) and in S10 (at 2973 cm^{-1} , extra band). The C-H stretch band at 2850 cm^{-1} in both membranes has disappeared and a shift in wavenumber from 663 (GR61) to 668 is due to PPG with a band at 665 cm^{-1} .

Figure 4 schematizes the procedure for obtaining difference spectra (spectrum subtraction). These difference spectra especially provide information about the chemical interaction between PSf and PPG, possibly elucidating the mechanism of adsorption. Interaction between PSf and PPG should be observed in differences in intensity, shifts or extra bands.

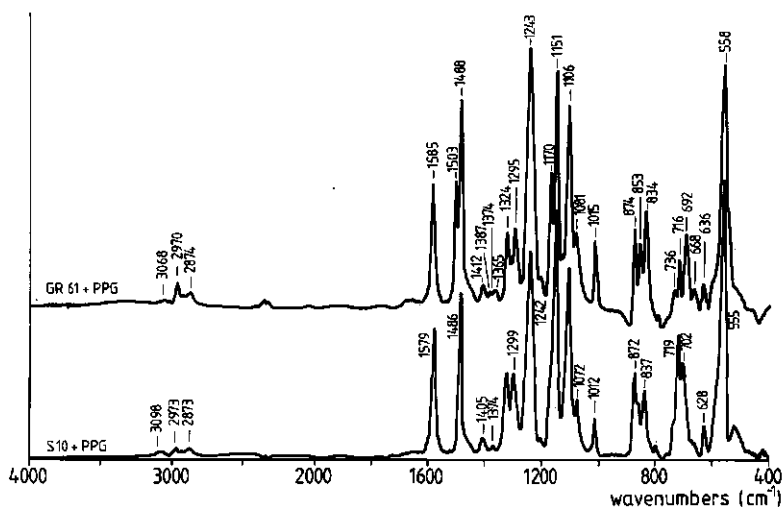


Figure 3. ATR IR spectra of the PPG fouled GR61 and S10.

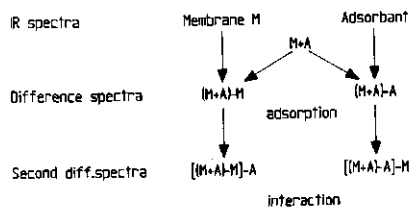


Figure 4. Schematic representation of the procedure for obtaining ATR IR difference spectra.

Better identification of PPG is best inferred from the difference spectra of the fouled and pristine GR61 and S10 (Table 6). The strong PPG C-O-C aliphatic ether band at 1099 cm^{-1} is distinguished from the 1106 cm^{-1} band of PSf. The dip-and-hump in the C-O-C aromatic ether band at 1242 cm^{-1} in both difference spectra of GR61 and S10 may be the result of an overlap with the 1263 cm^{-1} band of PPG or the indication of an interaction of PPG with the aromatic ether structure in PSf.

Table 6. Some characteristic ATR IR bands (cm^{-1}) in PPG and in pristine and PPG fouled GR61 and S10, as well as their appearance (shifts and dip-and-humps) in the difference spectra of the fouled PSf.

GR61	GR61+PPG	(GR61+PPG)-GR61	PPG	(S10+PPG)-S10	S10+PPG	S10
2969	2970	2973	2970	2973	2973	-
1585	1585	1586	-	1585\1577	1579	1579
1503	1503	1507	-	1507	-	-
-	-	1472 and 1464	1456	1473 and 1463	-	-
-	1374	1375	1373	1374	1374	-
1242	1243	1245\1224	(1263)	1244 and 1238	1242	1242
1106	1106	1114 and 1093	1099	1120 and 1100	1106	1106
663	668	668	665	668	-	-
558	558	555	-	570 and 556\551	555	558

The C-H stretching of the CH_3 group featuring in both GR61 PSf and PPG shows up at 2973 cm^{-1} in the difference spectra of GR61 as well as of S10 (Table 6). Also the C=C stretch band at 1503 cm^{-1} , typical for the aryl-C-aryl (Ar-C-Ar) structure in Udel PSf, appears to have shifted towards 1507 cm^{-1} , probably indicating an interaction with PPG. The same band is equally unexpectedly as obviously present in the difference spectrum of S10. Related to this new vibration is the dip-and-hump observed in the C=C stretch band at 1579 in S10. A band at 1585 cm^{-1} appears in the S10 difference spectrum. The presence of 1585 and 1507 cm^{-1} in this difference spectrum (also observed for GR61) can be explained by the smaller amount of Udel PSf along with the major compound Victrex PESf, present in the S10 surface and not deeper in the bulk, as observed by XPS and FAB MS. Due to the favoured interaction of PPG with the Ar-C-Ar structure in Udel, the appropriate vibration bands are accentuated in S10. Because the difference spectra of the surface IR (ATR IR) highlight the phenomena at the surface of the membranes, the vibration bands at 1507 cm^{-1} and at 1585 and 1579 cm^{-1} are clearly observed, being spectral features characteristic of Udel.

A second characteristic in the S10 difference spectrum is the sharp doublet at 1473 and 1463 cm^{-1} , which in a minor intensity is also observed in GR61 (1472 and 1464 cm^{-1}). This vibration region is related with the CH_2 deformation and CH_3 asymmetrical deformation and is associated with an interaction of the CH_2 and CH_3 groups in PPG with PSf. A small shift in the 1373 cm^{-1} CH_3 symmetrical deformation in PPG towards 1374 and 1375 in the difference spectra of GR61 and S10, respectively, and the shift in the C-H stretch (CH_3) from 2970 cm^{-1} towards 2973 , supports this type of interaction. It may be

concluded that the main interaction between PSf and PPG proceeds by the (hydrophobic) CH_3 group in PPG and the (hydrophobic) $\text{Ar-C(CH}_3)_2\text{-Ar}$ configuration in PSf. Probably the dip-and-hump in the difference spectra of GR61 and S10 at the C-O-C aromatic ether band (1242) is also caused by the altered vibrations in the aromatic rings attached to the aliphatic carbon (bisphenol A part in Udel PSf) due to this interaction. The SO_2 vibration bands at 1150 and 1324 cm^{-1} always appear unshifted, indicating that this SO_2 group is not involved in the interaction.

These ATR IR data emphasize again that hydrophobic groups in membrane and foulant are more responsible for adsorption (and thus for flux reduction during ultrafiltration) than hydrophilic structures.

In the appropriate wavenumber regions the reverse difference spectra of the fouled membranes with the foulant, (membrane + PPG) - PPG, show the PSf contributions with rather high intensity bands, sometimes concealing the typical PPG bands. Nevertheless, for example, the altered C-H stretch (aliphatic, below 3000 cm^{-1}), a C-H deformation region (\pm 1340 - 1390) and a shift of the 663 band to 668 cm^{-1} are obviously indicating the presence of PPG on and its interaction with the PSf membranes.

The second difference spectra (the difference of the differences) are not more elucidating than the first difference spectra. The high number of manipulations and assumptions involved, can only produce doubtful interpretations.

5.4. CONCLUSIONS

The surface spectroscopic analysis of the PSf GR61 and S10 membranes fouled by adsorption of PPG obviously reveals the presence of an additional layer upon the membrane, which can be assigned to PPG indeed. The XPS atomic and Cls composition of the membranes alters towards the composition of PPG. Typical m/z fragments in FAB MS, such as multiples of the monomeric mass 58, and typical vibration bands in ATR IR at 1373 cm^{-1} and 1099 cm^{-1} , observed in the combination spectra, are characteristic for PPG.

In FAB MS both fouled PSf membranes show new m/z ions that do neither appear in the spectra of the pristine membranes, nor of the PPG. Defining the adsorption mechanism by way of these additional m/z fragments appears to be impossible due to their complex structures. ATR IR analysis of the combination PSf + PPG shows that the entities responsible for interaction are the

hydrophobic CH_3 and CH_2 functions in PPG and the $\text{Ar-C}(\text{CH}_3)_2\text{-Ar}$ structure in PSf. It also illustrates the enormous possibilities of this technique in designing new surfaces for specific applications.

All data, particularly that obtained when comparing membranes before (Part I, chapter 4) and after adsorption, result in the schematic topographic model proposed in Figure 5. The hydrophobic interaction is also indicated.

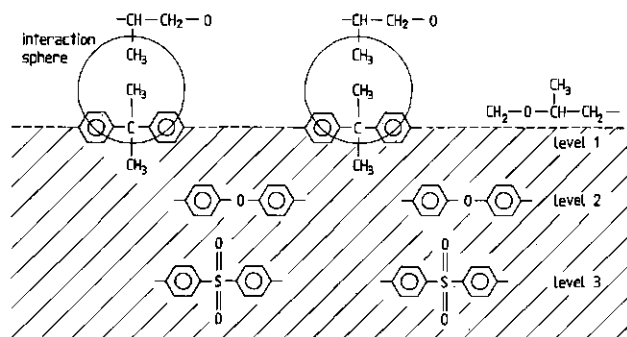


Figure 5. Schematic topographic model for the configuration of PPG on the PSf surface.

This model is a simplification of reality, of course the indicated levels with their constituents are not strictly located. Some flexibility of the molecules will still be present and adsorbed water will also influence the interaction. Nevertheless, the data observed by surface-selective spectroscopy qualitatively support the proposed model.

Although the IR spectrum of PSf is complex with some unassigned bands, the further analysis of the spectra of the fouled PSf membranes results in the elucidation of the interactive chemical groups. ATR IR, together with XPS and FAB MS, are thus shown to be very powerful techniques in the characterization of pristine and fouled surfaces. This type of research can lead to the development of better membranes, applicable for typical processes.

ACKNOWLEDGEMENTS

Mr. M.E.F. Biemond (Akzo Corporate Research, Arnhem, NL) and dr. D. Johnson (Surface Analysis Service, UMIST, Manchester, GB) acquired the XPS and FAB MS data, respectively. Dr. M. Oldani (ABB, Corporate Research, Baden, CH) and mr. J.M. Weseman (RIKILT, Wageningen, NL) contributed by providing helpful tips and taking part in stimulating discussions on the

ATR IR.

This investigation was financed by the Programme Committee on Membrane Technology (PCM) of the Dutch Ministry of Economic Affairs.

REFERENCES

- 1 E. Matthiasson. The Role of Macromolecular Adsorption in Fouling of Ultrafiltration Membranes. *J. Membrane Sci.*, 1983, **16**, 23-36.
- 2 E. Matthiasson, B. Hallström and B. Sivik. Adsorption Phenomena in Fouling of Ultrafiltration Membranes. In: *Engineering and Food*. Vol. 1. Ed. B.M. McKenna. [Proceedings from the Third International Congress on Engineering and Food, Dublin, Ireland, September, 1983.], Elsevier, 1984, 139-149.
- 3 J.A.G. Weldring and K. van 't Riet. Physical Properties of Sodium Carboxymethyl Cellulose Molecules Adsorbed on a Polyacrylonitrile Ultrafiltration Membrane. *J. Membrane Sci.*, 1988, **38**, 127-145.
- 4 J.H. Hanemaaijer, T. Robbertsen, Th. van den Boomgaard and J.W. Gunnink. Fouling of Ultrafiltration Membranes. The Role of Protein Adsorption and Salt Precipitation. *J. Membrane Sci.*, 1989, **40**, 199-218.
- 5 J.-Y. Chen and W. Pusch. Solute-Membrane Interactions in Hyperfiltration. *J. Applied Polymer Sci.*, 1987, **33**, 1809-1822.
- 6 G.B. van den Berg and C.A. Smolders. The Boundary Layer Resistance Model for Unstirred Ultrafiltration. A New Approach. *J. Membrane Sci.*, 1989, **40**, 149-172.
- 7 A.W. Adamson. *Physical Chemistry of Surfaces*. Interscience Publishers, 1967, 2nd Ed.
- 8 W. Pusch and A. Walch. Membrane Structure and its Correlation with Membrane Permeability. *J. Membrane Sci.*, 1982, **10**, 325-360.
- 9 I. Jitsuhara and S. Kimura. Structure and Properties of Charged Ultrafiltration Membranes of Sulfonated Polysulphone. *J. Chem. Eng. Japan*, 1983, **16**(5), 389-393.
- 10 L.J. Zeman. Adsorption Effects in Rejection of Macromolecules by Ultrafiltration Membranes. *J. Membrane Sci.*, 1983, **15**, 213-230.
- 11 T.D. Long, D.L. Jacobs and J.L. Anderson. Configurational Effects on Membrane Rejection. *J. Membrane Sci.*, 1981, **9**, 13-27.
- 12 J.A. Gardella Jr.. Review. Recent Advances in Ion and Electron Spectroscopy of Polymer Surfaces. *Applied Surface Sci.*, 1988, **31**, 72-102.
- 13 M. Oldani and G. Schock. Characterization of Ultrafiltration Membranes by Infrared Spectroscopy, ESCA and Contact Angle Measurements. Submitted.
- 14 M. Fontyn, B.H. Bijsterbosch and K. van 't Riet. Chemical Characterization

- of Ultrafiltration Membranes by Spectroscopic Techniques. *J. Membrane Sci.*, 1988, **36**, 141-145.
- 15 J.T.F. Keurentjes, J.G. Harbrecht, D. Brinkman, J.H. Hanemaaijer, M.A. Cohen Stuart and K. van 't Riet. Hydrophobicity Measurements of Microfiltration and Ultrafiltration Membranes. *J. Membrane Sci.*, 1989, **47**, 333-344.
 - 16 H.A. Willis and V.J.I. Zichy. The Examination of Polymer Surfaces by Infrared Spectroscopy. In: *Polymer Surfaces*. Ed. D.T. Clark and W.J. Feast, Wiley & Sons, 1978, p287-307.
 - 17 W.A.P. Luck, D. Schiöberg and U. Siemann. Infrared Investigation of Water Structure in Desalination Membranes. *J. Chem. Soc. Faraday Trans 2*, 1980, **76**, 136-147.
 - 18 J.L. Koenig. Fourier Transform Infrared Spectroscopy of Polymers. In: *Polymer Spectroscopy*. Springer Verlag, 1985.
 - 19 R. Kellner, G. Götzinger and F. Kashofer. In situ FTIR-ATR Spectroscopic Study of the Protein Adsorption on Hydrophilic and Hydrophobic Surfaces. *Colloquium Spectroscopicum Internationale*, 24 (CSI 24), Garmisch Partenkirchen, West-Germany, September 15-20, 1985. Volume I, p 172-173.
 - 20 R. Kellner, G. Fischböck, G. Götzinger, E.Pungor, K. Toth, L. Polos and E. Lindner. FTIR-ATR Spectroscopic Analysis of Bis-Crown-Ether Based PVC-Membrane Surfaces. *Fresenius Z. Anal. Chem.*, 1985, **322**, 151-156.
 - 21 R. Iwamoto and K. Ohta. Quantitative Surface Analysis by Fourier Transform Attenuated Total Reflection Infrared Spectroscopy (FT-ATR-IR). *Applied Spectroscopy*, 1984, **38**, 359-365.
 - 22 F. Garbassi and E. Occhiello. Spectroscopic Techniques for the Analysis of Polymer Surfaces and Interfaces. *Anal. Chim. Acta*, 1987, **197**, 1-42.
 - 23 D. Briggs. SIMS for the Study of Polymer Surfaces: a Review. *Surface Interf. Anal.*, 1986, **9**, 391-404.
 - 24 M. Fontyn. Unpublished results.

CHAPTER 6

GENERAL DISCUSSION

In this chapter the main conclusions that have been reached in this study will be emphasized and it will be assessed to which extent the original objectives of the study have been met. Some possibilities for further research and applications will be indicated.

In this thesis the problem of membrane fouling has been approached from very different (experimental) points of view and the results can be integrated to interesting conclusions.

Ultrafiltration is a complex process of which the sieving effect is only one aspect. Especially adsorption phenomena, governed by the chemical nature of membrane and adsorbing compound, play an important role in the way the resistance to flow is built up during ultrafiltration. In search of a parameter that can quantitatively characterize this interaction the hydrophilic-lipophilic balance (HLB) as applied to the adsorbates on a polysulfone (PSf) membrane appeared to be successful to some extent. Increasing the HLB of a model compound caused a decreasing adsorption resistance under the conditions used, but the effect of the molecular mass (MM) is not fully accounted for by this parameter. Obviously, the hydrophobicity of a membrane is not easy to express in a parameter at all. The interfacial tension of detachment (γ_d) [1] might ultimately prove to be a useful characteristic parameter. However, it remains an open question how to combine the γ_d of the membrane and the HLB of the solute in order to predict the behaviour of the two components during ultrafiltration.

The hydrophilic/lipophilic characteristic of the membrane has been assessed qualitatively by a combination of three surface-sensitive spectroscopic techniques (X-ray photoelectron spectroscopy (XPS), fast atom bombardment mass spectrometry (FAB MS) and attenuated total reflection Fourier transform infrared spectroscopy (ATR FTIR)). Similarities and differences between DDS GR61 and Dorr Oliver S10, both PSf membranes, have been illustrated. For both membranes a gradient in hydrophobicity towards the surface is inferred. SO₂ structural groups are more oriented towards the bulk and CH₃ and Aryl-C-Aryl functions towards the surface.

In fouling, the composition of the surface of the membrane rather than that of

the bulk seems to be determining the nature of the interaction. In a polypropylene glycol (PPG)-fouled GR61 PSf membrane the same spectroscopic techniques indicated the hydrophobic CH_3 and CH_2 functions in PPG and the Aryl- $\text{C}(\text{CH}_3)_2$ -Aryl structure in PSf to be the entities responsible for the interaction.

Flux measurements showed that the HLB parameter could qualitatively be related to fouling and therewith adsorption. The spectroscopic measurements indicated that the interactions of solute and membrane surface are hydrophobic of nature. These two phenomena, measured with totally different methods, agree to a large extent. This means that a further search for parameters that characterize the hydrophobic character of solute and membrane is useful and could eventually lead to a quantitative relation to predict adsorption properties of a solute.

The combination of spectroscopic techniques considered in this thesis is shown to be very powerful in indicating the chemical structures responsible for the fouling and the flux decrease in membranes, which is the entry in handling the problem. Designing new surfaces for specific applications, developing better membranes that are applicable for typical processes, or formulating cleaning agents to eliminate the mutual interactions and complexing agents to keep the fouling compounds away from the membrane surface, are some of the possible future applications.

For PPG on PSf, avoiding and/or abolishing the interactions by means of displacers has been investigated [2]. Small organic molecules and surfactants that probably show a higher affinity for the PSf than PPG were tested on their effectiveness. The capacity of the surfactants to displace PPG from PSf appears to be more pronounced than the defouling capacity of the small organic molecules. All data of this investigation indicate a displacement mechanism in which PPG is badgered from the PSf surface by the displacer that is taking over its adsorption sites, rather than solubilization of the PPG in a displacer micelle. A displacer taking over the PPG adsorption sites should have a hydrophobicity better matching that of the PSf than that of PPG.

Rather than displacing foulants from the membrane by appropriate compounds, can a chemical modification of the surface possibly prevent the potential foulants being adsorbed. Presorption of ethylene oxide (EO) / propylene oxide (PO) block copolyethers on the surface of PSf membranes [3] has been shown to reduce membrane fouling during ultrafiltration of protein solutions. An optimal chain length in both the EO and the PO part has been found for which protein ultrafiltration exhibits the lowest hydraulic resistance.

Hydrophilicity of the presorbed layer also influences the total resistance to flow. Higher hydrophilicity of the presorbed block copolyethers reduces the degree of protein fouling afterwards. So, for block copolyethers too it can be concluded that to a fair extent the HLB determines the effectiveness of their anti-fouling action.

Also the macroscopic properties (pore size distribution (PSD)) of a membrane have to be taken into account in order to reach the required flux. The procedure for obtaining PSDs elaborated in this thesis enables to compare pristine and fouled membranes. In the interpretation of adsorption of PPG on PSf, three categories of pores have been distinguished. After adsorption has taken place, the small pores are blocked, pores intermediate in size remain unaltered and large pores are narrowed. Having established how the pores in the PSf membrane contribute in the fouling by PPG, it is possible to selectively alter these pore characteristics by adapted membrane preparation techniques, in order to diminish the flux decrease.

In obtaining information on the mechanism of anti-fouling by presorbed polymers Elbers and Brink [4] have employed the same type of PSf membrane (GR61) as studied in this thesis. The MM of methylcellulose (MC) has been found not to influence the degree of fouling. This is in agreement with the conclusions drawn in chapter 2 of this thesis that the MM of a compound is not determining the fouling capacity in terms of flux. The polymer gets adsorbed in the pores, but no distinction between different pore sizes in the membrane has been made. However, the effect of fouling on the flux becomes less severe as the pore diameter (cut-off) is increased (GR81, GR61 and GR51). The presorption mechanism of MC as proposed by Elbers and Brink only mentions the alteration of category III pores in the model presented in chapter 3 of this thesis.

The treatment of these membranes [4] by poly(vinylmethylether) (PVME) has been suggested to lead to the pore opening being covered by PVME. For the adsorption of MC and PVME pore covering and pore narrowing form the basis for the flux decrease of the GR-series of PSf membranes.

In perspective, the combination of physical chemical research on membrane fouling (adsorption, optimization of membrane and solution) with the process engineering approach (concentration polarization, optimization of the process conditions) will probably prove to be very rewarding. In this way the causes of fouling can be further assessed and thus the possibilities to prevent the capacity decrease during membrane filtration or even to abolish it, come within easy reach.

REFERENCES

- 1 J.T.F. Keurentjes, J.G. Harbrecht, D. Brinkman, J.H. Hanemaaijer, M.A. Cohen Stuart and K. van 't Riet. Hydrophobicity Measurements of Microfiltration and Ultrafiltration Membranes. *J. Membrane Sci.*, 1989, 47, 333-344.
- 2 M. Fontyn, M.A. Geluk, K. van 't Riet and B.H. Bijsterbosch. Displacement of Foulants Adsorbed on Ultrafiltration Membranes. International Membrane Technology Conference (IMTEC'88), the University of New South Wales, Sydney, Australia, 15-17 November, 1988.
- 3 J.K. de Roo, L.E.S. Brink and B. de Ruiter. Crosslinked Copolyethers as an Anti-Fouling Presorbed Layer on Polysulfone Ultrafiltration Membranes. *Membraantechnologie in Nederland*, 1990, 5, 66.
- 4 S.J.G. Elbers and L.E.S. Brink. Mechanism of the Anti-Fouling Action of Polymers Presorbed on Ultrafiltration Membranes. *Membraantechnologie in Nederland*, 1990, 5, 68.

SUMMARY

In this thesis the problem of membrane fouling has been considered from different points of view. The aim of the study is to gather information on the physical and chemical mechanisms of membrane fouling, so that selective solutions can be introduced to overcome or to diminish the problem.

Anti-foaming agents (AFA) are by necessity widely used in the process industry. The severe problems during membrane filtration have been shown to be caused by AFA used in upstream process steps. AFA are amphiphilic compounds that exhibit strong adsorption on polysulfone (PSf) membranes and thus cause the first, strong, flux decline before the usual, less severe, flux decrease during permeation (chapter 1).

Polypropylene glycol (PPG) as a representative of these AFA was selected as the model foulant and the DDS GR61 PSf membrane as the model membrane.

The molecular mass of the solutes appears to affect the hydraulic resistance after adsorption (R_a) as do the chemical natures of solute and membrane (chapter 2). Experiments with ethylene oxide / proylene oxide (EO/PO) block copolymers indicate hydrophobicity to be of major importance. Expressing this parameter in terms of the hydrophilic - lipophilic balance (HLB) does not provide a very useful parameter, although it illustrates the qualitative tendency of R_a to decrease with decreasing hydrophobicity of the polymer.

Specific surface area determination (chapter 2) has illustrated that these membranes are highly porous materials. As compared to the flux through the support layer of the GR61 membrane (large pores), the flux through the PSf layer plays a dominant role due to the smaller pores. In view of this knowledge the characterization of the porosity (pore size distribution (PSD)) of the membrane was concluded to be important.

The macroscopic consideration of the porosity of the PSf membrane has prompted the development of a technique for measuring PSDs (chapter 3). Herefore, dextrans were selected as calibration compounds. The retention measurements were standardized such that adsorption, configuration and concentration polarization effects were minimized. The method is applicable for pristine and fouled membranes.

It has been established that the PSD within one type and even within one batch of PSf membranes shows differences. To enable the interpretation of the adsorption mechanism on PSf membranes the PSD of the fouled membrane always should be compared to that of the corresponding pristine membrane.

A schematic model for the physical adsorption mechanism of PPG on PSf has been proposed. Due to adsorption small pores are blocked and do not contribute to the flux anymore. Pores intermediate in size remain unaltered after adsorption. Large pores are narrowed so that the flux through these pores after adsorption has decreased. The applicability of this model to other combinations of membranes and solutes has not been investigated.

To characterize the membrane on a molecular scale, surface-sensitive spectroscopic techniques have been selected (chapter 4). Only a combination of data obtained from photoelectron spectroscopy (XPS), fast atom bombardment mass spectrometry (FAB MS) and attenuated total reflection infrared spectroscopy (ATR IR) appeared feasible in revealing the surface properties of the PSf. Similarities as well as differences between DDS GR61 and Dorr Oliver S10, both PSf membranes, were established. Criteria to distinguish between both samples have been developed.

Exploiting the depth profiling properties of the three spectroscopic techniques a gradient in hydrophobicity of the membranes was established. The SO₂ chemical functions of the PSf are mainly oriented towards the bulk, whereas the hydrophobic CH₃ and Aryl-C-Aryl structures are more oriented towards the surface.

Application of the surface-sensitive spectroscopic techniques to the PPG fouled PSf membrane (chapter 5) revealed indeed an additional layer of PPG. The question if particular chemical groups could be indicated as being responsible for the interaction in membrane and adsorbing compound could be answered affirmatively. The entities CH₂ and CH₃ in PPG and Aryl-C(CH₃)₂-Aryl in PSf form a hydrophobic interaction.

In general, more insight in and knowledge on the system DDS GR61 PSf membrane and PPG as a foulant has been gathered. A PSD determination method also applicable to the fouled membrane and a molecular characterization method consisting of a combination of three spectroscopic techniques have been developed. These methods are now available for application to other membrane and foulant combinations.

A general discussion (chapter 6) combines the different points of view on the PPG foulant - PSf membrane system and the obtained results. The factor hydrophobicity influences the membrane fouling. R_a is for the major part determined by hydrophobicity and the interaction between PPG and PSf has been indicated as a hydrophobic one. Also the pore size alteration after PPG fouling has been established. The knowledge gathered in this study leads to a discussion about the possibilities to abolish and to avoid the fouling on membranes.

SAMENVATTING

In dit proefschrift wordt het membraanvervuilingsprobleem vanuit verschillende invalshoeken benaderd. Het doel van het onderzoek is informatie te verzamelen over de fysische en chemische mechanismen van membraanvervuiling. Als resultaat hiervan kunnen selectieve oplossingen worden voorgesteld om het probleem tegen te gaan of te verminderen.

Antischuimmiddelen (ASM) worden uit noodzaak veel gebruikt in de procesindustrie. Het is gebleken dat grote problemen bij de membraanfiltratie veroorzaakt worden door ASM die worden gedoseerd in processtappen vóór de filtratie. ASM zijn amfifiele produkten die sterk adsorberen op polysulfon (PSf)-membranen en daardoor de eerste, sterke, fluxafname vóór de gebruikelijke, minder snelle, fluxafname gedurende de permeatie veroorzaken (hoofdstuk 1).

Polypropyleenglycol (PPG) is representatief voor deze ASM en werd geselecteerd als de modelvervuiler. Als het modelmembraan werd DDS GR61 PSf gekozen.

De molecuulmassa van de te filtreren componenten, zowel als de chemische aard van component en membraan beïnvloeden de hydraulische weerstand na adsorptie (R_a) (hoofdstuk 2). Via experimenten met ethyleenoxide / propyleenoxide (EO/PO) blok-copolymeren is de hydrofobiciteit als belangrijkste factor naar voren gekomen. Deze parameter wordt uitgedrukt in de hydrofiel-lipofiel balans (HLB). Het is niet een kwantitatief bruikbare parameter maar de kwalitatieve tendens van verminderende R_a met verminderende polymeer-hydrofobiciteit wordt duidelijk.

Specifieke-oppervlakmetingen (hoofdstuk 2) hebben geïllustreerd dat GR61-membranen zeer poreuze materialen zijn. In vergelijking met de flux door de steunlaag van het GR61-membraan (grote poriën), speelt de flux door de PSf-laag een dominante rol vanwege de kleine poriën. Vanwege dit feit werd de karakterisatie van de porositeit (poriegrootteverdeling (PGV)) als belangrijk beoordeeld.

De macroscopische zienswijze op de porositeit van het PSf-membraan heeft geleid tot de ontwikkeling van een techniek om PGVn te meten (hoofdstuk 3). Hiervoor werden dextransen als ijkingsmateriaal geselecteerd. De retentiemetingen werden gestandaardiseerd zodat adsorptie, configuratie en concentratiepolarisatie-effecten zijn geminimaliseerd. De methode is toepasbaar op schone en vervuilde membranen.

Er werd vastgesteld dat de PGV binnen één type en zelfs binnen één batch van PSf-membranen verschillen vertoont. Om het adsorptiemechanisme op PSf-membranen te kunnen interpreteren, moet de PGV van het vervuilde membraan altijd vergeleken worden met dat van datzelfde schone (ongebruikte) membraan.

Een schematisch model voor het fysisch-adsorptiemechanisme van PPG op PSf werd opgesteld. Door adsorptie worden kleine poriën geblokkeerd die daardoor niet meer bijdragen tot de flux. Poriën met een gemiddelde poriegrootte blijven onaangetast door adsorptie. Grote poriën worden kleiner zodat de flux door deze adsorptie wordt verlaagd. De geldigheid van dit model voor andere combinaties van membranen en oplossingen werd niet onderzocht.

Om het membraan op moleculaire schaal te karakteriseren werden oppervlakte-gevoelige technieken gekozen (hoofdstuk 4). Alleen een combinatie van "photoelectron spectroscopy (XPS)", "fast atom bombardment mass spectroscopy (FAB MS)" en "attenuated total reflection infrared spectroscopy (ATR IR)" bleek de oppervlakte-eigenschappen van het PSf te kunnen ophelderen. Gelijkenissen en verschillen tussen DDS GR61 en Dorr Oliver S10, beide PSf membranen, werden duidelijk aangetoond. Criteria om beide te kunnen onderscheiden werden opgesteld.

Door de mogelijkheden te gebruiken om met de drie spectroscopische technieken diepteprofielen te maken, werd een gradiënt in hydrofobiciteit in de membranen gevonden. De SO_2 -chemische functies van het PSf-membraan zijn meer naar de bulk georiënteerd, terwijl de meer hydrofobe structuren CH_3 en Aryl-C-Aryl meer naar het oppervlak toe georiënteerd zijn.

Toepassing van deze oppervlakte-gevoelige technieken op het met PPG-vervuilde PSf-membraan (hoofdstuk 5) toonde inderdaad een additionele laag PPG aan. De vraag of bepaalde chemische groepen als verantwoordelijk voor de adsorptie konden worden aangeduid werd positief beantwoord. De groepen CH_2 en CH_3 in PPG en Aryl-C(CH_3)₂-Aryl in PSf vormen een hydrofobe interactie.

In het algemeen werd meer inzicht verkregen in en kennis vergaard over het systeem DDS GR61-membraan en PPG als vervuiler. Een PGV-bepalingsmethode die ook toepasbaar voor vervuilde membranen is en een moleculaire karakterisatiemethode bestaande uit een combinatie van drie spectroscopische methoden werden ontwikkeld. Het staat nu open deze methoden toe te passen op andere combinaties van membraan en vervuiler.

Een algemene discussie (hoofdstuk 6) combineert de verschillende gezichtspunten op het PPG-vervuiler - PSf-membraan systeem en de verkregen resultaten. De factor hydrofobiciteit is van invloed op de membraanvervuiling. De R_a wordt er voor het grootste gedeelte door bepaald en de interactie tussen PPG en PSf werd als een hydrofobe interactie aangeduid. Ook de verandering van poriegrootte na vervuiling met PPG is aangetoond. De kennis opgebouwd via dit onderzoek biedt aangrijpingspunten voor een bespreking over de mogelijkheden om vervuiling van membranen te verwijderen en te vermijden.

CURRICULUM VITAE

Marleen Fontyn werd geboren te Leuven (B) op 9 juni 1961. Zij volgde de Humaniora (Latijn-Grieks waarna Latijn-Wetenschappen) eerst aan het Ursulineninstituut te Mechelen (B), dan aan het Virgo-Fidelisinstituut te Vilvoorde (B). In hetzelfde jaar van beëindiging van de middelbare school (1979) is zij gestart met een studie aan de Landbouwfaculteit van de Katholieke Universiteit Leuven (K.U.Leuven).

In 1981 behaalde Marleen Fontyn het kandidaatsdiploma Landbouwkundig Ingenieur en in 1984 studeerde zij af met grote onderscheiding als Ingenieur voor de Scheikunde en de Landbouwindustrieën, specialisatie Technologie en Bedrijfsleiding van Landbouw- en Voedingsnijverheden.

In september 1984 trad zij in dienst van de Landbouwuniversiteit Wageningen, bij de vakgroepen Levensmiddelen-technologie (sectie proceskunde) en Fysische en Kolloïdchemie, alwaar het in dit proefschrift beschreven onderzoek werd uitgevoerd.

Sinds september 1989 is zij werkzaam bij TNO Voeding te Zeist.